

VITAL EKG

A Wearable Multi-Sensor System for Medical Diagnostics and Patient Monitoring

Giacomo Zanichelli

A Master's Thesis submitted to the
Department of Electronics and Telecommunications
in partial fulfillment of the requirements for Master Degree in
Electronic Engineering of Politecnico di Torino.

Torino

Friday 14th December, 2018

Advisor:

Prof. Eros Pasero

Co-Advisor:

Vincenzo Randazzo

Committee President:

Prof. Carlo Ricciardi

Thesis Committee:

Prof. Eugenio Brusa
Prof. Matteo Cocuzza
Prof. Roberto Garello
Prof. Fabrizio Giorgis
Prof. Andrea Lamberti
Prof. Eros Pasero
Prof. Paolo Prinetto
Prof. Carlo Ricciardi

Colophon

Typeset in X_ET_EX
and the memoir class
created by *Peter Wilson*.

The body text is set 12pt
with Minion Pro.
Other fonts include
Monaco and Myriad Pro.

Drawings typeset in
TikZ/PGF packages.

Credits

Vincenzo Randazzo
for the Android™ app.

Elisa Valli and Alessia Mauro
for the case design.

Licenced under the Creative
Commons Attribution 4.0
International Licence.

To view a copy of this licence,
visit [creativecommons.org/
licenses/by/4.0/](http://creativecommons.org/licenses/by/4.0/).



Research Places



NEURONICA LABS



*Android is a trademark of
Google LLC.*



Proudly Written by

Giacomo Zanichelli

Executive Summary

Continuous vital signs monitoring is of utmost importance for many people. Consequently, devices able to perform such monitoring, also called Personal Health System (PHS), have been gaining a lot of research and market interest in the last few years.

This thesis work deals with the design of a multi-sensor PHS able to perform I-Lead EKG, measure heart rate and Peripheral Capillary Oxygen Saturation (SpO_2) as well as monitoring skin temperature and humidity and tracking activity.

VITAL EKG has a wrist band form factor. This choice simplifies the management of the device with respect to chest straps; EKG trace and SpO_2 and heart rate readings are offered on demand and require the user to place two fingers on the device.

VITAL EKG has been designed using off the shelf, modern surface mount components. The layout of a Semi-Flex printed circuit board is also considered to account for assembly in the 3D printed case.

Heart rate and SpO_2 measurements accuracy have been checked against a professional Vital Sign Simulator; furthermore, real-life tests have been performed and results have been confronted with a professional Fingertip Pulse Oximeter.

EKG traces provided by VITAL EKG have been tested as well against professional medical equipment.

To sum up, further studies could use hardware and firmware developed in this work to provide detailed informations about anomalies of the heart, such as atrial fibrillation.

To the memory of my grandfather *Giuliano*.

Acknowledgments

I would like to express my gratitude to Prof. Eros Pasero, Vincenzo and Jacopo, who guided me throughout the development of this work.

This thesis would not have been possible without the precious support of my mom Alessandra, my dad Massimo, my brother Daniele and my grandmother Teresa, who encouraged me everyday.

My friends Luca, Elvio, Marcello, Alessandra and Leonardo, Elisa and Antonio, Kristjane and Marco and my colleagues Corrado, Christian and Giuseppe also deserve a special mention because I would not be what I am without them.

Finally, I would like to thank my girlfriend Sonia, who demonstrated incredible strength and patience during these last few months of interminable work at the lab. Anyone would have given up in front of my stubbornness and irreparable temper.

Extended Summary

In the last few years, many studies have shown the possibility of developing compact electronic devices able to monitor continuously most of vital signs. These devices are often called Personal Health Systems (PHS), because are intended to accompany the user during most, if not all, the daily activities.

Heart rate and activity are routinely and reliably tracked using single LED Photoplethysmography (PPG) and compact MEMS motion units, respectively. Other parameters, like SpO₂ and blood pressure, are already measured easily using non-invasive techniques, which however require the user to physically perform an action and use a dedicated tool (e.g. cuff-based blood pressure measurement).

This thesis work focuses on the design and production of a new generation of multi-sensor, compact electronic devices potentially able to measure a large number of parameters. VITAL EKG is available in a wrist-band, watch-like form factor.

The electronic circuitry is based on low-cost off-the-shelf components. Heart rate and SpO₂ measurements are performed exploiting PPG technique; the sensor of choice is Maxim Integrated MAX30102, which includes both red and infrared LEDs and photodetector in a small Organic Land Grid Array (OLGA) package. Skin temperature and humidity, as well as tracking of activity, have been considered while compiling the specifications for VITAL EKG to make it a complete PHS able to give a fast response about the general health status of the user.

A single lead Electrocardiogram (EKG) analog front-end completes VITAL EKG. The metal electrodes are placed on the case. The first is in contact with the skin of the wrist; the second, located in the top part of the case, is placed beside the PPG sensor. This positioning allows the user to perform concurrent acquisitions of 10 s, thus minimizing the required time, the number of actions required by the user and enabling the correlation of the signals to gain more informations about the health status (promising studies show the possibility of computing the blood pressure in this way).

The design of the VITAL EKG has been based on the older ECG Watch by Neuronica Labs, Politecnico di Torino. The analog front-end has been completely redesigned with modern, ultra low-power components. Moreover, it has been simplified greatly by replacing most of the analog filters with digital filters.

Most of the digital processing is performed onboard. A novel PPG algorithm has been designed, implemented and tested to produce reliable heart rate and SpO₂ values. A more standard autocorrelation-based routine is used to confirm the results of the processing, thus allowing to establish a confidence level for the measurement. The processing is performed in batch; however, most of the routines are designed to be easily customizable and extendable to fully-online use cases.

EKG processing has been kept simple and included only to demonstrate the capabilities of the analog front-end. Currently, heavy distortions are present as a consequence of a steep High-Pass filter. A follow-up work is already in progress to improve VITAL EKG from this point of view.

The absence of a screen does not incur in more difficult interaction with the user and ensures a significant saving on battery power. Bluetooth 4.2 is the communication protocol of choice, due to its ubiquitous presence on smart devices. An application (currently only for Android devices) is in development at Neuronica Labs. The user interface has been designed to be extremely easy to use. VITAL EKG user base is believed to be the elderly, with particular focus on people affected by heart issues which would benefit from continuous monitoring. A state based firmware allows the device to be responsive in all situations, minimizing deadlock conditions. To further enhance the user experience, three LEDs have been included in the design to inform when the device is on and the battery is in recharge and fully charged. In this preliminary prototype, LEDs color are not compliant with CE regulations.

VITAL EKG is powered by a small rechargeable battery with a capacity of 300 mA h. Fuel gauge dedicated circuitry allows the user to always have up to date information about the state of charge of the device. Low power design allows to perform an estimated number of acquisitions greater than 3000 with a single charge.

A few hardware problems have been detailed in this document. This first prototype of VITAL EKG has always been intended as a proof of concept, to be completed and extended in future works. A Semi-Flex Printed Circuit Board (PCB) has been planned for the next hardware revision, to minimize the number of connectors on the board, improve the quality of the signals and further reduce the assembly costs.

This document is organized as follows. The first Chapter introduces the topic with a general description of typical features of a PHS.

Chapter 2 focuses on the analysis of vital signs of interest for this work. A description of the human heart is also given, since this provides the basis for both EKG and PPG techniques.

Chapter 3 introduces a few devices which are already on the market, describing their positive and negative aspects.

Chapter 4 and 5 are the core of the work. The former deals with the design of VITAL EKG from a hardware point of view; the latter is about firmware and includes a detailed description of the algorithms used for signal processing.

Chapter 6 presents the verification of VITAL EKG and highlights a few problems encountered during the tests.

Finally, Chapter 7 closes the document by underlining design faults and suggesting a direction for future development of VITAL EKG.

Contents

Contents	xi
List of Figures	xiv
List of Tables	xvi
List of Listings	xvii
Acronyms	xix
1 Introduction	1
1.1 Requirements	3
2 Vital Signs	5
2.1 The Human Heart	5
2.1.1 Anatomy	5
2.1.2 The Cardiac Cycle	7
2.1.3 The Cardiac Conduction System	8
2.2 Electrocardiogram	10
2.2.1 Standard 12-lead EKG	10
2.2.2 I-Lead EKG	17
2.3 Heart Rate and Blood Oxygen Level	17
2.3.1 Theory of Photoplethysmography	17
3 State of the Art	21
3.1 Chest Straps	21
3.1.1 QARDIOCORE	21
3.1.2 CALM.	23
3.1.3 Discussion	24
3.2 Wrist Trackers	24
3.2.1 FITBIT	24
3.3 Finger Clips	24

3.4	ECG Sensor	25
4	Vital EKG	27
4.1	Requirements	27
4.2	Specifications	29
4.3	Hardware	30
4.3.1	Circuit Design	30
4.3.2	PCB Layout	44
4.4	Case Design and Fabrication	46
5	Firmware	49
5.1	BLE 4.2	49
5.1.1	Physical Layer	49
5.1.2	Host and Controller	50
5.1.3	GATT Layer	50
5.1.4	GAP Layer	52
5.1.5	LE Data Length Extension	53
5.1.6	Security	53
5.1.7	Throughput	54
5.2	General Architecture	54
5.2.1	BLE Dispatcher	55
5.2.2	MAX30102 Manager	57
5.2.3	EKG Manager	58
5.2.4	Monitoring Task	60
5.2.5	Flash Memory Manager	61
5.2.6	Memory Configuration	61
5.3	Digital Signal Processing	61
5.3.1	PPG	61
5.3.2	EKG	70
5.3.3	QRS complexes identification	76
5.4	Android Application	76
6	Testing and Discussion	79
6.1	Patient Simulator	79
6.1.1	EKG	79
6.2	Testing on Patients	82
6.2.1	EKG	83
6.2.2	MAX30102	83
7	Conclusions	87
7.1	Limitations and Future Work	87

7.1.1	Pull-up Resistors	87
7.1.2	Micro SD card Support	87
7.1.3	TI REF2033 Symbol Error	88
7.1.4	TDK Invensense MPU-9250 Connection Error	89
7.1.5	MAX30102 Errors	89
7.1.6	Acquisition and Processing Global Buffer	90
7.1.7	EKG Processing	90
7.1.8	Calibration of TI HDC2010	90
7.1.9	TDK Invensense MPU-9250 Motion Tracking Algorithm	91
7.1.10	Blood Pressure Estimation	91
7.2	Concluding Remarks	91
A	PCB Design Material	93
A.1	Gerber Files	93
B	Reference	97
B.1	BLE Dispatcher Commands	97
B.2	BLE Dispatcher Status Codes	97
B.3	I2C Events	100
B.4	NV Events	100
B.5	BLE Dispatcher Response Messages	101
B.5.1	Profile Messages	101
B.5.2	EKG Messages	102
B.5.3	MAX30102 Messages	103
B.5.4	Other Messages	105
B.6	MAX30102 Events	106
B.7	EKG Events	108
B.8	Monitoring Task Events	109
C	MAX30102 Manager	111
D	EKG Manager	121
	Bibliography	129

List of Figures

21	Anatomy of the heart	6
22	Cardiac Cycle	8
23	Cardiac Conduction System	9
24	The Einthoven's Triangle.	12
25	EKG Waves	14
26	Standard 12-lead EKG	15
27	The hexaxial reference system.	16
28	Arteries expansion	19
31	QARDIO QARDIOCORE	22
32	CALM.	23
33	FITBIT Charge 3.	25
41	TEXAS INSTRUMENTS (TI) CC2640R2FRGZ	31
42	MCU section	33
43	GPIO section	34
44	Power section	36
45	RF analog front end options.	37
46	Analog front-end schematic.	38
47	Simulation of differential section.	40
48	Simulation of filter section.	42
49	Digital peripheral schematic.	43
410	Summary of case design.	47
51	Communication diagram	56
52	MAX30102 output	62
53	IR Butterworth Low Pass Filter (LPF)	64
54	IR Butterworth LPF	65
55	Threshold locations	67
56	Frequency Domain (FD) Digital Signal Processing (DSP)	69
57	Autocorrelation Function (ACF) of Infrared (IR) channel	71

58	Raw EKG	72
59	Spectrum of raw EKG	73
510	Comb Notch Filter	74
511	Comb filtered EKG	75
512	Final EKG	77
513	Android app rendering. Results window.	78
61	ProSim 3 waveform 1	80
62	ProSim 3 waveform 2	80
63	ProSim 3 waveform 3	81
64	ProSim 3 waveform 4	81
65	ProSim 3 waveform 5	82
66	ProSim 3 waveform 6	83
67	Faulty FIFO acquisition	84
71	REF2033 Symbol Error	88
72	MPU-9250 Connection Error	89
A1	Top Layer	93
A2	Bottom Layer	94
A3	Assembly Top Layer	94
A4	Assembly Bottom Layer	95

List of Tables

41	Vital EKG Specifications	29
42	Bessel LPF specification	41
43	MAX30102 LEDs specifications	44
61	PPG Results	85

List of Listings

C.0.1 MAX30102 Manager finite state machine.	111
D.0.1 EKG Manager finite state machine.	121

Acronyms

- ACF** Autocorrelation Function. xiv, 69–71
- ADC** Analog-to-Digital Converter. 23, 25, 29, 32, 41, 44, 55, 58, 59, 70, 72, 79, 89
- API** Application Public Interface. 55
- ATT** Attribute Profile. 50
- AV Node** atrioventricular node. 10, 14, 15
- BLE** Bluetooth Low Energy. 22–24, 26, 28, 29, 32, 37, 49–57, 59, 61, 76, 97, 100–106, 109
- Bluetooth SIG** Bluetooth Special Interest Group. 51
- BPF** Band Pass Filter. 68
- BPM** Beats per Minute. 66, 70
- CCS** Code Composer Studio. 55
- CO₂** Carbon Dioxide. 18
- DCT** Discrete Cosine Transform. 70
- DFT** Discrete Fourier Transform. 68, 69
- DSP** Digital Signal Processing. xiv, 30, 57, 61, 62, 64, 70, 83, 87, 90
- EKG** Electrocardiogram. ix, x, xiv, xvii, 2, 7, 10, 11, 13–17, 21–30, 35, 39, 41, 44, 45, 50, 54, 56–60, 70, 72–77, 79–83, 90, 91, 97–99, 101–103, 106–109, 121
- FD** Frequency Domain. xiv, 62, 68, 69, 84
- FFT** Fast Fourier Transform. 69, 70, 73, 79

- FIFO** First-In, First-Out. 42, 44, 57, 58, 83, 84, 89, 90, 98, 106
- FSK** Frequency-Shift Keying. 49
- FSM** Finite State Machine. 57–60, 107, 109
- GAP** Generic Access Profile. 51, 52, 55, 56
- GATT** Generic Attribute Profile. 50–52
- GPIO** General Purpose Input Output. 32, 34, 35
- Hb** Hemoglobin. 17, 18
- HCI** Host Controller Interface. 50, 53
- HHb** Deoxyhemoglobin. 18, 19
- HR** Heart Rate. 2, 20, 24, 28, 29, 44, 61, 62, 64, 66, 68–71, 84, 85, 91, 105
- I²C** Inter Integrated Circuit. 32, 35, 42, 44, 45, 55, 100
- IDE** Integrated Development Environment. 55
- IIR** Infinite Impulse Response. 63, 66, 68, 69, 72
- IR** Infrared. xiv, 18, 19, 24, 57, 62, 66, 68, 70, 83
- L2CAP** Logical Link Control and Adaptation Layer Protocol. 50, 54
- LA** Left Arm Electrode. 10, 11, 13, 29, 79
- LE** Low Energy. 50, 53
- LiPo** Lithium-Ion Polymer. 22, 23, 30, 35
- LL** Left Leg Electrode. 10, 11, 13
- LPF** Low Pass Filter. xiv, 41, 42, 63, 64, 68, 76
- MCU** Microcontroller. 30, 32
- MUX** Multiplexer. 32
- O₂** Oxygen Molecules. 17, 18
- O₂Hb** Oxyhemoglobin. 18–20

- OLGA** Organic Land Grid Array. ix, 44
- OpAmp** Operational Amplifier. 39–41
- PCB** Printed Circuit Board. x, 30, 37, 44–46, 87–89, 93
- PDU** Protocol Data Unit. 50, 53, 54, 59
- PHS** Personal Health System. iii, ix, x, 1–3, 24, 27, 91
- PHY** Physical Layer. 49, 50, 52–54
- PPG** Photoplethysmography. ix, x, 17, 20, 24–26, 29, 57, 59, 61, 71, 75, 79, 83, 84, 91, 97
- RA** Right Arm Electrode. 10, 11, 13, 29, 79
- RL** Right Leg Electrode. 10
- RTOS** Real-Time Operating System. 54, 55, 60, 61
- SA Node** sinoatrial node. 8, 10, 14, 16
- SCE** Sensor Controller Engine. 30, 32, 61
- SDK** Software Development Kit. 55
- SDU** Service Data Unit. 50
- SMT** Surface Mount Technology. 46
- SNR** Signal-To-Noise Ratio. 20, 25, 85
- SPI** Serial Peripheral Interface. 32, 42, 45, 55
- SpO₂** Peripheral Capillary Oxygen Saturation. iii, ix, 2, 17, 20, 24, 28, 29, 44, 61–63, 66–68, 83–85, 91
- TD** Time Domain. 62–64, 68, 79, 84
- TI** Texas Instruments. xiv, 29–32, 35, 37, 39, 41, 42, 44–46, 49, 50, 53–55, 57, 58, 60–62, 72, 87, 88, 90
- UART** Universal Asynchronous Receiver-Transmitter. 45, 46
- UUID** Universal Unique Identifier. 51, 52
- WLCSP** Wafer Level Chip Scale Package. 42

CHAPTER

1

Introduction

WEARABLE HEALTH DEVICES have been gaining a lot of attention in the last few years. Two main concepts which are critical to understand the reasons are **Personal Health System (PHS)** and **patient empowerment**.

A PHS, in its generic definition, is a device which is able to monitor the health status of an individual. Besides physical devices, it can also include smartphone application or a combination of both. The purpose of these devices are summarized below:

- enable continuous health monitoring over extended periods of time (days/weeks);
- favour domestic monitoring of vital parameters and decrease saturation of family medical practitioners and hospitals in developed countries;
- increase diffusion of vital signs tests in less developed countries by drastically reducing costs;
- help the recovery from a medical intervention or body injury;
- evaluate general health status of workers in hazardous situations and environments, such as firefighters, powerline technicians and military personnel.

The technology related to the monitoring of many vital signs has developed quickly in the last few years. Traditional testing methodologies require people to physically move to an hospital or laboratory to perform a test. This requires a considerable amount of time, which can be broadly split into the following categories:

- waiting lists - often waiting lists to perform routine tests which are included in the national healthcare are several months long due to hospitals and laboratories saturation [1];

- commuting time - large cities and rural areas inhabitants may experience long commutes to reach hospitals or laboratories;
- processing time - analyses require the intervention of specialized technicians which process the samples manually. As a consequence, results are available with a delay of several days.

Furthermore, many vital signs, such Heart Rate (HR), Peripheral Capillary Oxygen Saturation (SpO_2), blood pressure and Electrocardiogram (EKG) (strictly speaking EKG is not a vital sign but can be seen as an augmentation of the HR), benefit from a continuous monitoring over long periods of time. This is clearly very difficult to achieve using traditional test methodologies, despite a dynamic EKG technique, first introduced in 1961 by Norman J. Holter, is routinely used to partially overcome this problem [2]. Despite its domestic use, it remains a not ideal solution because the test is limited to 24 h and requires the positioning of a full set of electrodes and wires, which affects the daily routine.

The responsabilization of patient, or “patient empowerment” as it is often called, is a concept which has an impact on both developed and less developed countries.

In the first case, overcrowding of medical facilities is an actual problem which stems from the widespread availability of vital signs tests and their relative moderate costs, often coupled with accomodating medical practitioners. The delocalization of a few simpler tests would help to simplify the identification of more serious health problems early: the reduction of the amount of samples specialized technicians need to process would allow a faster publishing of results. Less developed countries face an opposite problem: the lack of structures where health tests can be performed and the relative prohibitively high costs of those make routine check ups not accessible to the vast majority of the population. Also in these cases, a mass produced consumer device would help to monitor general health status and take action when necessary.

The availability of reliable PHS considerably reduces prolonged hospitalization after treatment of body injuries and surgeries. In these cases, especially when the interventions are planned in advance, hospitalization has the only aim to monitor vital signs for an extended period of time to reduce as much as possible the onset of complications [3].

A further use case of wearables is the monitoring of laborers in hazardous fields, such as military personnel, powerline technicians and firefighters. In these cases, the availability of a PHS would help to reduce the redundancy of individuals performing the same task for security reasons and discover critical conditions before they can actually manifest in dangerous environments.

1.1 Requirements

Any wearable device should comply with a few common requirements in order to enter the market successfully. Among others:

- due to their inherent portable nature, wearables should be *zero-power* or *low-power* devices with a battery life as long as possible;
- wearables should be *reliable* enough to be used as a solid base for further medical tests; both false positives and non detected conditions should be minimized;
- *continuous operation* should be ensured; the idea of a PHS intrinsically requires continuous health monitoring;
- *seamless integration* with the daily routine of the user/patient is of foremost importance; a wearable health device should be worn as often as possible to enable the discovery of critical conditions and this is possible only if the device features an unobtrusive design, is comfortable and does not block natural body movements;
- data collection and consulting should be user friendly and not time and energy consuming; today's widespread diffusion of smart devices and fast and reliable wireless communication technologies pair nicely with this requirement and enable a zero-effort flow of information from the patient to medical staff;
- *aesthetic*, despite often regarded as a second level requirement by electronic designers and not strictly required to enable most of the benefits of wearable health devices, is important because it directly affects the willingness of the patient to wear the device throughout the day in public;
- the results of the monitoring should be available in *real-time* to minimize the delay of the treatment;
- *cost* is an important factor to consider, especially if the device is targeted to less developed countries.

An in-depth analysis of these requirements and others is carried out in [4].

CHAPTER 2

Vital Signs

THIS chapter intends to give a brief introduction about the principles behind non invasive automatic vital signs monitoring by exploring anatomy and physiology of the organs involved, along with benefits and limitations of the techniques currently in use.

2.1 The Human Heart

HEART related diseases account for a large percentage of the total deaths worldwide, according to the World Health Organization. Ischaemic heart disease and stroke have been the two biggest killers from 2000 to 2016, reaching almost 27% of the total deaths. For this reason, monitoring continuously the health of the heart is considered particularly important.

2.1.1 Anatomy

From a structural point of view, the heart can be described as a couple of muscular pumps with valves. Even though the two pumps share a few common structures, they are physiologically independent. Thus, it makes sense to talk about right and left heart.

Each half is composed by an atrium and a ventricle. The fundamental structure of the atria is alike, even though left and right cavities present substantial differences which are related to their role. The same holds for ventricles.

Right Atrium

The right atrium is one of the upper chambers of the heart and is positioned slightly below its left counterpart. It receives deoxygenated blood which returns from the systemic

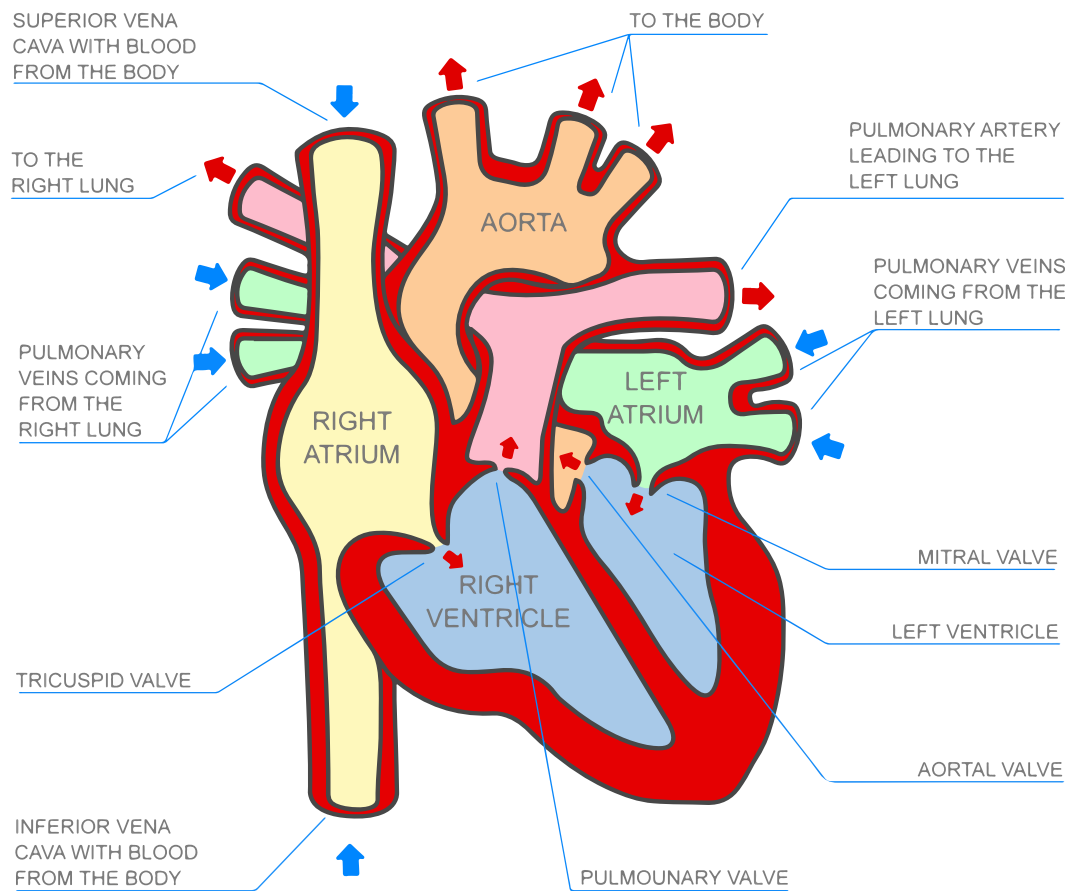


Figure 21: Anatomy of the heart.

circulation through the superior and inferior vena cava and the coronary sinus. The atria do not have valves at their inlets to favour the accumulation of blood in the cavities. The superior vena cava is located in the upper and posterior part of the right atrium; it receives venous return from the upper part of the body. The inferior vena cava receives instead venous blood from the inferior part of the body. Since it enters the right atrium at the lower right, back side of the heart, it has valves to prevent blood to flow down via gravity.

Right Ventricle

The right ventricle is one of the two large chambers of the heart positioned in the lower part. It receives deoxygenated blood from the right atrium through the tricuspid valve; the blood is pumped in the pulmonary artery via the pulmonary valve.

Left Atrium

The left atrium is located on the right posterior side of the heart and is separated from the right atrium by the atrial septum. The blood enters the left atrium through the pulmonary vein and is pumped into the left ventricle through the mitral valve.

Left Ventricle

The left ventricle is the fourth and last cavity of the heart. It is located in the bottom left portion of the heart and is separated from the right ventricle by the ventricular septum. It receive blood from the left atrium and pumps it in the aorta artery.

2.1.2 The Cardiac Cycle

The human blood circulation system can be divided into **pulmonary circulation** and **systemic circulation**. It is convenient to describe the cardiac cycle starting from the second phase of the systemic circulation. Deoxygenated blood returns from the body to the right heart and is accumulated in the right atrium. The right atrium pumps it in the right ventricle through the tricuspid valve. Then, the blood is pumped to the lungs through the pulmonary artery and at this point the pulmonary circulation starts. Functionally speaking, the sole presence of the ventricles would still ensure the separation of oxygenated and deoxygenated blood. The presence of the atria, though, increases the cardiac output of more than 75% by ensuring an uninterrupted venous flow to the heart and preventing circulatory inertia [5]. In the pulmonary circulation, deoxygenated blood flowing from the heart reaches the lungs where it is oxygenated. In the second phase, the blood returns to the heart flowing in the pulmonary vein. In the left part of the heart, the oxygenated blood is accumulated in the left atrium and pumped out in the aorta artery. The cardiac cycle concludes with the first phase of the systemic circulation: blood reaches the cells where the oxygen it carries is used. Despite having the same volume, the efficiency of the ventricles is different. The left ventricle is considerably thicker than the right one because it has to provide blood to the entire body whereas blood which is pumped by the right ventricle only reaches the lungs.

From the description of the cardiac cycle, four periodic contraction and relaxation phases can be indentified. A cardiac contraction is called a **systole**; a cardiac relaxation phase is called a **diastole**. Systoles and diastoles, along with all the phases of the cardiac cycle, can be clearly identified in a EKG.

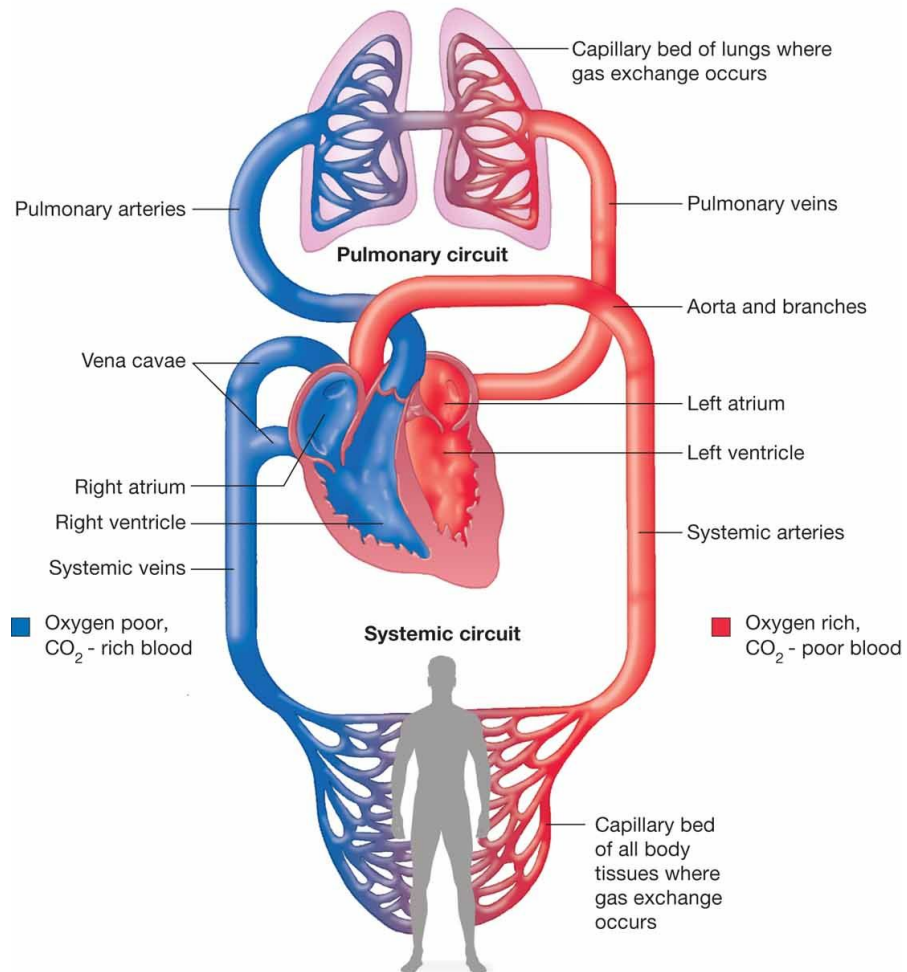


Figure 22: Cardiac cycle. Pulmonary and systemic circulation are highlighted.

2.1.3 The Cardiac Conduction System

The cardiac conduction system is responsible for the propagation of electrical signals which control systoles and diastoles.

The heart contraction originates from the **sinoatrial node (SA Node)**, which is located in the upper wall of the right atrium, close to the superior vena cava. It is effectively the pacemaker of the heart. The signal generated by the SA Node is directly responsible for the contraction of the atria (systolic phase). Its pace is regulated by autonomic nerves of the peripheral nervous system and can be increased by sympathetic

Electrical System of the Heart

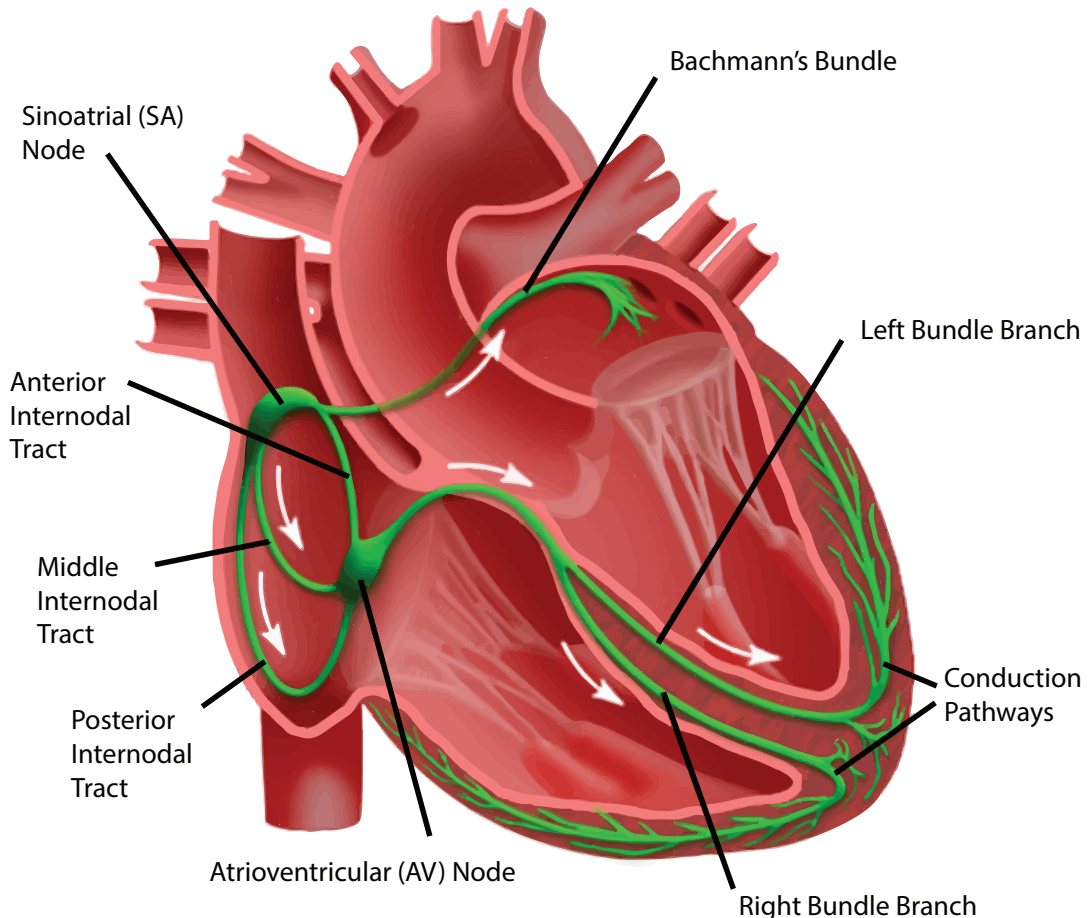


Figure 23: Cardiac Conduction System.

nerves or slowed down by parasympathetic ones.

The conduction of the electric impulse happens exploiting *cell depolarization*: the normally negative internal potential of cells of the heart walls, measured with respect to the exterior, undergoes depolarization when it becomes temporarily positive. A second phase, called *repolarization* follows and brings the internal potential back to its negative value [6].

The efficiency of a four chambers heart structure is mainly due to the delay between the atrial and ventricular systoles. The delay between the two contractions greatly reduces the inertia of the venous blood [5]. Since contractions and relaxations of the heart are electrically controlled, the signal which causes depolarization of the ventricles must be delayed with respect to the one responsible for depolarization of atria. The electrical

signal originated from the SA Node propagates to the **atrioventricular node (AV Node)**, which is located on the right bottom side of the interatrial septum and is responsible for the required delay. The AV Node acts as a relay, introducing delay which lies between 120 ms and 200 ms for healthy hearts[7].

The AV Node also acts as a backup pacemaker in case of failure of the SA Node, in particular preventing arrhythmias, such as **atrial fibrillation**, from spreading to the ventricles at dangerous rates.

From the AV Node, the electrical signal spreads to the ventricular walls. The **Bundle of His**, composed by two bundle branches, is responsible for propagating the electrical signal through the interventricular septum. Each branch serves a ventricle by feeding the signal to the **Purkinje fibers**.

To conclude this section and better understand the basics of EKG, it is important to remark that cardiac conduction is clearly split into two phases to delay the ventricular contraction with respect to atrial contraction; furthermore, during depolarization the electric potential increases while repolarization causes a decrease of the same quantity.

2.2 Electrocardiogram

THE EKG is a graph which shows the electrical activity of the heart. The cardiac muscle **T** cells behave like an electric dipole. As a consequence, given two points carefully chosen on the skin, it is possible to measure a potential difference which varies according to the activity of the heart. The modern EKG was developed by Willem Einthoven and Étienne-Jules Marey at the beginning of 20th century [8].

Before delving in the description of acquisition and processing of EKG signals, it is necessary to describe a standard EKG to understand what to expect and how to interpret the data.

2.2.1 Standard 12-lead EKG

When dealing with professional electrocardiographs, such as the ones listed in [9], it is necessary to understand the concepts of **electrode** and **lead**, as well as the importance the correct placement of the electrode to obtain a reliable EKG.

A 12-lead EKG requires 10 electrodes, positioned as detailed below [10]:

- Right Arm Electrode (RA) : anywhere between the right shoulder and the wrist;
- Left Arm Electrode (LA) : anywhere between the left shoulder and the wrist;
- Right Leg Electrode (RL) : anywhere above the right ankle and below the torso;
- Left Leg Electrode (LL) : anywhere above the left ankle and below the torso;

- V_1 : 4th intercostal space to the right of the sternum;
- V_2 : 4th intercostal space to the left of the sternum;
- V_3 : midway between V_2 and V_4 ;
- V_4 : 5th intercostal space at the midclavicular line;
- V_5 : anterior axillary line at the same level as V_4 ;
- V_6 : midaxillary line at the same level as V_4 and V_5 .

A **lead** is defined as an electric potential difference obtained by a suitable linear combination of electrodes. As already mentioned, a standard EKG is composed by 12 leads, or 12 different voltage signals. Leads are grouped in 3 categories: **limb leads** (unipolar limb leads), **augmented limb leads** (or bipolar limb leads) and **precordial leads** (also called unipolar chest leads).

Leads are obtained as follows.

Limb Leads

$$\begin{aligned} I &= LA - RA, \\ II &= LL - RA, \\ III &= LL - LA. \end{aligned} \tag{2.1}$$

Limb leads are bipolar leads because they are expressed as potential differences between two electrodes. Limb leads are the vertices of the **Einthoven's triangle**, shown in Fig. 24, which was invented and used by W. Einthoven.

The Einthoven's triangle has an important property: the sum of the voltages around any closed path around it equals zero. As a consequence, a virtual ground point can be derived from limb leads. A convenient choice leads to the definition of the **Wilson's central terminal** V_w as the average of the vertices of the triangle [11].

$$V_w = \frac{1}{3}(RA + LA + LL). \tag{2.2}$$

The Wilson's central terminal is a measure of the average potential of the body and can be taken as a reference for the unipolar leads.

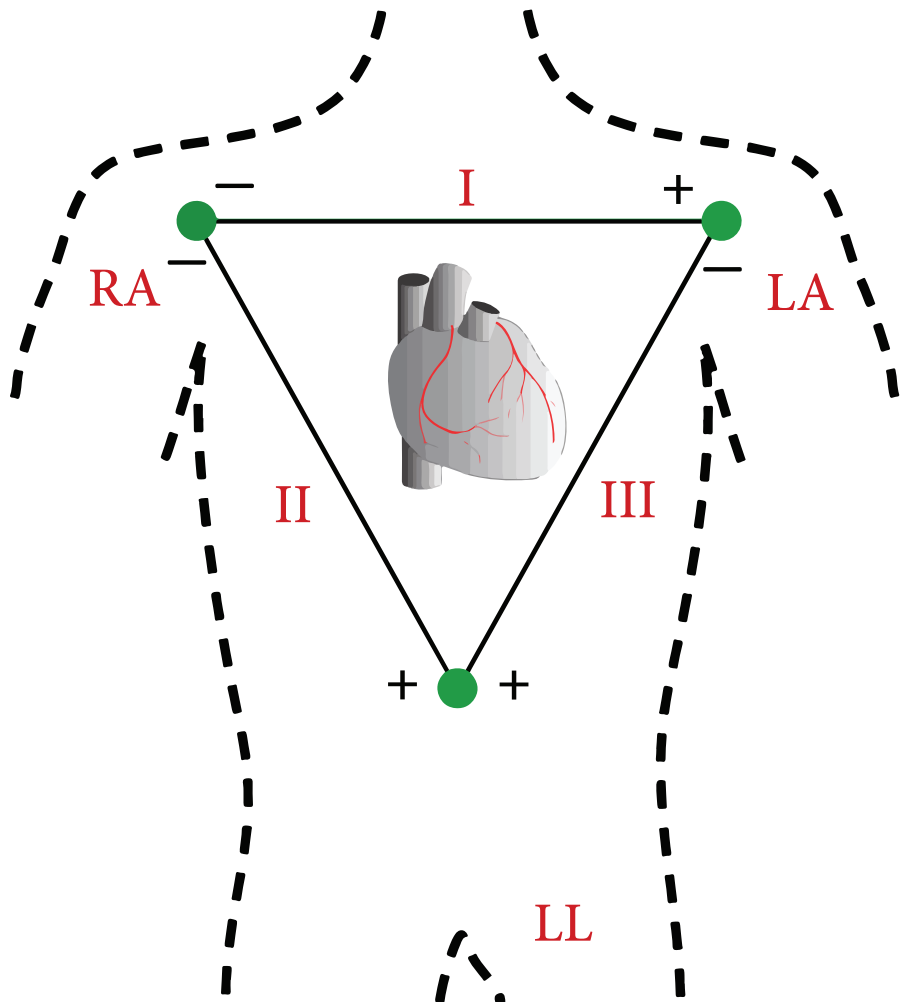


Figure 24: The Einthoven's Triangle.

Augmented Limb Leads

Augmented limb leads are obtained from the same electrodes which give limb leads. However, only one terminal at a time is used to define each of these leads, along with a reference terminal. Having defined the Wilson's central terminal, a natural choice would be to use it as a negative pole for unipolar limb leads. However, Joseph Goldberger showed that a voltage output 50% greater was possible by defining for each unipolar lead a central terminal formed by an average of the electrodes of Einthoven's triangle not used as positive pole [12]. This discovery motivated the renaming of unipolar limb leads to augmented limb leads.

Goldberger's central terminals are defined as follows:

$$\begin{aligned} V_G^R &= \frac{1}{2}(LA + LL), \\ V_G^L &= \frac{1}{2}(RA + LL), \\ V_G^F &= \frac{1}{2}(RA + LA), \end{aligned} \tag{2.3}$$

where R stands for right arm, L for left arm and F for left foot. The augmented limb leads are then given by 2.4.

$$\begin{aligned} aVR &= RA - V_G^R, \\ aVL &= LA - V_G^L, \\ aVF &= LL - V_G^F. \end{aligned} \tag{2.4}$$

Limb leads and augmented limb leads give informations about the electrical activity of the heart in the frontal (vertical) plane.

Precordial Leads

Precordial leads, also called unipolar chest leads, are given by the potential difference between the electrodes V_i and V_w . They provide insight on the activity of the heart in the transverse (horizontal) plane.

Lead Polarity

The electric potential of each lead can be associated with an axis whose direction and polarity depend on the position of the poles of the lead (unipolar and bipolar leads are considered composed by two poles in the following, one of which can be a reference terminal). By considering the direction of the lead axis and the activity of the heart, it is possible to predict the polarity of the EKG trace associated to each lead. Indeed [13]:

- a depolarization (repolarization) whose direction is aligned to lead axis produces a positive (negative) deflection;
- a depolarization (repolarization) whose direction is opposite to the lead axis produces a negative (positive) deflection;
- a depolarization or repolarization whose direction is orthogonal to the lead axis produces a isoelectric trace.

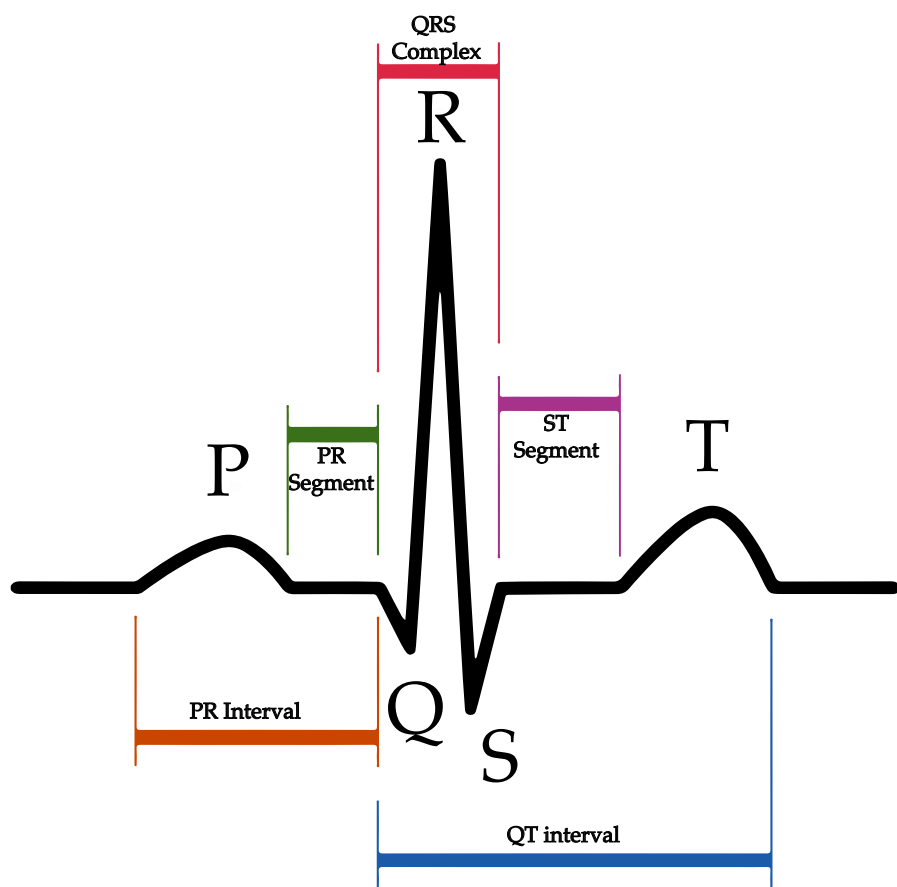


Figure 25: Waves of an EKG trace.

EKG Waves

A typical EKG trace is composed by periodic traces in which peaks and valleys can be identified (Fig. 25).

In order to better understand the meaning of each wave, the polarity should be ignored. Indeed, the polarity of each peak depends on the lead axis but the presence of a deflection and the time interval among deflections are the important points to be remembered to identify a cardiac condition.

A typical cardiac cycle begins with the generation of an electrical impulse in the SA Node. The signal flows at the same time to the AV Node and to the muscle cells in the atria. The **P wave** represents atrial depolarization which causes atrial systole.

The atrial contraction precedes the ventricular contraction as a consequence of the presence of the AV Node. When the electrical signal reaches the ventricles, it causes their depolarization. This phenomenon is typically the most visible and distinctive part of an EKG and is called **QRS complex**. It is formally composed by 3 close waves: a

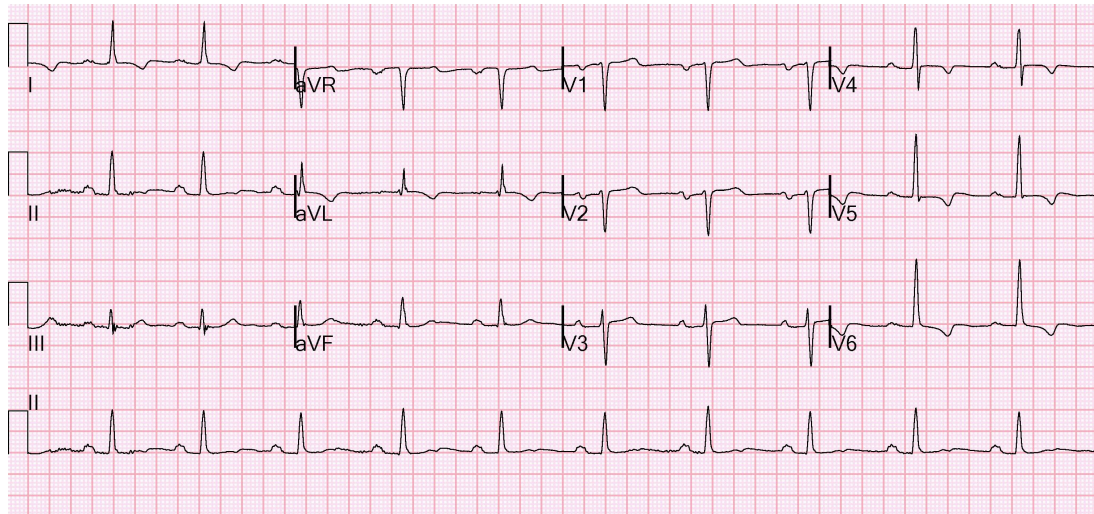


Figure 26: A standard 12-lead EKG. The polarity of the waves depend on the lead.

negative deflection (**Q wave**) which represents the depolarization of the interventricular septum, a positive peak (**R wave**) immediately followed by a new negative deflection (**S wave**). The amplitude of the R wave is typically much larger than the P wave because ventricular systole involves a much larger number of muscle cells than atrial systole. The QRS complex has a typical length which spans from 60 ms to 100 ms. During ventricular depolarization, atria repolarize. A deflection opposite to the P wave is superimposed to the QRS complex but cannot be appreciated due to the larger magnitude of the QRS complex.

The role of the AV Node is highlighted by the **PR interval**, which usually lasts between 120 ms and 200 ms.

The **ST segment** and **T wave** are usually analyzed together to gain insights about the repolarization of the ventricles. The ST segment is usually isoelectric because it represents the time delay between ventricle depolarization and repolarization in which no electrical signal propagates. The T wave should be asymmetric, with the first portion longer and less steep than the second portion.

Finally, the **QT interval** shows the activity of the ventricles in a full cardiac cycle.

A standard 12-Lead EKG is shown in Fig. 26. The QRS complex is positive in all the leads which have the positive pole in the left part of the body (left arm and left leg).

The Cardiac Axis

As a conclusion, the concept of **cardiac axis** and **hexaxial reference system** is presented with reference to Fig. 27.

Hexaxial Reference System

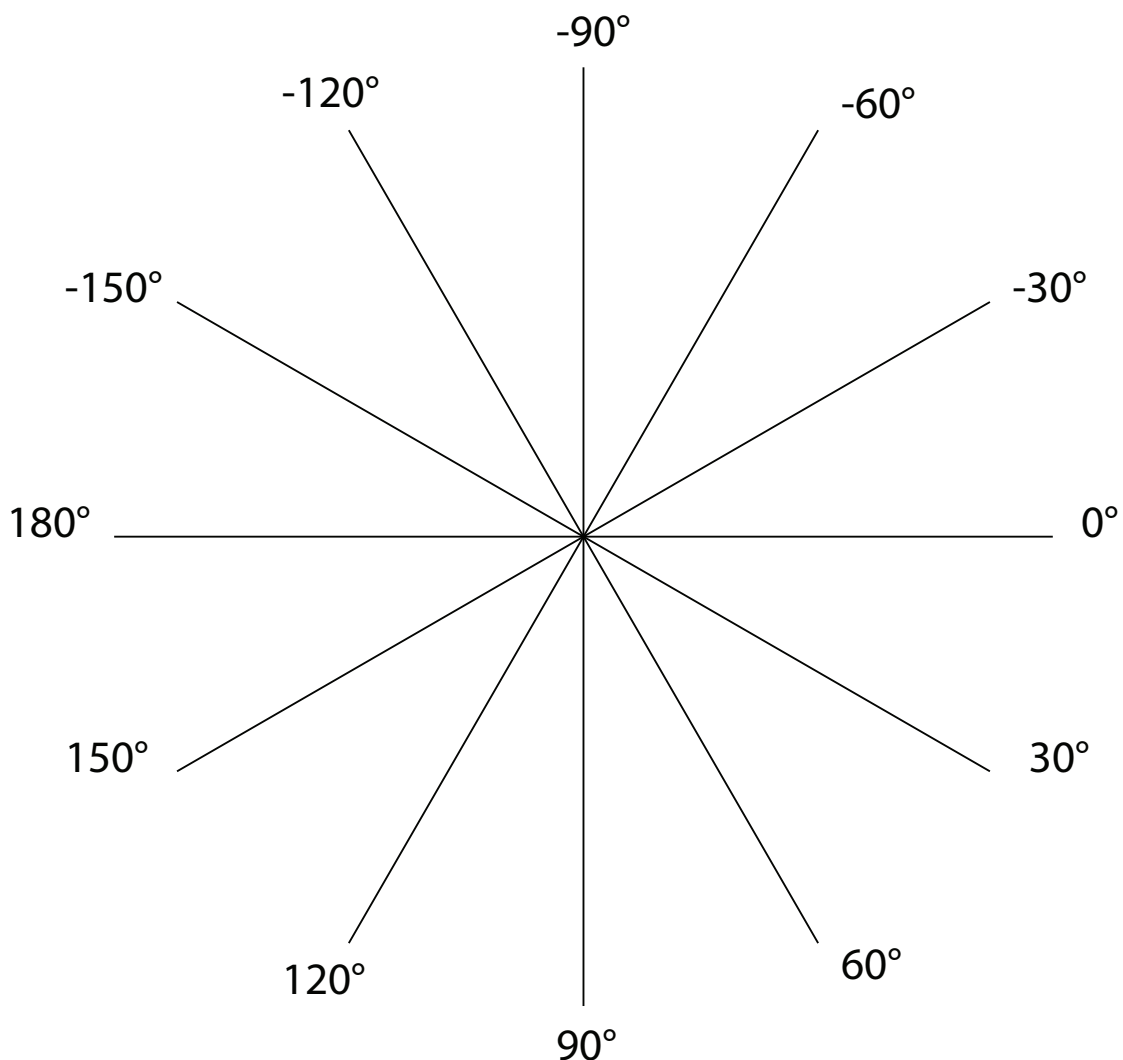


Figure 27: The hexaxial reference system.

Recalling 2.1.3, the direction of depolarization of atria and ventricles follows the electrical signal which originates in the SA Node. It is possible to understand the direction of this signal by constructing a hexaxial reference system: the 3 bipolar limb leads are moved in order to cross the Goldberger's reference terminal. The result is the diagram shown in Fig. 27. By inspecting a 12-lead EKG, it is possible to determine which lead has the largest QRS complex and associate a positive or negative angle to the lead

axis, according to Fig. 27. The cardiac axis normally lies between -30° and 90° . When the cardiac axis is lower than -30° we refer to left cardiac deviation; conversely, when the cardiac axis is greater than 90° we refer to right cardiac deviation.

2.2.2 I-lead EKG

The heart is a complex structure with many paths for electrical signals. A 12-lead EKG is required to get thorough insights about its health because each lead is able to show particular anomalies associated to signals which propagate in a direction orthogonal to the lead axis. Limiting the number of EKG leads clearly limits the amount of information which is possible to extract.

The reduction of the number of electrodes is required to make the EKG portable and wearable-friendly. The minimum number of electrodes clearly cannot be lower than two, since a lead is a differential signal. The minimization of electrodes automatically excludes augmented limb leads because at least two poles are required for the definition of a central reference terminal, beside the positive pole used for the specific lead. Chest leads V_1 and V_2 are a possible choice for a single lead EKG and are usually exploited by chest straps devices; an alternative choice is any of the bipolar leads, keeping in mind that positioning a leg electrode is surely less convenient for the user than using electrodes positioned on the arms. At this point, the most obvious choice is Lead-I, with electrodes positioned on the left and right arms.

2.3 Heart Rate and Blood Oxygen Level

ESTIMATION of SpO_2 is of utmost importance to evaluate general health status. Indeed, it has been regarded as a 5th vital sign by many authors [14].

The technique routinely used for its estimation, which dates back to 1972, was invented by Takuo Aoyagi, a Japanese bioengineer [15]. Its importance lies in its non invasive nature, real time availability of results and possibility to test many patients quickly without replacing consumables.

2.3.1 Theory of Photoplethysmography

Plethysmography is a generic term which refers to a technique to measure changes in volume of organs or whole body. It is commonly used to estimate pulmonary capacity exploiting Boyle's Law [16].

Photoplethysmography (PPG) is derived from classic Plethysmography but relies on the detection of changes in light absorbances to estimate changes in volume.

During systemic circulation, oxygenated blood is pumped from the heart to the body periphery through the arteries (2.1.2). Oxygen Molecules (O_2) carried by Hemoglobin

(Hb) are provided to all body cells and Carbon Dioxide (CO_2) is picked up in return. Oxygenated Hb is commonly referred as Oxyhemoglobin (O_2Hb) while O_2 -free Hb is called Deoxyhemoglobin (HHb).

O_2Hb has the property of absorbing more Infrared (IR) light (850 nm to 940 nm) than RED light (635 nm to 700 nm). Remarkably, HHb features the opposite property, absorbing more RED light than IR light.

Classic Lambert-Beer Law relates the absorption of light in a solution to the physical properties of the solution:

$$A = -\ln \left(\frac{I_{out}}{I_{in}} \right) = \ell \sum_{i=1}^N \varepsilon_i c_i. \quad (2.5)$$

In practice, for N attenuating species in case of **uniform attenuation**, the absorbance A depends on the arterial length of light through the sample ℓ , the concentration c and the molar attenuation coefficient ε . The absorption clearly depends on the amount of light provided to the solution (I_{in}) and the amount of light which is transmitted through the solution (I_{out} , which refers to both reflected and transmitted light).

Since O_2 is transported by O_2Hb in arterial blood, its detection is related to the detection of O_2Hb . Given the different light absorption properties of O_2Hb and HHb, a convenient quantity to define is the **RED:IR modulation ratio R** :

$$R = \frac{A_{RED}}{A_{IR}} \quad (2.6)$$

where A_{RED} is the absorption of RED light and A_{IR} the absorption of IR light.

When a systemic circulation cycle starts with the contraction of the left ventricle, the blood pressure has a sudden increase (systolic blood pressure). As a consequence, the arteries undergo a cyclic expansion and contraction which follow the cardiac cycle. Conversely, veins are much stiffer and their diameter stays fairly constant. The concept is illustrated in Fig. 28.

This fact can be exploited to ease the computation of R . Indeed, a tissue bed can be considered composed of a pulsatile part, that is essentially composed by arterial blood which changes periodically with cardiac cycle, and a constant non-pulsatile part (venous blood, fat, skin, bones) [17]. By modifying Eq. 2.6 with time derivatives of absorption, the effect of non-pulsatile tissue components can be excluded obtaining

$$R = \frac{\frac{\partial A_{RED}}{\partial t}}{\frac{\partial A_{IR}}{\partial t}} \quad (2.7)$$

PPG Signal Components

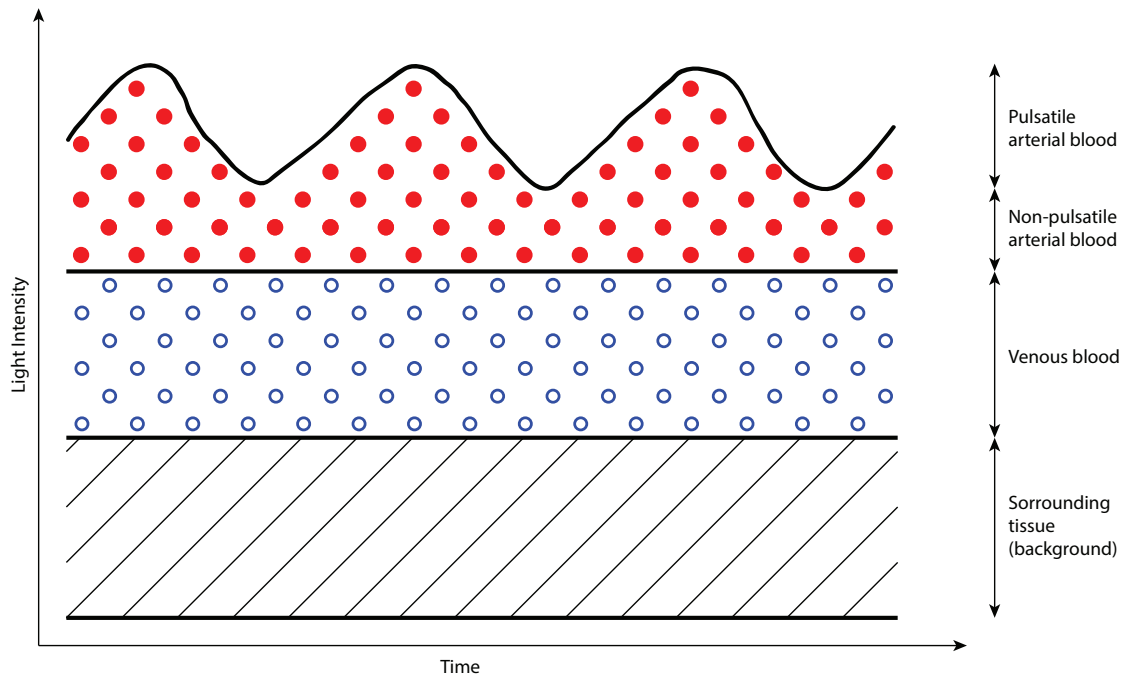


Figure 28: Arteries and veins behaviour during a cardiac cycle.

and, by using the first equality of Eq. 2.5,

$$R = \frac{\frac{\partial}{\partial t} \left[-\ln \left(\frac{I_{out}(t)}{I_{in}} \right) \right]_{RED}}{\frac{\partial}{\partial t} \left[-\ln \left(\frac{I_{out}(t)}{I_{in}} \right) \right]_{IR}}. \quad (2.8)$$

By considering that $I_{out}(t)$ is time dependent (because of the presence of the pulsatile component) and I_{in} is not, we can finally obtain:

$$R = \left[\frac{I_{out}^{ac}}{I_{out}^{dc}} \right]_{RED} \cdot \left[\frac{I_{out}^{ac}}{I_{out}^{dc}} \right]_{IR}^{-1}, \quad (2.9)$$

where ac and dc refer to pulsatile and non-pulsatile components, respectively. Both channels are expected to present a behaviour in time similar to the envelope of Fig. 28.

The RED:IR modulation ratio is expected to increase for low blood oxygen saturation. Indeed, in this condition the amount of O_2Hb is low with respect to HHb; since O_2Hb absorbs more IR and less RED light, the fraction in 2.9 increases.

At this point, it should be noted that the choice of the body location for a PPG measurement is extremely important to obtain a reliable result. Indeed, ear lobes and fingertips are normally considered ideal spots because they are well blood-perfused tissues. Recently, the forehead has been indicated as a potential third body location for PPG measurements [18].

A further important point to be discussed is the choice between *transmittance* and *reflectance* PPG techniques. From the photo-detector point of view, as a matter of fact it is not particularly important if the device has light source and photo-detector on the same side (surface device) or on opposite sides of a tissue bed if their distance is sufficiently large. In case of transmittance based devices, the separation is guaranteed by the thickness of the finger or ear lobe; in case of reflectance based devices, the required separation is ensured by considering that the mean-free-path of photons in a tissue bed is approximately 1 mm and this is sufficient for photons to lose the history of their past [18].

Once that R has been computed according to Eq. 2.9, it is necessary to make one final step to obtain a SpO_2 value.

If the second equality of Eq. 2.5 is used in Eq. 2.7, the following expression can be derived:

$$R = \left[(S\varepsilon_a + (1 - S)\varepsilon_v) \cdot \frac{\partial(c_a\ell_a)}{\partial t} \right]_{RED} \cdot \left[(S\varepsilon_a + (1 - S)\varepsilon_v) \cdot \frac{\partial(c_a\ell_a)}{\partial t} \right]_{IR}^{-1} \quad (2.10)$$

where S is the true SpO_2 value (the unknown, ranging from 0 to 1) and the only time dependent variable are the concentration c_a of O_2Hb and ℓ_a . The product $c_v\ell_v \simeq 0$ as a consequence of the greater stiffness of the veins.

By coupling Eq 2.9 with 2.10 and solving for S , the SpO_2 value can be estimated [18]. Practically, c_a and ℓ_a are hard to estimate. As such, off-the-shelf devices, which integrate both light sources and the photodetector, are often already characterized exploiting a relation such as Eq. 2.11:

$$S = \frac{k_1 + k_2 R}{k_3 + k_4 R}, \quad (2.11)$$

where eventually one or more constants k_i can be zero.

Finally, the HR comes for free from SpO_2 estimation. Indeed, a clean heart rate is required to evaluate R and HR estimation is simply a matter of calculating the main frequency component of a PPG channel. The choice of the wavelength at which this computation is performed depends on the Signal-To-Noise Ratio (SNR) of the channels which, ultimately, links to the quality of the light source and photo-detector.

CHAPTER 3

State of the Art

HERE are many systems already on the market which promise to perform monitoring of vital signs. This chapter presents a review of a few examples, along with positive and negative sides of each device. As evident from Chapter 2, the location of the device on the body is a core decision to be made during the very first stages of development of a vital signs monitoring device. Currently available systems can be roughly divided in three categories:

- chest straps;
- wrist trackers;
- finger clips.

3.1 Chest Straps

CHEST straps are devices which normally focus on acquiring a single lead EKG signal close to the heart. The device is placed on the chest and the two electrodes are located on opposite sides of the heart. The lead is also non standard, because V_1 and V_2 are used together to obtain a bipolar lead instead of being referred to a central reference terminal.

3.1.1 QARDIOCORE

A first example of chest straps comes from QARDIO [19] QARDIOCORE (Fig. 31).

Qardiocore is able to perform continuous single lead EKG signal measurements and monitor heart rate, respiratory rate, skin temperature and activity. Furthermore, an indication of the heart rate variability is also provided.



Figure 31: QARDIO QARDIOCORE chest strap.

The device is equipped with Bluetooth Low Energy (BLE) version 4.0 to enable wireless communication with iOS devices; an app is available to display EKG waveforms and interact with the device.

From the hardware point of view, Qardiocore performs 16 bit acquisitions at a frequency of 600 Sa s^{-1} . The frequency response is claimed to be 0.05 Hz to 40 Hz. The Lithium-Ion Polymer (LiPo) battery is able to power the device up to one day without recharging. Finally, Qardiocore weighs 130 g including the battery and is dust tight and water jets resistant (IP65).



Figure 32: CALM chest strap.

Due to its positioning on the body Qardiocore lacks the ability to monitor arterial blood oxygen level. Furthermore, its current price is €499 which is quite above the average for similar devices. Finally, it lacks compatibility with Android smartphones.

3.1.2 CALM.

CALM. [20] is another example of chest straps (Fig. 32). CALM. is a simpler device which only performs single lead EKG continuous monitoring. Also this device uses V₁ and V₂ electrodes together to obtain a non-standard lead. The electrodes are disposable gel pads which must be purchased separately (first set included).

It features a 12 bit, 250 Sa s⁻¹ Analog-to-Digital Converter (ADC), BLE version 4.0 connectivity and smartphone apps are available for both Android and iOS devices. It is equipped with a 200 mA h LiPo battery which ensures up to 72 h of battery life. Furthermore, it has a 3-axis accelerometer and the sensor device weighs only 14 g.

Finally it is splash resistant and the retail price is set to \$120.

3.1.3 Discussion

Chest straps devices have the advantage of not requiring user interaction to perform measurements. However, the presence of the chest belt is probably not enough to ensure the stability of the device, which is extremely important to get reliable EKG acquisitions. A further downside of chest straps devices is the inability to provide informations about SpO₂; besides being an important indicator by itself, it is also a requirement to perform cuff-free blood pressure checks.

3.2 Wrist Trackers

ACTIVITY trackers are devices whose core functionality is to analyze motion data and recognize common daily activities, such as walking and running and provide indications about performances, such as number of steps, pace and excessive sedentary lifestyle. A few trackers feature also HR monitoring.

3.2.1 FITBIT

FITBIT [21] is a US based company which sells a wide range of smartwatches and trackers. These devices should not be confused with a PHS. Indeed they are not able to provide EKG and SpO₂ measurements and are only intended to monitor the lifestyle. The latest FITBIT activity tracker, featuring HR monitoring, is shown in Fig. 33.

They are typically well connected, feature BLE and well designed smartphone apps to record data. As they are intended to be always worn, they are waterproof and are ideal to provide statistics about daily workouts. These devices feature a battery life which can last up to one week, due to their simpler low power design.

HR is measured using GREEN leds to detect peak blood pressure. Studies have shown the superiority of green light (530 nm) for measurements on the wrist, where RED and IR leds exhibit poor performances [22]. Clearly, a single led measurement does not allow to compute the RED:IR modulation ratio from which SpO₂ can be derived.

3.3 Finger Clips

FINGER clips deserve a mention in this chapter because they are an example of the widespread use of PPG to measure HR and SpO₂. Clearly, they are not wearable devices and their use is limited to hospitals and clinics. The challenge which all other devices presented in this chapter face is to keep up with the accuracy of finger clips.



Figure 33: FITBIT Charge 3.

Indeed, their design minimize the amount of external light which hits the photodetector, greatly increasing the SNR. Typical designs exhibit leds on one side and photodetector on the other side. As such, they perform transmittance based PPG measurements. One of this devices has been used for the validation of VITAL EKG. More information are included in Chapter 6.

3.4 ECG Sensor

THE last part of this chapter is devoted to the description of **ECG Sensor**, a device developed at Neuronica Lab, Politecnico di Torino. VITAL EKG can be considered a spin-off evolution of ECG Sensor.

ECG Sensor is a bracelet device which can perform EKG bipolar leads measures. One electrode is positioned on the bottom side and the other on the top side. The analog differential signal is processed to remove noise from the grid and muscular noise. The analog to digital conversion is performed at 10 bit with a rate of 1 kSa s^{-1} , using the ADC integrated in the MSP430 microcontroller. Data are sent to a smartphone device using Bluetooth technology. This device features a few problems which led to the development of VITAL EKG.

- Analog filtering is too aggressive, causing a non isoelectric ST segment.

- The Bluetooth module is external and data are sent to it using UART protocol. A few recently developed microcontrollers integrate BLE onboard, enabling greater power savings.
- The digital processing is not performed on board but after transmission to the smartphone. This leads to Bluetooth communication even though no critical heart conditions are detected. Since the RF section is the single most power hungry part of the board, implementing on board processing could strongly influence the battery life.
- EKG is not enough to gain sufficient insight on vital signs. Other biometrics signals, such as PPG, skin temperature and humidity and activity, could enable more advanced techniques to estimate general health conditions of the user.

Detailed informations about ECG Sensor can be found in [23]. A feasibility study on VITAL EKG, based on the ECG Sensor, is detailed in [24].

CHAPTER 4

Vital EKG

AFTER a brief review of the state of the art, including commercial devices, crowdfunded projects and literature in Chapter 3, a device which can be considered a complete PHS has not been found. This chapter provides detailed information about the design of such a system, both from hardware and firmware points of view.

Requirements and specifications of the VITAL EKG are highlighted first; then, the several stages of development of the product are described.

4.1 Requirements

BEING a wearable device, VITAL EKG must at least be compliant with the requirements of this class of devices. The general requirements of a PHS, as described in detail in Chapter 1, are reported here for convenience.

1. Zero-power or low-power;
2. Reliability;
3. Continuous operation;
4. Real-time processing;
5. Seamless integration with the daily routine of the user;
6. Zero-effort flow of information from the patient to medical staff;
7. Aesthetically pleasant;

8. Cost-effective.

To these general requirements, the following VITAL EKG specific design goals have been added and considered to guide the development of the product.

- i. *LEAD I* EKG acquisition;
- ii. SpO₂ meter;
- iii. HR meter;
- iv. Activity tracking;
- v. Skin temperature and humidity indications;
- vi. Systolic blood pressure indication;
- vii. On-board data storage;
- viii. BLE connectivity;
- ix. Wrist-band/watch form factor;
- x. Rechargeable battery.

At this point, an important remark is necessary. Requirements 3, i, ii, ix are impossible to be satisfied at the same time with current technology.

Requirement i dictates a design able to perform a differential measurement and, thus, the presence of 2 electrodes positioned on opposite sides of the heart. Even though one of the augmented limb leads were chosen for the the measurement (also misleadingly called single ended leads), the reader should note that more than one electrode would still be required to define Golberger's central terminals or Wilson's central terminal (2.3 and 2.4).

Moreover, requirement ii (and 2) suggests that only finger tips or ear lobes should be used for SpO₂ measurement. The incompatibility with requirement ix is thus evident.

The solution commonly adopted is to neglect requirements ii and ix and design a chest strap device, such as the ones already described in 3.1.1 and 3.1.2.

The solution proposed here takes a different direction: requirement 3 is partly neglected and replaced with the following:

- I. *LEAD I* EKG acquisition on request;
- II. SpO₂ meter on request;
- III. HR meter on request;

Table 41: Technical specification summary of VITAL EKG.

Item	Value
Case Size	50 mm x 30 mm x 20 mm
BLE	v4.2
Working Voltage	3.3 V
Battery Voltage Range	3.4 V to 4.0 V
Battery Capacity	300 mA h
Recharge Method	Micro-USB cable
Acquisitions with a single charge	min 3000
Acquisition Time	11 s
ADC Sampling Frequency	500 Sa s ⁻¹
Effective Sample Size	14 bit
MAX30102 Effective Sampling Frequency	50 Sa s ⁻¹
MAX30102 Sample Size	18 bit, 2 channels

IV. Continuous activity tracking;

V. Continuous skin temperature and humidity indications.

VITAL EKG is designed to be a wrist-band product which performs *LEAD I* EKG, SpO₂ and HR measurements **upon request**. The user interacts with VITAL EKG using its smartphone (or BLE enabled device) to initiate the measurement; two fingers of the right hand (left hand) must be placed on the device while it is worn on left wrist (right wrist). One finger is used to perform PPG while the other serves as RA (LA) electrode.

4.2 Specifications

After compiling the general requirements, detailed technical specifications of VITAL EKG have been clearly stated and are summarized in Table 41. This section provides a general summary of hardware and firmware capabilities of the device; for a more thorough discussion the reader is invited to proceed to 4.3 and 5, respectively.

The power consumption of VITAL EKG has been measured in worst case conditions, that is while performing concurrent PPG and EKG acquisitions, sustaining a Bluetooth connection and with continuous monitoring enabled. The analog front-end was powered on, as well as Texas Instruments (TI) HDC2010, TDK Invensense MPU-9250 and Maxim Integrated MAX30102. The current draw was 10 mA with a power supply voltage for most components of 3.3 V; the voltage regulator MAX1759, the reference REF2033 and

the fuel gauge MAX17048 are powered from the battery instead but all these components feature quiescent currents lower than 50 mA.

A LiPo battery with nominal voltage of 3.7 V and 300 mA h capacity allows to perform an ideal maximum of 6000 acquisitions, according to Eq. 4.1.

$$N = \frac{3.7 \text{ V} \cdot 300 \text{ mA} \cdot 3600 \text{ s}}{3.3 \text{ V} \cdot 10 \text{ mA} \cdot 3600 \text{ s}} = 6054. \quad (4.1)$$

Clearly, continuous reading of temperature and humidity, as well activity tracking and battery monitoring and consume battery power even when the user is not performing an acquisition. The activity tracking potentially allows to monitor when the device is worn, eventually turning all the equipment in low-power standby mode. Thus, a conservative maximum number of acquisitions with a single battery charge is expected to be around 3000.

The ECG Watch, which is the reference device which drove the development of VITAL EKG, allowed roughly 400 acquisitions with the same battery and was only able to perform EKG.

4.3 Hardware

THIS section provides detailed informations about hardware design, including circuit operation and Printed Circuit Board (PCB) layout.

4.3.1 Circuit Design

The circuit design can be organized in several sections, conceptually independent: microcontroller, power, RF, analog front-end, digital peripherals.

Microcontroller

The choice of Microcontroller (MCU) is critical from many points of view. Being VITAL EKG a product with many peripherals, all of which need Digital Signal Processing (DSP) a fast 32 bit MCU is mandatory. Nonetheless, a power hungry MCU would invalidate requirement 1 and costs must be kept under control to obey 8.

The TI CC2640R2FRGZ has been chosen for VITAL EKG. A system block diagram is shown in Fig. 41.

TI CC2640R2FRGZ exhibits the following characteristics, among others [25]:

- ARM® CORTEX® M3;
- Ultra-Low Power Sensor Controller Engine (SCE) with 16 bit architecture;

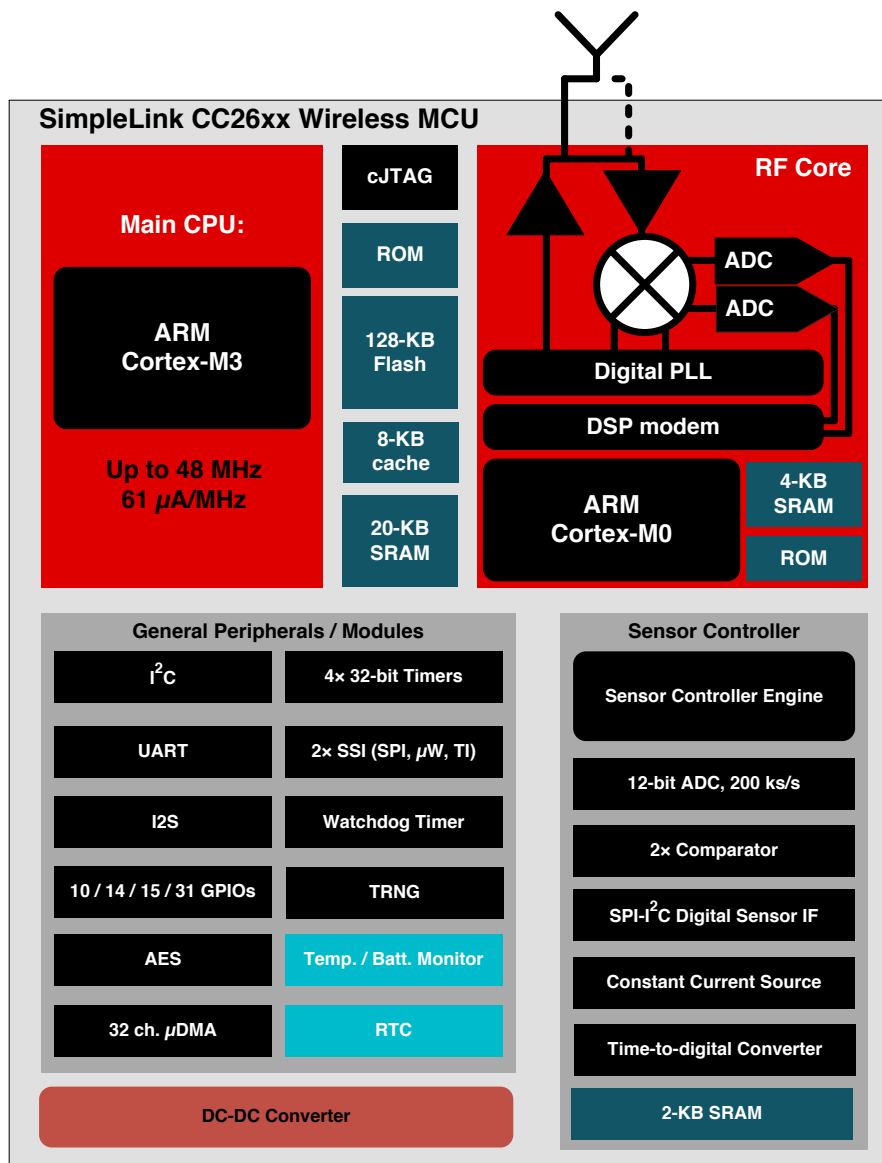


Figure 41: TI CC2640R2FRGZ system block diagram (Copyright ©2016, Texas Instruments Incorporated).

- Up to 48 MHz clock speed;
- 275 kB of Non-Volatile Memory;
- 128 kB of In-System Programmable Flash;
- 20 kB of Ultra-Low Leakage SRAM;

- 8 kB of Cache, which can be repurposed as RAM;
- 2 kB of Ultra-Low Leakage SRAM dedicated to Sensor Controller Engine which can be repurposed as ARM® CORTEX® M3 RAM;
- 2-Pin cJTAG and JTAG Debugging;
- 31 General Purpose Input Output (GPIO);
- 12 bit, 200 kSa s^{-1} ADC with 8 channels analog input Multiplexer (MUX);
- Inter Integrated Circuit (I^2C) driver;
- Serial Peripheral Interface (SPI) driver.

TI also specifies the following power consumption specifications:

- Normal operation power supply voltage range from 1.8 V to 3.8 V;
- Active-Mode BLE RX: 5.9 mA;
- Active-Mode BLE TX at 0 dB: 6.1 mA;
- Active-Mode BLE TX at 5 dB: 9.1 mA;
- Active-Mode MCU: $61 \mu\text{A MHz}^{-1}$;
- Active-Mode SCE: $0.4 \text{ mA} + 8.2 \mu\text{A MHz}^{-1}$;
- Standby-Mode (RAM/CPU Retention): 1.1 μA ;
- Shutdown-Mode (Wake Up on External Events): 100 nA.

TI CC2640R2FRGZ only requires few external components. Power supply traces require decoupling and bulk capacitors; a ferrite bead is also used to suppress high frequency noise. Two crystals have been used in VITAL EKG design. Schematic pages about TI CC2640R2FRGZ are reported in Fig. 42 and 43.

The 24 MHz crystal is required for BLE operations and is internally doubled to 48 MHz. ARM® CORTEX® M3 has a software selectable internal capacitor array to better tune BLE carrier frequency. Thus, external capacitors are not required for correct operation[26].

The 32 kHz crystal is technically speaking optional; however, a high accuracy crystal (better than $\pm 500 \text{ ppm}$) is required if BLE connection has to be maintained while the ARM® CORTEX® M3 is in standby mode. Hence, to enable the maximum power savings (1) while acquisitions are not performed (I, II, III), it has been added to the design.

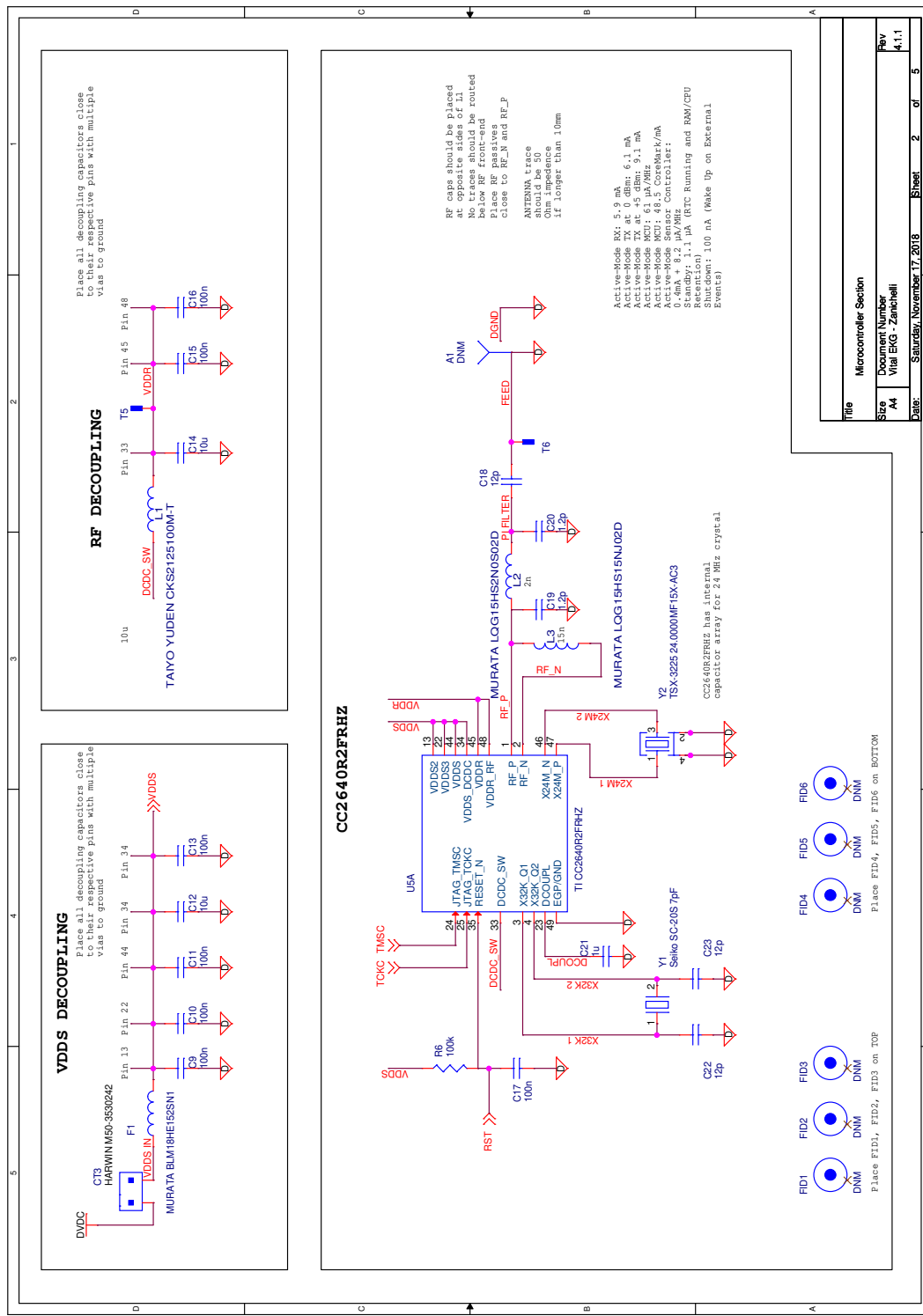


Figure 42: VITAL EKG schematic, microcontroller section.

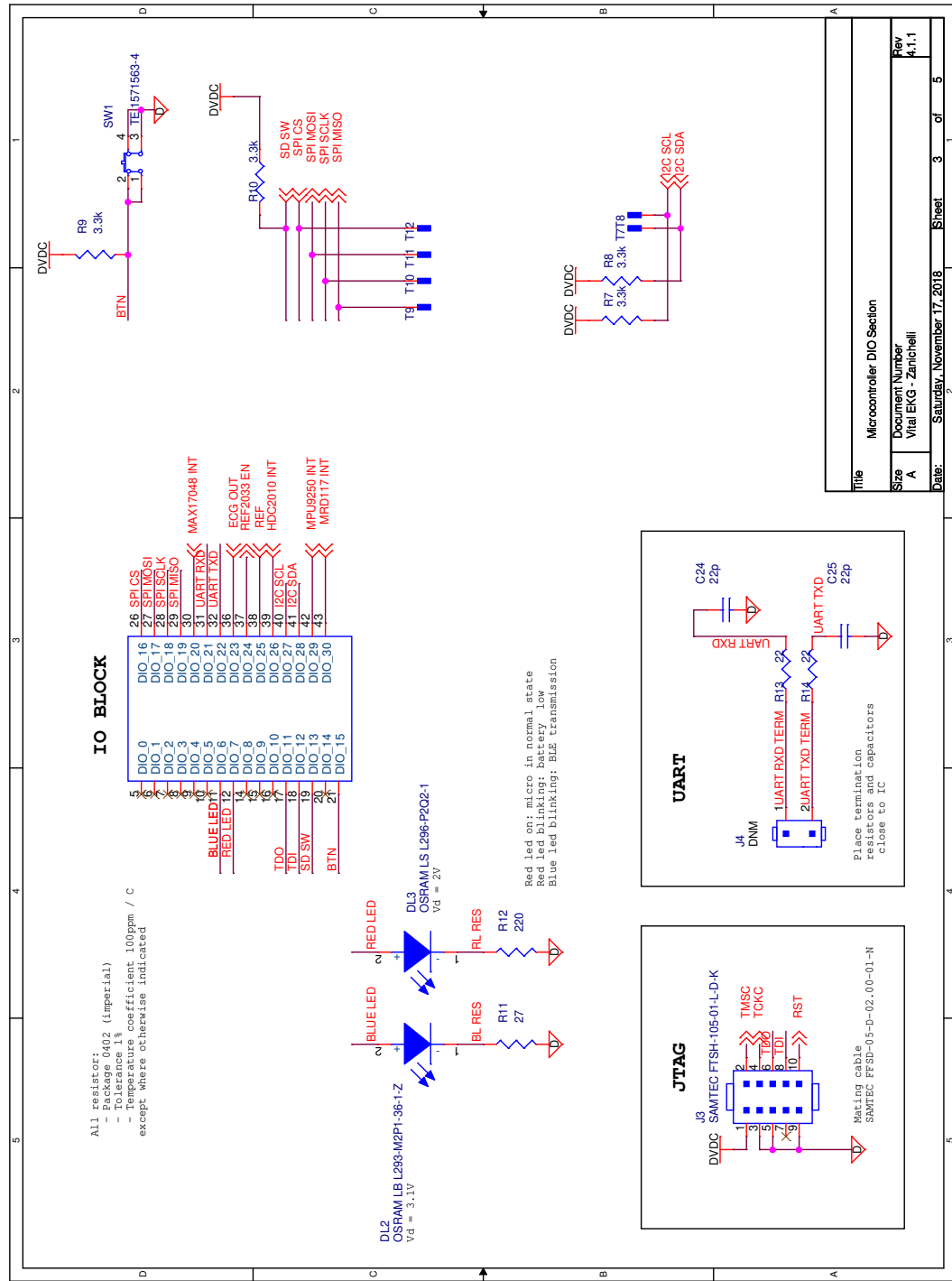


Figure 43: VITAL EKG schematic, microcontroller GPIO section.

Power

Given the complexity of VITAL EKG, a rechargeable LiPo battery has been chosen as power source. This choice obviously requires circuitry to recharge it, as well as to monitor the voltage output and provide the user an estimation of the state of charge. Furthermore, LiPo cells typically require protection circuits to avoid permanent damage to the battery. The schematic of the power section is shown in Fig. 44.

A micro USB connector has been selected to recharge the LiPo battery. MAX1555 by Maxim Integrated [27] allows to safely recharge a single cell LiPo. Its input voltage ranges from 3.7 V to 6.0 V; typical output current is 100 mA, considering that the device itself is powered by USB connector during a recharge. Finally, the Power OK (POK) output is low when the battery is recharging. This fact has been exploited to bias a green LED, which turns on in this condition. A careful evaluation of the prototype during testing underlined that LED colors should be made compliant with CE certification in a future revision. Thus, it would be best to connect the green LED to the TI CC2640R2FRGZ to allow multiple informations to be delivered through blink patterns.

Battery voltage needs to be regulated to power the digital circuitry. This would not be strictly required for TI CC2640R2FRGZ because it has its own internal regulator. MAX1759 by Maxim Integrated [28] provides voltage regulation using a Buck/Boost charge pump. The output voltage is programmable and it has been set to 3.3 V. Output current is guaranteed to be at least 100 mA. Quiescent supply current is 50 μ A. Finally, only 3 ceramic capacitors are required, making it an ideal choice for spaced constrained designs.

The analog front end is powered by REF2033 by TI [29]. It conveniently provides both a 3.3 V and 1.65 V voltage references, which is ideal for single supply systems. Input voltage is taken directly from the battery; outputs can be disabled (high impedance) to minimize the power consumption (1) using EN input, directly connected to a GPIO. This feature is really important because the analog section can be completely turned off most of the time, given that VITAL EKG is designed to provide only on-demand EKG measurements.

The last component of the power section is MAX17048 by Maxim Integrated [30], which is a tiny current fuel gauge for LiPo cells. It provides battery voltage measurements with a precision of ± 7.5 mV as well the state of charge, which is estimated using a proprietary algorithm (ModelGauge™[31]). It conveniently provides I²C interface and separate (configurable) interrupt pin, which has been connected to TI CC2640R2FRGZ GPIO.

RF

TI CC2640R2FRGZ integrates a dedicated ARM® CORTEX® M0 processor to manage time critical aspects of RF communication. The RF Core must be completed with an analog RF

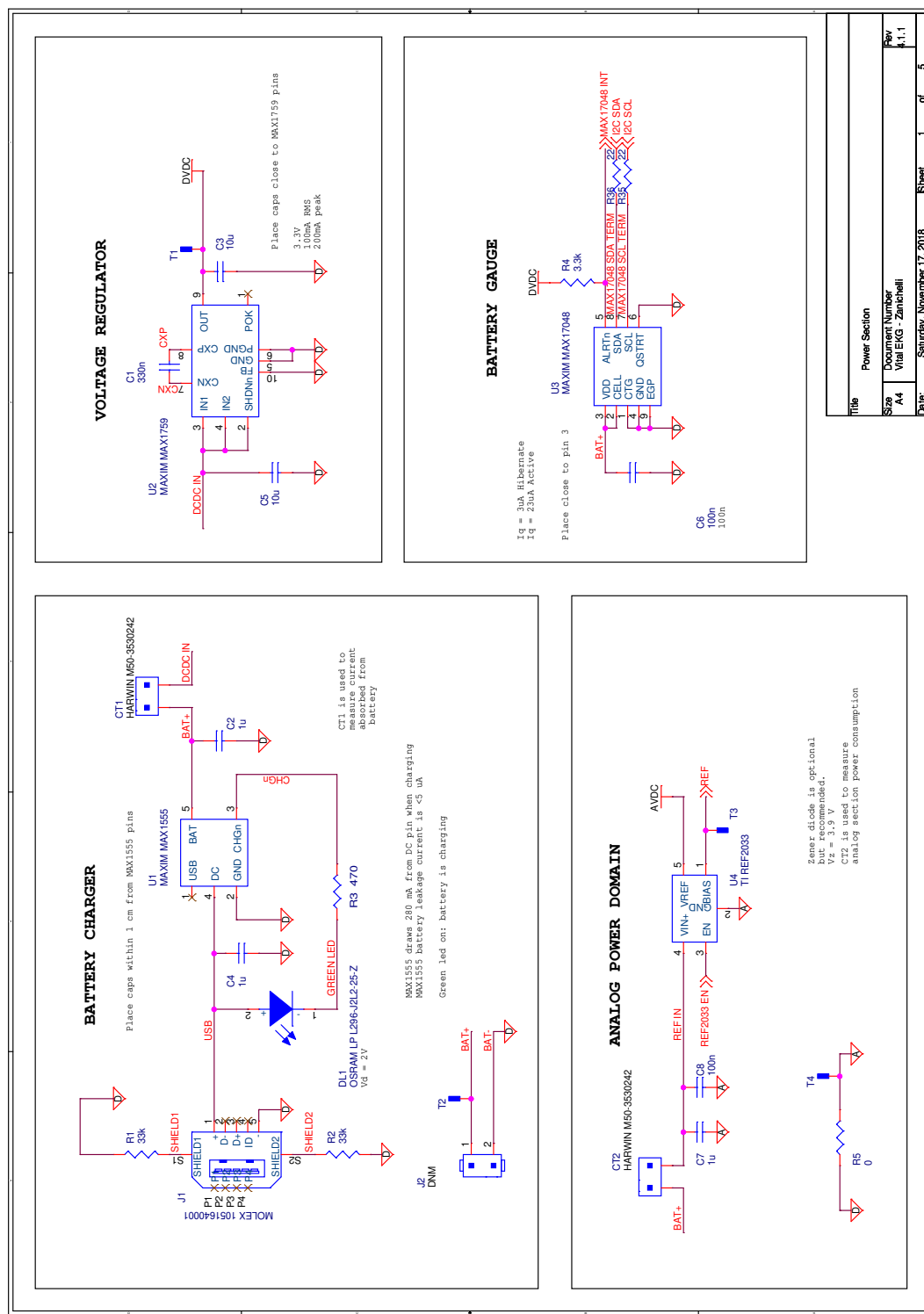


Figure 44: VITAL EKG schematic, power section.

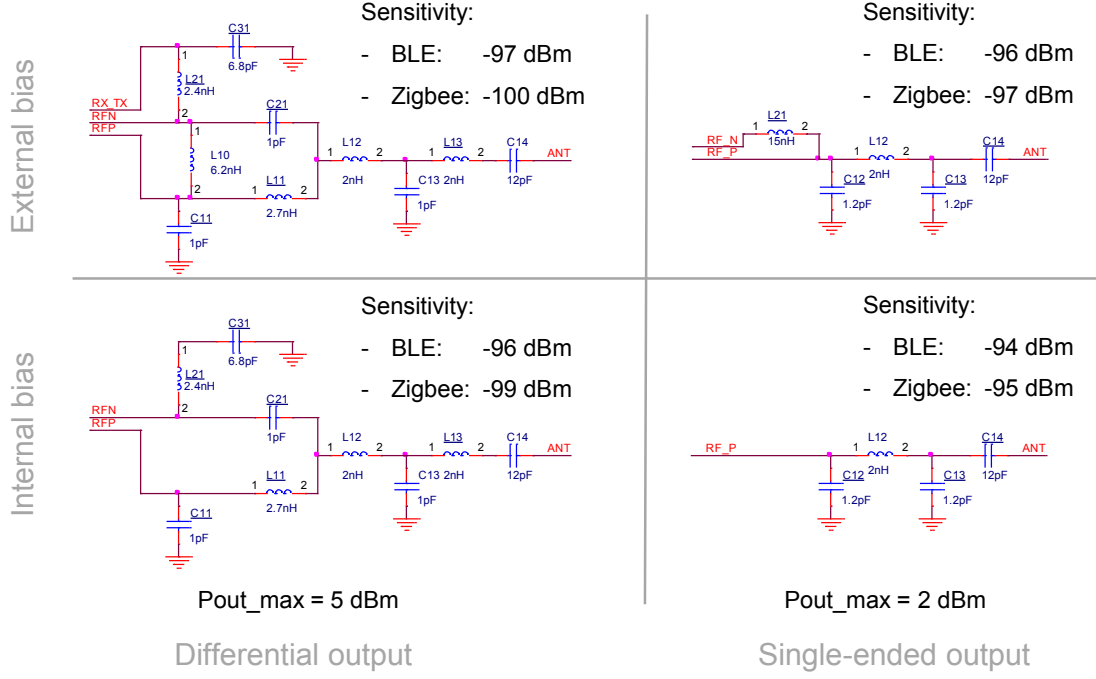


Figure 45: RF analog front end options.

front end and an antenna to provide BLE capabilities.

TI recommends several proven designs, which are shown in Fig. 45 [32].

Single-ended output with external bias has been chosen due to PCB space constraints (ix). The presence of an additional inductor as a trade off to increase the sensitivity of 2 dBm seemed reasonable, also considering that TI suggests to avoid placing any component too close to the RF analog front end.

Antenna selection is also critical to obtain desired performances. Chip antennas have the advantage of being small and a few have been considered during VITAL EKG component selection. However, they have the disadvantage of being considerably more expensive (8) than patch antennas (which are indeed free, if the production cost of a slightly larger PCB is neglected). After comparing performances of both antenna types, one of the patch antennas provided by TI was selected. Detailed performance analysis are provided in [33].

Analog Front-End

The analog front-end schematic is reported in Fig. 46.

It can be essentially subdivided in four sections. Before analyzing each section in full detail, a few general points will be highlighted. The single-rail 3.3 V power supply

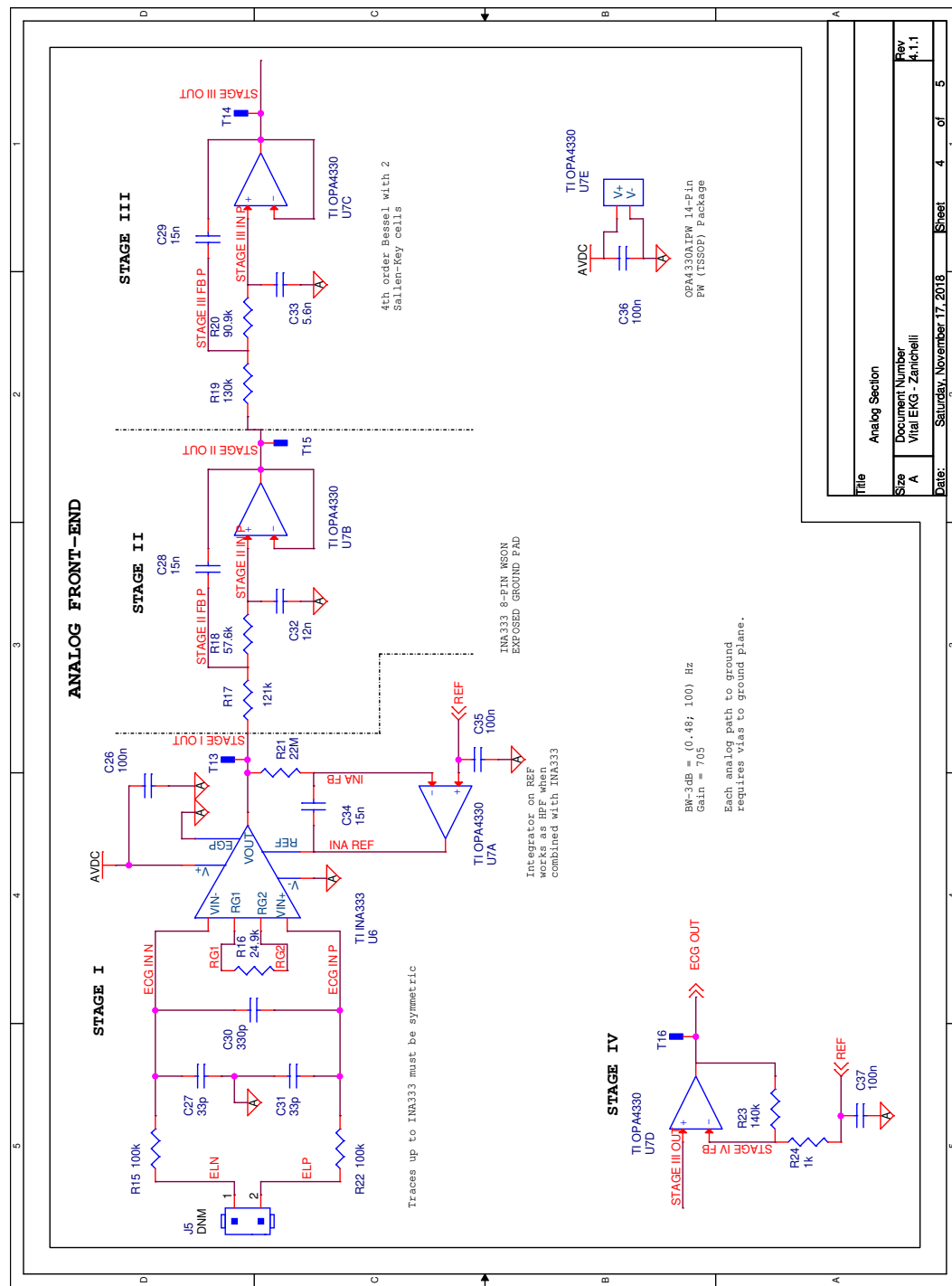


Figure 46: Analog front-end schematic.

is provided by TI REF2033 reference, which outputs also a 1.65 V mid-range reference voltage.

The analog front-end is essentially structured around two integrated circuits: TI INA333 [34] and TI OPA4330 [35], which have been selected among other similar parts for their low-power specifications.

The first section is the **differential section**. Its input is *LEAD I* EKG signal, whose amplitude is expected to be few mV.

The differential section inputs feature 1st order low pass filters to remove very high frequency components. The cut-off frequency has been set to 48.229 kHz. Furthermore, the capacitor across the inputs (C30) helps to minimize common mode noise. It behaves as a differential low pass filter when combined with resistors R15 and R22, with a cut-off frequency of 4.823 kHz.

The core of this section is TI INA333 instrumentation amplifier. The input signal, besides being only a few mV in amplitude, is expected to be superimposed to a DC offset, which must be removed from the output. The DC offset, whose amplitude depends on the electrodes, is present because the bias currents of operational amplifiers charge the electrodes, which behave like the plates of a capacitor. 22 MΩ resistors to ground would provide a path to ground for these currents. In practice, such resistors did not really make a clear difference on the output since no baseline has been detected. This has been verified in a first breadboard prototype of the analog front-end.

Metal electrodes plated with Silver Chloride have been selected for VITAL EKG because disposable EKG electrodes are not really compatible with the wrist-band form factor (ix). The DC offset which these electrodes can introduce is of the order of 300 mV.

The DC offset must be filtered out before amplifying the signal to avoid saturation. To this end, an integrator is used as INA333 feedback network. A first order Operational Amplifier (OpAmp) integrator, on its own, is highly unstable: the output quickly saturates towards one of the supply rails. Conversely, when it is used as a negative feedback network, its input is lowered (increased) by the INA333 whenever the output increases (lowers), stabilizing the system as a whole. Since an integrator has a Low-Pass response, when used as a negative feedback network the overall response is High-Pass. The -3 dB cut-off frequency is set by the integrator resistor (R21) and capacitor (C34), according to Eq. 4.2:

$$f_c = \frac{1}{2\pi RC} = \frac{1}{2\pi \cdot 15 \text{ nF} \cdot 22 \text{ M}\Omega} = 0.48 \text{ Hz.} \quad (4.2)$$

The -3 dB cut-off frequency f_c has been selected as a trade-off between removal of low frequency signals introduced by the user's body (e.g. breathing, muscular noise) and the duration of the step response transient, which increases as f_c does.

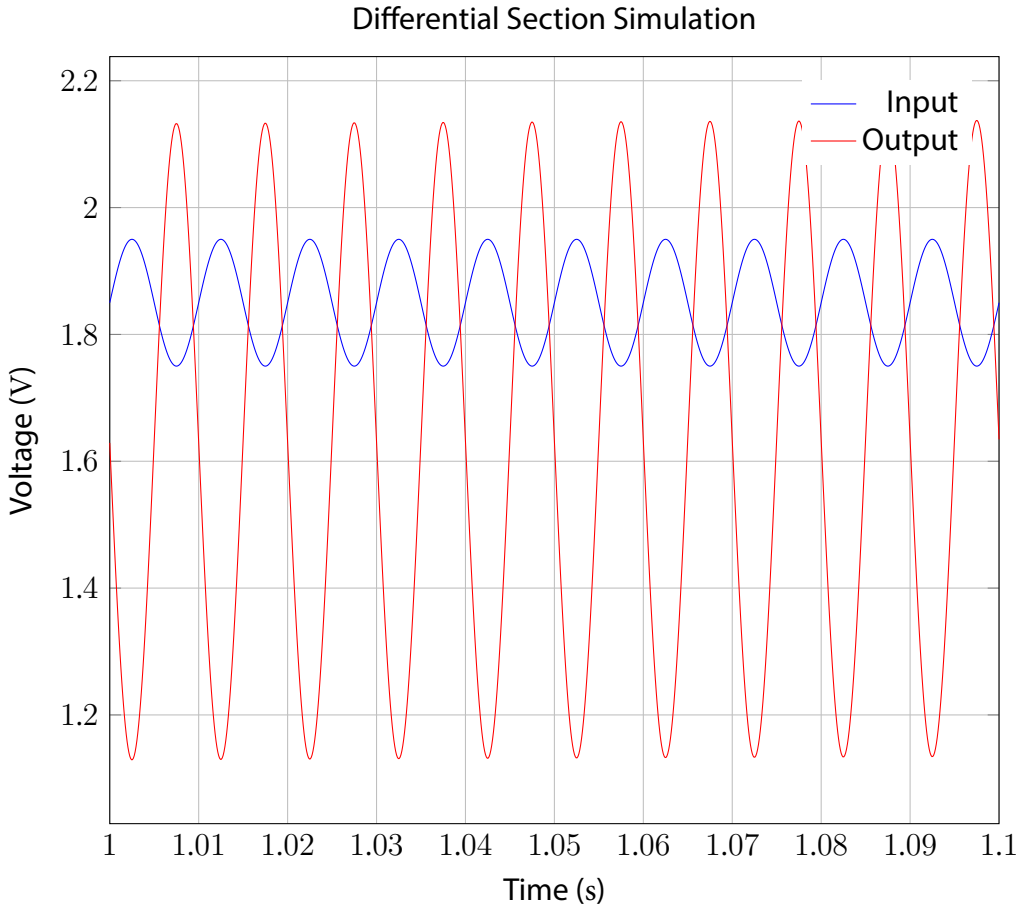


Figure 47: Simulation of differential section.

INA333 gain is set to 5.02 V/V (Eq. 4.3).

$$G = 1 + \frac{100 \text{ k}\Omega}{R_G} = 1 + \frac{100 \text{ k}\Omega}{24.9 \text{ k}\Omega} = 5.02 \text{ V/V.} \quad (4.3)$$

G has been chosen deliberately low to avoid the saturation of the INA333 due to the presence of the differential DC offset. It should be noted that presence of the feedback network would not help in case of OpAmp saturation.

The differential section has been simulated with Cadence PSpice to verify the correct behaviour of the negative feedback network. As such, the input capacitors and the power supply network (REF2033) have not been simulated.

The positive input has been connected to a constant voltage $V^+ = 1.65 \text{ V}$; the negative input has been set with a DC signal $V_{DC}^- = 1.85 \text{ V}$ and a sinusoidal signal $V_{pp}^- = 100 \text{ mV}$ with a frequency of $f = 100 \text{ Hz}$. Input and output are shown in Fig. 47.

Table 42: Fourth order Bessel Low-Pass filter specifications. Sallen-Key topology.

Parameter		First Stage	Second Stage	Units
Gain	G	1	1	1
Frequency Scaling Factor	FSF	1.4192	1.5912	1
Quality Factor	Q	0.5219	0.8055	1
Cut-off Frequency	f_c	100	100	Hz

The second and third section, which can be considered together as a **filter section**, implement a 4th order Bessel Low Pass Filter (LPF) using two Sallen-Key cells. Bessel topology has been preferred to Chebyschev because the last presents ripple in pass-band and the roll-off in transition band is too steep; much like Chebyschev, Butterworth filters present excessive roll-off in transition band. The presence of relatively high-frequency components in the QRS group of an EKG trace dictates the specifications which the filter should have. A fast impulse response transient, in particular, is important to avoid ringing when a R wave is filtered.

Specification of the filter are reported in Table 42; detailed design information are reported in [36].

The Bessel LPF has also been simulated to verify its frequency response. The simulation has been performed from 10 Hz to 1000 Hz with 100 data points per decade. The frequency response is shown in Fig. 48.

The last section is an **amplifier section**. An OpAmp in non-inverting configuration provides an amplification of 141. The overall gain of the analog front-end is then $5 \cdot 141 = 705$ V/V. Since a typical EKG signal is no more than a few mV in amplitude, the analog front end could have been designed with a total amplification up to 1000 V/V; nonetheless, a conservative gain have been preferred to avoid saturation of the ADC due to signal offset and noise (e.g. muscular noise, mains).

Digital Peripherals

The digital peripherals section is composed of the following:

- TI HDC2010 : temperature and humidity sensor;
- TDK - InvenSense MPU-9250 : 9-axis motion-tracking unit;
- Maxim Integrated MAX30102 : integrated pulse oximetry and heart-rate monitor module.

The schematic page which details digital peripheral section circuitry is shown in Fig. 49.

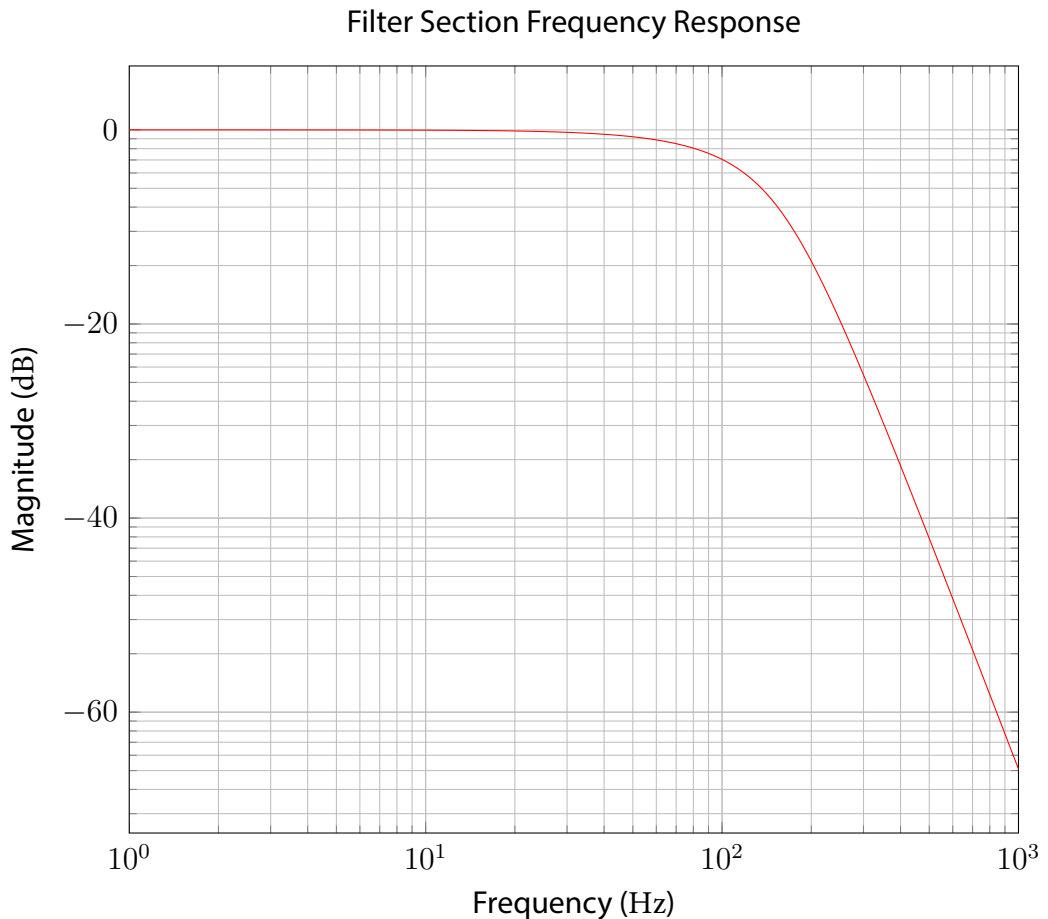


Figure 48: Frequency response of 4th order Bessel LPF with Sallen-Key topology.

TI HDC2010 [37] is a digital temperature and humidity sensor, specifically designed for low power battery operated products. It has a 6 pins Wafer Level Chip Scale Package (WLCSP) which occupies only 1.45 mm^2 . Both temperature and relative humidity are 11 bit wide with an accuracy of $\pm 0.2 \text{ }^\circ\text{C}$ and $\pm 2\%$, respectively. Average supply current is only 500 nA in active mode when both temperature and humidity measurements are performed. Digital interface is provided through I²C and an interrupt pin. Interrupt functionality is configurable both with respect to source and frequency.

TDK Invensense MPU-9250 is a digital 9-axis motion-tracking unit. It ships in 24 pins 3 mm x 3 mm QFN package, which is ideal for space constrained designs. It supports both I²C and SPI and can also be configured as a master. It is equipped with a 512 B First-In, First-Out (FIFO) memory which allows to read many acquisitions with a single protocol transaction, thus reducing the overhead associated to slave address and register address (I²C).

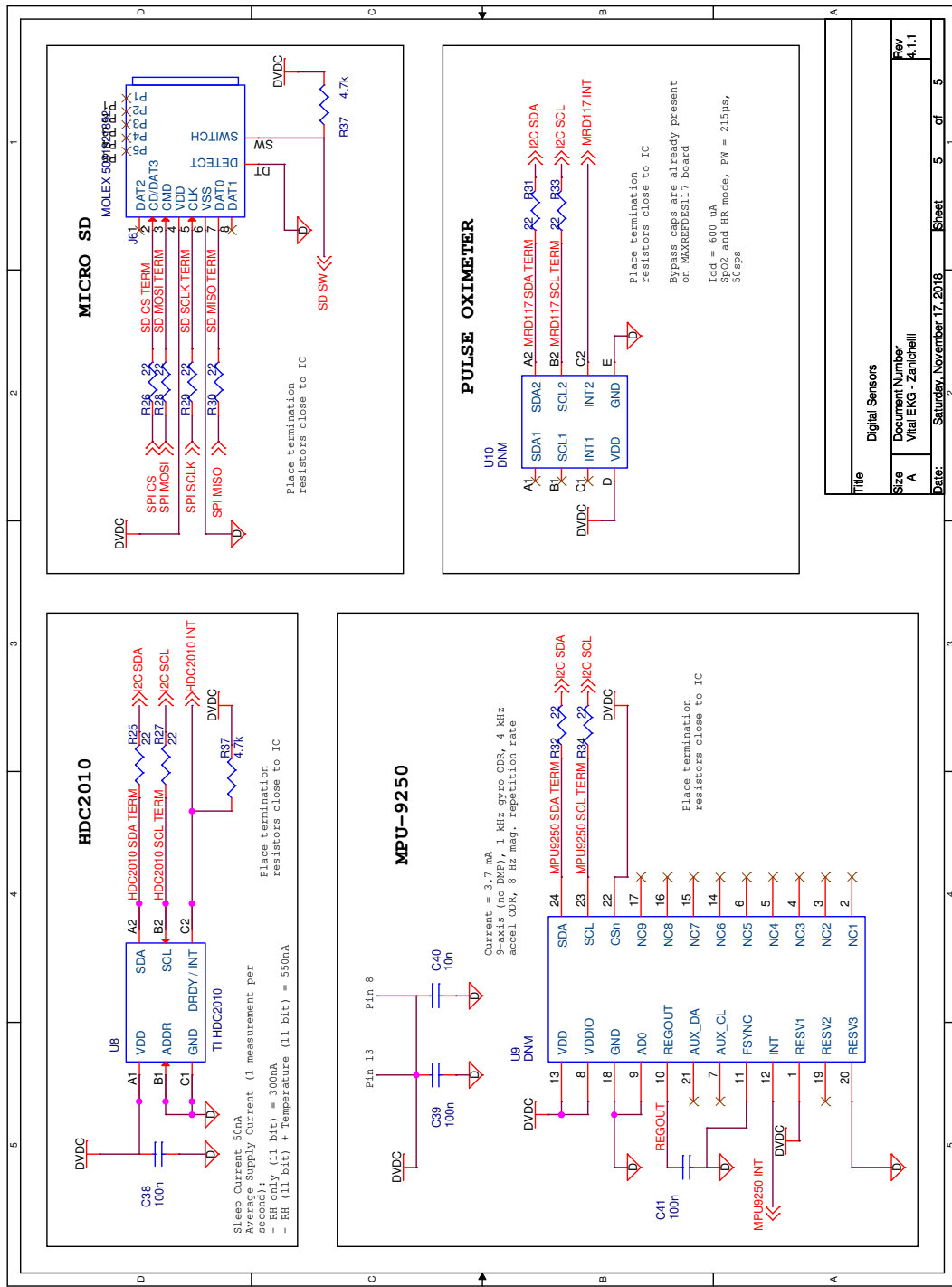


Figure 49: Digital peripheral schematic.

Table 43: Maxim Integrated MAX30102 LEDs specifications.

Characteristics		IR	RED	Units
LED Peak Wavelength	λ_P	880	660	nm
Full Width at Half Max	$\Delta\lambda$	30	20	nm
Forward Voltage	V_f	1.4	2.1	V
Radiant Power	P_O	6.5	9.8	mW

Maxim Integrated MAX30102 is an integrated module which allows to measure HR and SpO₂. It features 2 LEDs, whose specifications are reported in Table 43 [38]. A photodetector with a Spectral Range of Sensitivity from 600 nm to 900 nm is also included in the module.

MAX30102 on itself is 5.6 mm by 3.3 mm and ships with an Organic Land Grid Array (OLGA) package. This is very convenient for production because it minimizes the footprint area. Nonetheless, it is not a good choice for a first prototype of VITAL EKG because it makes the debug of any hardware problem very hard. Moreover, recommended power supply is $V_{DD} = 1.8$ V, plus and $V_{DD}^{led} = 5$ V for LEDs, while the working voltage for VITAL EKG is 3.3 V.

For all these reasons, MAX30102 has been replaced by MAXREFDES117, which is a development PCB module designed by Maxim Integrated for rapid prototyping [39]. It includes MAX30102, along with MAX14595 (I²C level translator) and MAX1921 (step-down converter) to adapt all the voltage levels.

A 18 bit ADC converts the analog reading of the photodetector to digital samples. MAX30102 is equipped with an internal 192 B FIFO memory. Since a sample is 6 B long, up to 32 samples can be stored. MAX30102 can be configured to trigger an interrupt whenever the FIFO memory is in *Almost FULL* condition, which means there are a user selectable number of free positions (from 0 to 15).

Finally, MAX30102 RED LED can be used to enable a **Proximity Interrupt**. Indeed, when the user places a finger on MAX30102, the value of the readings substantially increases because RED light which was previously diffused into the environment is absorbed by the photodetector. This feature is very important because it has been exploited to start synchronously both MAX30102 acquisition and TI CC2640R2FRGZ internal ADC conversion for EKG.

4.3.2 PCB Layout

The PCB layout have been done with Cadence Allegro PCB Designer. Even though the PCB described in this work is intended as a first prototype and proof of concept for VITAL EKG, many effort have been made to keep the size of the PCB as small as possible.

The PCB is a two-layer board. Copper layers have a thickness of 18 µm. The minimum trace width and minimum trace distance have been set to 110 µm. Minimum values have been used for digital signals (e.g., I²C and SPI buses, interrupts signals), which are not particularly affected by noise and do not suffer from increased trace resistance. Wider traces, up to 400 µm, have been used for more delicate signals; these includes power supply traces (300 µm and 400 µm, depending on how much current the specific trace segment is expected to carry) and analog signals (200 µm). All the vias have been designed with 450 µm round pad and 250 µm drill size. It should be noted that the drill size is merely the size of the tool used by the manufacturing company; finished hole size varies according to the plating specifications. Eurocircuits¹ specifies 100 µm decrease in diameter for plated vias.

The components have been placed according to datasheets recommendations. The RF and the analog sections have been positioned at opposite sides of the board to minimize high frequency noise components in the EKG signal. The input traces of the analog front end have been routed as a differential pair to minimize the differential noise picked up by before the instrumentation amplifier. All passive components have been kept as close as possible to ICs.

The position of the antenna is critical. Ideally, it should not have components and traces placed nearby or below to maximize performances. In practice, this is a difficult condition to achieve given the constraints on PCB area. The antenna have been placed in a corner and TI CC2640R2FRGZ have been positioned accordingly to minimize the length of the RF front end.

Via arrays connected with a trace on the top plane have been used to shield the antenna and the analog front-end. Via matrices have also been used to increase the thermal dissipation of TI CC2640R2FRGZ and INA333, as recommended by datasheets. Finally, decoupling capacitors have been connected with three vias (in a few occasions only two vias have been used due to lack of space) to the ground plane on the bottom layer to minimize the resistance. Decoupling capacitors have been placed as close as possible to the pins to minimize the inductance introduced by the trace segment.

A solid copper pour have been used as ground plane on the bottom layer. Two layers layout forced to route a few trace segments on the bottom layer. However, whenever possible traces on the bottom layer have been removed or kept short to prevent long return paths for currents. No copper have been placed below the antenna, as recommended by TI. Moreover, no traces have been routed below the RF front end and TI CC2640R2FRGZ.

Symbol interference is a problem which generally affects digital communication buses, such as I²C, SPI and Universal Asynchronous Receiver-Transmitter (UART). A symbol pulse might reflect at the end of trace and interact with the following symbol. If

¹<https://www.eurocircuits.com/>

the traces are short, the propagation time is also short and the symbol amplitude reduces to negligible values before the following symbol is sent. Conversely, the symbols might interact and digital communication may fail. To minimize this problem, 22Ω series termination resistors have been used on these traces.

Gerbers files are included in Appendix A.

4.4 Case Design and Fabrication

THE PCB presented earlier in this Chapter (4.3.2) has been designed to provide a proof of concept and to ease the development of the firmware.

The design of a production ready PCB with Semi-Flex technology was also planned. The main board has a reduced size, which was possible due to the removal of all test points, UART protocol support and Maxim Integrated MAXREFDES117 development module. Two satellite boards, connected with a Semi-Flex PCB, are necessary to ensure correct placing of sensors. TI HDC2010 requires a small satellite board because it needs to be attached to the lower shell of the case to minimize the distance between the sensor and the skin. A second satellite board is necessary because Maxim Integrated MAX30102 needs to be visible from the outside, along with the Surface Mount Technology (SMT) LEDs. To satisfy these requirements, the PCB was designed following the open source Maxim Integrated MAXREFDES117 documentation.

A 3D-printable plastic case has been designed in partnership with two students of Department of Architecture and Design (DAD) of Politecnico di Torino. A summary of the design files is reported in Fig. 410. The size of the case is approximately 50 mm x 30 mm x 20 mm. The case has been first 3D-printed at Politecnico di Torino. However, a better quality result was obtained with a professional 3D-printing service.

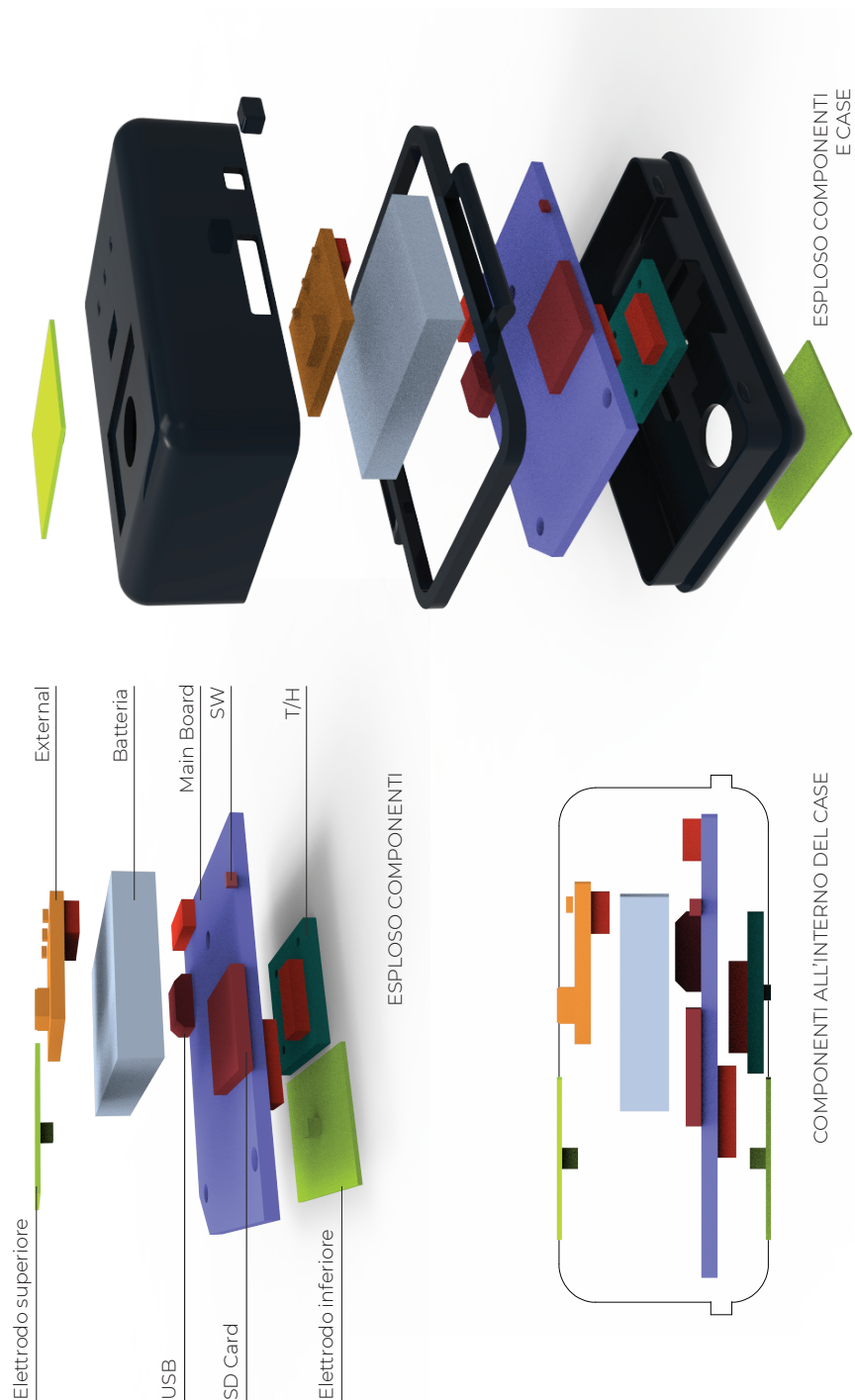


Figure 410: Summary of case design.

5

CHAPTER

Firmware

THIS chapter has a double aim. On the one hand, it documents the firmware and the algorithms which power VITAL EKG; on the other hand, it serves as a *Getting Started* document to provide a basis for future development of VITAL EKG. Sections 5.1 and 5.2 serve specifically this second purpose.

5.1 Introduction to BLE 4.2 Protocol

AN in depth discussion about Bluetooth Low Energy 4.2 is well beyond the scope of this document. Nonetheless, a short introduction is necessary to understand why certain decisions have been made during the design of the Custom Profiles which sit above the TI BLE 4.2 protocol stack. All the information regarding this section can be found covered in full depth in the Bluetooth Core Specification Version 4.2 [40].

5.1.1 Physical Layer

The BLE Physical Layer (PHY) operates in the unlicensed industrial, scientific and medical band in the range from 2.4 MHz to 2.485 MHz. It uses a 1 Mbit s^{-1} Gaussian Frequency-Shift Keying (FSK) modulation, which reduces the out-of-band high signal components caused by sudden symbol switching of traditional FSK modulation. To improve robustness of the protocol, an adaptive frequency-hopping scheme is also implemented.

Each device can be in any of the following five states:

- Standby;
- Advertising;

- Scanning;
- Initiating;
- Connected.

There are a total of 40 channels, each separated by 2 MHz. Connected devices can use up to 37 channels for frequency-hopping; 3 are reserved to advertisement.

Advertisers broadcast Protocol Data Unit (PDU) on dedicated channels to announce their availability for a connection. Scanners listen PDU broadcasted by advertisers. Both these roles are connectionless. When a scanner responds to an advertiser's connection request, it assumes the initiator state. If the connection is successfully established, the initiator becomes the master (Central role) and the advertiser becomes the slave (Peripheral role). Central and Peripheral roles are not mutually exclusive and can be assumed by the same device. During a connection, Central and Peripheral devices switch channel periodically. Each time they switch channel a new **connection event** begins.

5.1.2 Host and Controller

The BLE protocol stack is split in two blocks: the **Host** and the **Controller**. The host groups the higher layers of the protocol stack; the controller includes the lower layers, from the PHY to the **Host Controller Interface (HCI)**. The HCI can either be defined in software or in hardware. The TI BLE protocol stack implements the HCI in software.

Above the HCI, on the host side, there is the **Logical Link Control and Adaptation Layer Protocol (L2CAP)**. The L2CAP is responsible for multiplexing, segmentation, and reassembly operations of higher layer packets. L2CAP input packets are technically called Service Data Unit (SDU); a PDU is composed by the L2CAP header and an SDU and represents the L2CAP output.

The default PDU size is 27 B; the L2CAP header is 4 B long, leaving at most 23 B for the SDU. The standard PDU size ensures full compatibility between BLE 4.2 and BLE 4.0/4.1. The Low Energy (LE) Data Length Extension feature of BLE 4.2 allows to increase the PDU size up to 255 B, loosing compatibility with BLE 4.0/4.1 devices.

Currently, VITAL EKG has been designed to support only BLE 4.2 devices. The PDU size increase request must be issued by the Central device to allow compatibility with **PAYLOAD** characteristic of EKG Profile, which is 202 B long.

5.1.3 GATT Layer

From the application standpoint, data communication is handled by the GATT layer of the protocol stack. The GATT layer is an abstraction of the **Attribute Profile (ATT)** layer. Each device which participates in a connection can either be a GATT client or a GATT

server. Servers are the devices which have data to share while clients are those asking for data. The GATT client/server roles are completely independent from the Generic Access Profile (GAP) roles.

GATT servers expose data using a formatted database. **Characteristics** are usually grouped to form a **service**; multiple services constitute a **profile**, even though the two terms are often used interchangably because it is common to find single service profiles.

A characteristic is a formatted, atomic abstract information which a GATT server exposes. To realize such abstract communication, each characteristic is composed of groups of bit fields called **attributes**. Generally, a characteristic is composed of the following attributes:

- **Characteristic Declaration.** The characteristic declaration informs the client about the properties of the characteristic.
- **Characteristic Value.** The characteristic value is the attribute where the actual information which the server wants to expose is stored.
- **Client Characteristic Configuration.** **Notification** or **indication** can be provided by configuring the client characteristic configuration. These messages, which have a dedicated bit field, are sent asynchronously by the server with or without client acknowledgement, respectively.
- **Characteristic user Description.** The characteristic user description is an ASCII string with a human readable description of the characteristic.

Each attribute is composed of a number of bit fields, listed below.

- **Handle.** The handle is a unique index which identifies an attribute.
- **Type.** The type, also called **Universal Unique Identifier (UUID)**, is a 128 bit field which informs the client about which kind of information is contained in the attribute. There is a number of predefined UUID provided by Bluetooth Special Interest Group (Bluetooth SIG) which have standard meaning. Custom UUID can be defined to encode custom application behaviour.
- **Permissions.** The permission flags define if the given attribute can be read (`0x02`), written with or without response (`0x08` and `0x04`, respectively), notified (`0x10`) or indicated (`0x20`) by the client. The flags, which are all single bit, can be combined to precisely describe the behaviour of the attribute.
- **Value.** The value is the payload of the attribute.

When a GATT client intends to request informations from a GATT server, it performs a **service discovery**. BLE specifications state that a client must be able to understand the

features of a service by only looking at the characteristic declarations. For this reason, a characteristic declaration attribute UUID must be `0x2803` and its value is a 5 B field with the following meaning:

- Byte 0 is a code which matches the permissions of the characteristic value;
- Byte 1-2 is the (reversed) attribute handle of the characteristic value;
- Byte 3-4 is the (reversed) attribute UUID of the characteristic value.

5.1.4 GAP Layer

The states and roles for BLE devices are defined by the top layer of the protocol stack: the GAP. The GAP layer is responsible for connection functionality. There are several connection parameters which an initiator device sends during a connection request which are controlled by the GAP.

Connection Interval

BLE uses an adaptive frequency-hopping scheme at the PHY layer. Devices which participate in a connection switch channel after a connection interval T , which is configurable in the range 7.5 ms to 4000 ms in steps of 1.25 ms. At the beginning of a connection interval, central and peripheral devices exchange packets even though the GATT client does not make any request to the GATT server. This is required by the BLE specification to maintain the connection. As a consequence, at the beginning of a connection interval an increase in current draw is normally observed and the power consumption increases proportionally. Increasing the connection interval has the direct consequence of lowering the power consumption. On the other hand, the throughput normally decreases.

Slave Latency

A peripheral device has the option of skipping a number of connection events equal to the slave latency S . This has the advantage of decreasing the number of packets transmitted by the Peripheral if no useful information needs to be sent, lowering its power consumption. Furthermore, it gives the Peripheral device more time to receive data transmitted by the Central device.

Both Peripheral and Central devices may adjust the connection parameters during an ongoing connection.

Effective Connection Interval

From the Peripheral point of view, the connection interval is not respected if the slave latency is greater than zero because it is allowed to skip connection events. It makes sense to define a new parameter, called effective connection interval T_{eff} , which describe the interval between two connection events in which the Peripheral device participate. It can be calculated according to Eq. 5.1.

$$T_{eff} = T \cdot (1 + S). \quad (5.1)$$

The slave latency S and the connection interval T must be configured such that the effective connection interval T_{eff} is lower than 16 s.

5.1.5 LE Data Length Extension

The LE data length extension is a feature introduced by the Bluetooth Core Specifications Version 4.2. It permits negotiation of the PDU size between the master and the slave and increases the maximum size to 251 B while in the connected state. This is a significant improvement over the Bluetooth Core Specification Versions 4.0 and 4.1, which set the maximum PDU size to 27 B. The maximum transmission time for a PDU, defined at the PHY layer symbol rate, has also been increased to 2120 μ s; previous BLE versions allowed a maximum transmission time of 328 μ s. It is important to notice that a device can only control its transmission PDU size and time and the reception PDU size and time of a peer device which participate to the connection. The symmetrical parameters are controlled by the peer device.

The dynamic negotiation of higher PDU size and time allows BLE 4.2 devices to maintain full compatibility with older devices. The negotiation is performed by the **Link Layer**, which is located in the controller; it sits above the PHY layer and below the lower HCI.

Increasing PDU size has a direct impact on the amount of RAM which the protocol stack needs. Indeed, the transmission and reception buffers, located in the lower HCI in the controller, require a larger space. The maximum size of these buffers is configurable: default values for TI BLE 4.2 protocol stack are 8 PDUs for the transmission buffer and 4 PDUs for the reception buffer.

5.1.6 Security

TI BLE 4.2 Stack implementation includes the **GAP Bond Manager**. It takes care of most security mechanisms, thus offloading the application from this task.

The Gap Bond Manager is responsible for managing the **pairing** and **bonding** processes. When two devices establish a connection, they generate and exchange keys (pairing). Optionally, the keys can be stored in non-volatile memory to ensure the

devices can recognize each other even during following connections (bonding). In order to enable bonding, the Gap Bond Manager needs to have access to non-volatile memory. This is provided by the SNV Driver. The Gap Bond Manager requires one page of flash memory (4 kB) and one page of Cache as temporary storage to perform memory compaction. The Gap Bond Manager can also be configured to use two pages of flash to enable backup of bonding keys. This method has been used in VITAL EKG, mainly because the 8 kB Cache memory has been repurposed as RAM.

5.1.7 Throughput

BLE Core Specification version 4.2 allows to extend the PHY packet size up to 255 B, greatly decreasing the overhead. Indeed, the L2CAP header is 4 B long regardless of PDU size.

Throughput is only meaningful when talking about transmission of EKG waveform. Indeed, all other sensors produce data which are processed onboard to provide the Central device only a short information, up to 2 B.

EKG waveform consists of 5000 samples of 2 B each. The processing is performed with a batch size of 200 samples. Thus, each batch is split in 2 packets. Further 2 B are appended to each packet to include the progressive number of the packet; this is done to ensure correct ordering of the packet at the receiver side. All in all, 50 packets of 202 B are sent.

To minimize the packet loss, the processing of a batch is started only after the Central device reads the second (and last) packet of the previous batch. This is possible because the BLE profiles include callback functions which the BLE stack invokes upon transmission of a packet. This choice is inherently slow and computing the throughput does not make sense, since it depends on the time the Central device takes to perform a read.

An alternative implementation of EKG waveform transmission would require a feedback characteristic NEXTPACKETOFFSET on EKG profile. Basically, VITAL EKG could process continuously all the batches, transmitting ready packets immediately. The Central device would read continuously (or subscribe to a notification) and verify the progression of packets. In case of missed packets, NEXTPACKETOFFSET would be used by Central device to let know to VITAL EKG which packet need to be transmitted again.

5.2 General Architecture

As already mentioned, TI CC2640R2FRGZ is based on ARM® CORTEX® M3. It can be used both *bare metal* or with a Real-Time Operating System (RTOS), conveniently provided by TI and called TI RTOS. Its documentation can be found in [41].

Firmware development can be carried out using either TI's proprietary Integrated Development Environment (IDE), Code Composer Studio (CCS), or IAR Embedded Workbench. In this work, CCS has been used.

TI RTOS is a **preemptive real-time operating system**. Threads (also called Tasks) run concurrently and a scheduler switches context based on a priority value associated to each Task.

A few thread-safe structures are part of TI RTOS kernel and simplify greatly inter-task communication (Semaphores, Events, Mailboxes, Queues among others). Application Public Interface (API) documentation can be found in [42]. Several drivers are also provided to ease the low level management of peripherals. Among others, I²C, SPI, ADC, ADCBuf, RF.

Using an operating system becomes imperative to exploit TI's implementation of BLE protocol stack. TI provides several pre-compiled BLE stack libraries, which cover all the GAP roles a BLE device can assume. In practice, the Stack project is linked to the Application project and provides a high level interface for BLE communication. More informations about the BLE protocol stack can be found in 5.1. TI's stack libraries for TI CC2640R2FRGZ are grouped within the SimpleLink™TI CC2640R2FRGZ Software Development Kit (SDK) (latest version at the time of writing is v2.30.00.xx); complete documentation can be found online at [43].

VITAL EKG assumes the Peripheral GAP role. A sample application project can be found by browsing the online resources from within CCS (Resource Explorer). BLE stack library can be accessed by the application using ICall software layer. The use of ICall is not mandatory, since all the standard BLE layers described by the Bluetooth Core Specification have their own API. However it is very convenient to simplify the communication with the stack library project. All the tasks which send requests over BLE must be ICall-aware and need to register with it before using any ICall API.

The application firmware is organized into several entities. Each entity can be generally thought as the manager of a sensor, even though this is not true in all the cases (the Continuous Monitoring entity manages the battery gauge, the temperature and humidity sensor and the motion tracking device).

Communication among entities is achieved using Events, Mailboxes and Queues. The first provides a data-less communication, where only situations are notified; the other modules implement structures which can carry data payloads as well as notifying a change of state. A communication diagram of VITAL EKG behaviour is shown in Fig. 51.

5.2.1 BLE Dispatcher

The entry point of the application is the BLE Dispatcher, which is in charge of the following:

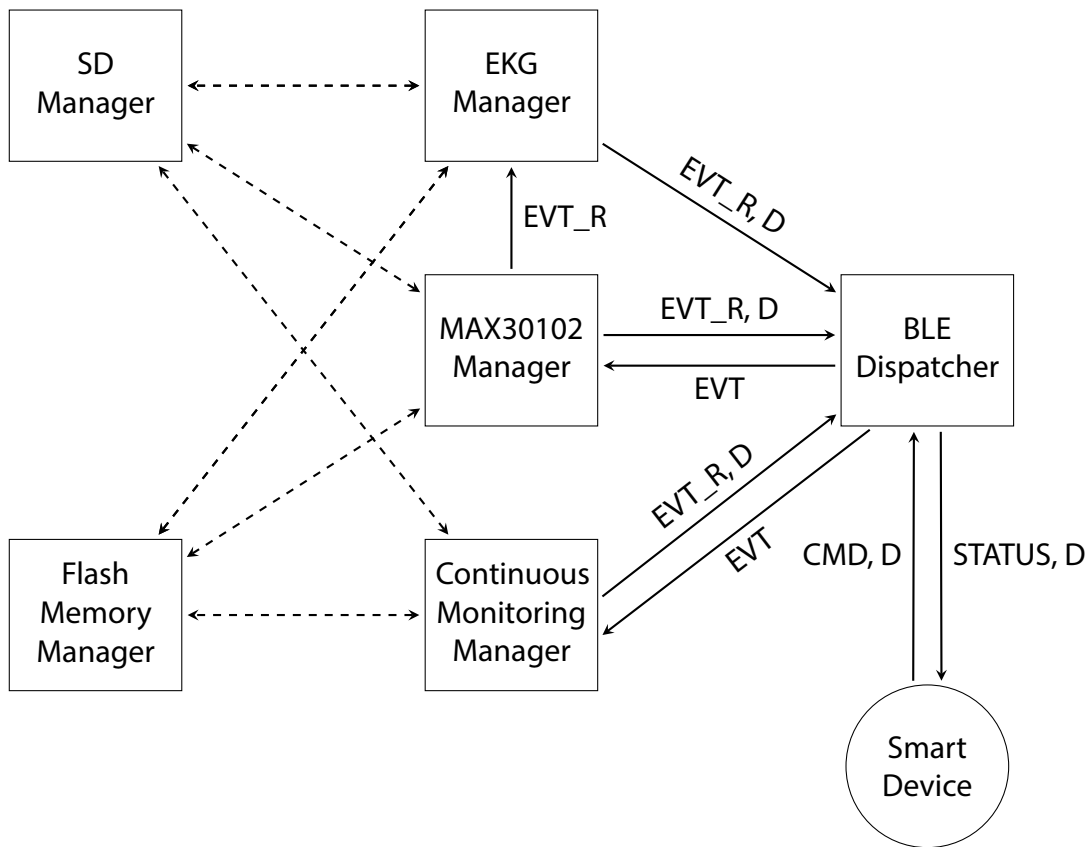


Figure 51: VITAL EKG communication diagram. Messages which involve data are marked with D.

- **dispatch** commands received from the Central device, which is the one which interprets the Central GAP role to the appropriate entity;
- **forward** status updates received from entities to the Central device;
- **forward** data received from entities to the Central device.

It is important to note that the BLE Dispatcher is a stateless asynchronous entity which does not produce or process any data. It is only in charge of managing BLE communication at data level and is used to separate conceptually the acquisition and processing of information from its transmission. Details about commands and status codes are included in Appendix B.

5.2.2 MAX30102 Manager

MAX30102 Manager is a Task which deals with Maxim Integrated MAX30102 sensor configuration, RED and IR channels data acquisitions and processing.

MAX30102 Manager is implemented as a Finite State Machine (FSM). This choice architecture prevents most deadlock conditions which might happen if BLE Dispatcher receives unexpected commands from Central device. Indeed, being the BLE Dispatcher stateless, it has no clues about correctness and timing of the commands it forwards.

The configuration of MAX30102 is performed before the FSM starts and is the first operation performed by the thread. Parameters are reported in Appendix C, along with heavily commented code about MAX30102 Manager execution.

MAX30102 Manager is also responsible of controlling the execution of the EKG Manager. Indeed, there is no way for the analog front-end to understand when the user is really ready for an acquisition (finger placed on the electrode), once the start command has been sent from the Central device. For this reason, the Proximity Sensor feature of MAX30102 has been exploited to synchronize the acquisitions of PPG and EKG signals. This is particularly important for a future development of the firmware, described in 7.1.10. Furthermore, the DSP of PPG and EKG signals are performed sequentially to reuse the same RAM block. The communication between MAX30102 manager and EKG Manager is realized using the Event module; complete reference is provided in Appendix B.

MAX30102 Manager FSM is sensible to an acquisition start command only in the idle state. If this is the case, the FSM proceeds only if the battery voltage is within the range 3.4 V to 4.0 V. MAX30102 Manager is sensible to two events posted by the Monitoring Task, which takes care of signaling the status of the battery. More informations can be found in the events reference (Appendix B).

MAX30102 Manager is also in charge of monitoring the execution of EKG Manager. In particular, it needs to know if the latter completed the processing and transferred all data to the Central device or if the processing is still in progress. In this last case, the ongoing EKG processing is cancelled and a new acquisition can start only when MAX30102 Manager receives an acknowledge from EKG Manager.

Once these preliminary checks have been completed, MAX30102 is turned on in SP02 mode with proximity sensor functionality enabled. The sensor generates an interrupt when the photodetector reading exceeds a programmable threshold. This happens whenever an object gets too close to the sensor, because the LEDs light is reflected by the object instead of being diffused into the environment. When the proximity interrupt is caught by TI CC2640R2FRGZ, the sensor is reconfigured to generate interrupts whenever the internal FIFO memory is almost full. This condition has been configured to be triggered when 20 new samples are collected, which means 12 positions are still available for new data. At the same time, an acquisition start message is sent to EKG Manager to let it start its acquisition. Upon FIFO almost full

interrupt, samples are read from the FIFO, and transferred to the Flash Memory Manager for non-volatile storage. All the samples are checked to make sure no saturation of MAX30102 ADC or FIFO occurred. More information on this problems are included in Chapter 7.1.5.

After completing the acquisition, the processing does not start until also EKG Manager has completed its acquisition. This synchronization is necessary to ensure thread safety. Indeed, a global memory buffer is used for EKG Manager acquisition and processing and MAX30102 Manager acquisition. Alternative design choices are detailed in Chapter 7.1.6. It should be noted that in general communication between FSMs have been assumed asynchronous. Whenever a message from an other FSM arrives, it is buffered until the receiver is ready to process said message.

At this point, MAX30102 Manager executes a data processing algorithm with a quasi-online approach; data are then processed according to different strategy to verify the results of the first algorithm. The processing phase is described in all detail in Section 5.3.

After the processing, a message is sent to EKG Manager to communicate the memory buffer is available and EKG waveform processing can start.

5.2.3 EKG Manager

EKG Manager is responsible for acquisitions of EKG signal. Also this Task is organized as a FSM. When MAX30102 Manager commands the start of an acquisition, the analog front-end is powered on by setting REF2033_EN pin high. The analog front-end is normally unpowered to increase battery life. TI REF2033 takes at most $500\ \mu s$ to stabilize the output signals with 0.1% accuracy. Since the sampling frequency is set to 500 Sa s^{-1} , the settling time is short enough to justify this operation at the beginning of each acquisition¹. The ADC driver which is used is ADCBuf, which provides continuous sampling with two buffers. A callback function is invoked when a buffer is full. The samples are saved in internal flash memory after a light processing.

Since the ADC has a maximum sampling frequency of 200 kSa s^{-1} , an **oversampling** strategy has been employed to increase the effective number of bits. Oversampling of 1 bit is done by accumulating 4 consecutive samples and dividing the results by 2. Clearly the sampling frequency must be increases of a factor 4 as well. An oversampling of 2 bit has been performed, obtaining samples with 14 bit effective resolution. The processing highlighted in Section 5.3.2 has been performed without oversampling to preserve the original signal and to evaluate the performances of the analog front end.

EKG Manager uses four buffers obtained from a unique array used for most of acquisition and processing. These are as follows:

¹Oversampling increases the sampling frequency by 4 times for each added bit of resolution. This fact does not impact the timing because the output waveform after oversampling has still a frequency of 500 Sa s^{-1} .

- 320 B ADC first buffer;
- 320 B ADC second buffer;
- 320 B ADC support buffer;
- 100 B memory transfer buffer.

The first two buffers of 320 B are used to accumulate 160 Sa of 12 bit, each stored on 2 B. After the oversampling processing, 10 Sa are obtained from each ADC buffer. The support buffer is used to transfer the samples from the ADC callback (it is provided as argument of ADCBuf conversion structure) to EKG Manager task context. This is necessary because the operation performed in callback context should be reduced as much as possible. Finally, the memory transfer buffer is used to save the samples in flash memory. This means flash memory is accessed during the acquisition once each 100 ms at 500 Sa s^{-1} effective sampling frequency.

After the acquisition is completed, the FSM releases the buffers by signaling to MAX30102 that they can be used for PPG processing.

Once PPG processing has been completed, MAX30102 Manager lets know EKG Manager that the memory buffer can be used for EKG processing. EKG Manager processes 200 Sa at a time, which are converted to 4 B signed integers before processing. A fixed point strategy with 10 fractional bits is used to represent fractions. This approach reduces the usable dynamics to $[-2^{21}; 2^{21} - 1]$ and about 3 decimal digits of accuracy. After the completion of the processing of the first batch of samples, EKG Manager signals to BLE Dispatcher that the batch is ready to be sent over BLE using the standard queue on which BLE Dispatcher listens to messages.

Processed samples are converted back to 16 bit signed integers before transmission. This allows to halve the amount of data to transmit (400 B for 200 Sa), drastically reducing power consumption. The output dynamics in this case is $[-2^{15}; 2^{15} - 1]$. However, no real information is lost in this process. In fact, the raw waveform after oversampling had a resolution of 14 bit.

Data Length Extension allows to send up to 251 B PDU and for this reason each batch of samples is split in two packets before transmission. A further 2 B are added at the end of each packet to indicate its progressive number and facilitate the reconstruction of the signal without ordering errors.

To minimize the probability of losing packets, a new batch of samples is loaded from flash and processed only when the Central device performs a read of both packets of the previously processed batch of samples. This feedback mechanism clearly introduces a misalignment between MAX30102 Manager and EKG Manager, with the former entering in idle state much earlier than the latter. To cover error situations in which MAX30102 Manager commands to EKG Manager to perform a new acquisition even

though the processing of the previous has not yet been completed, MAX30102 Manager has the possibility to cancel an ongoing EKG processing.

Appendix D includes commented code about EKG Manager execution.

5.2.4 Monitoring Task

The Monitoring Task handles all the functionalities of VITAL EKG which do not depend on the interaction of the user with Central device. These are:

- skin temperature and humidity monitoring, using TI HDC2010;
- battery monitoring, using Maxim Integrated MAX17048;
- activity tracking, using TDK Invensense MPU-9250.

As all tasks, the basic structure is a never ending loop which blocks on events. For this task, a FSM is not required because the interaction with other entities is minimal and the events are periodic.

TI HDC2010 is configurable to generate an interrupt on a dedicated pin with specified timeout. The interrupt pin requires a pull-up resistor which was not included during the design of the schematic. More information about this error are included in Chapter 7.1. Since skin temperature and humidity monitoring needs to be continuous, a workaround using a timer (Clock module of TI RTOS) has been used. The timer timeout is longer than the sensor reading interval, to be sure to read always updated data.

Maxim Integrated MAX17048 has been configured to provide interrupts when the battery voltage rises above 4.0 V or falls below 3.4 V. In both cases, the Central device is notified of the situation. In the first case, no other action is required since the notification is only intended to let the user know the battery is fully charged. In the second case, the battery level is dangerously low, considering that the working voltage is 3.3 V. Hence, the Monitoring task takes care of notifying MAX30102 Manager, which does not allow any acquisition to be started. In both situations, the interrupts are disabled until the voltage level returns within normal range. The voltage level is monitored by periodically reading MAX17048 registers; the reading interval is decreased when threshold interrupts are generated to reduce the latency associated to the restoring of normal operation.

The current version of VITAL EKG does not support activity tracking, despite the hardware is fully operational (a design fault is documented in Chapter 7.1.4). A low level library has been designed to allow configuration, reading and calibration of TDK Invensense MPU-9250. A first approach which allows to classify the types of movement and implement a pedometer is suggested in Chapter 7.1.9.

5.2.5 Flash Memory Manager

The Flash Memory Manager handles the internal non-volatile storage using the NVS Driver. The management of the flash memory storage has been offloaded to a dedicated Task mainly to ensure thread-safety. The Task structure consists of a never ending loop which blocks waiting for a Mailbox message. Entities which intends to perform a memory operation are required to enqueue a message in the mailbox using a specified format. In case of write operations, no response is given, except when errors occur; in case of read operations, data is returned using a response Mailbox message, which the caller entity provides in the request Mailbox message.

The Flash Memory Manager source code file includes instructions on how to add support for Micro-SD card operations using FAT32 file system. This feature is not supported in the current version of VITAL EKG because too much RAM is required as working memory to operate a file system.

5.2.6 Memory Configuration

TI CC2640R2FRGZ features 128 kB of non-volatile flash memory, which is shared among the BLE stack, the application and eventual data. Furthermore, it is equipped with 147 kB ROM, which are factory programmed with RTOS code.

Volatile storage includes 20 kB of ultra low-leakage main RAM, further 2 kB of RAM dedicated to SCE and 8 kB of Cache.

Since SCE is not used in this version of VITAL EKG, its memory has been reconfigured as main RAM. It can be found in the linker configuration file as AUXRAM. Furthermore, also the Cache needed to be repurposed as RAM to fit the whole application. Clearly this choice trades speed and power consumption for memory size. Indeed, the Cache, which is found in the linker configuration file as GPRAM, is not an ultra-low-leakage memory and TI CC2640R2FRGZ runs at slightly reduced speed without Cache memory.

5.3 Digital Signal Processing

THIS section illustrates the algorithms which have been employed for DSP. Generally, all the presented algorithms have been developed in MATLAB first to quickly test their effectiveness and reliability on data samples. A second phase has required the translation of MATLAB code to C code, compatible with ARM® CORTEX® M3.

5.3.1 PPG Digital Signal Processing

The implementation of a dedicated algorithm to extract HR and SpO₂ values has been a core activity of this thesis project.

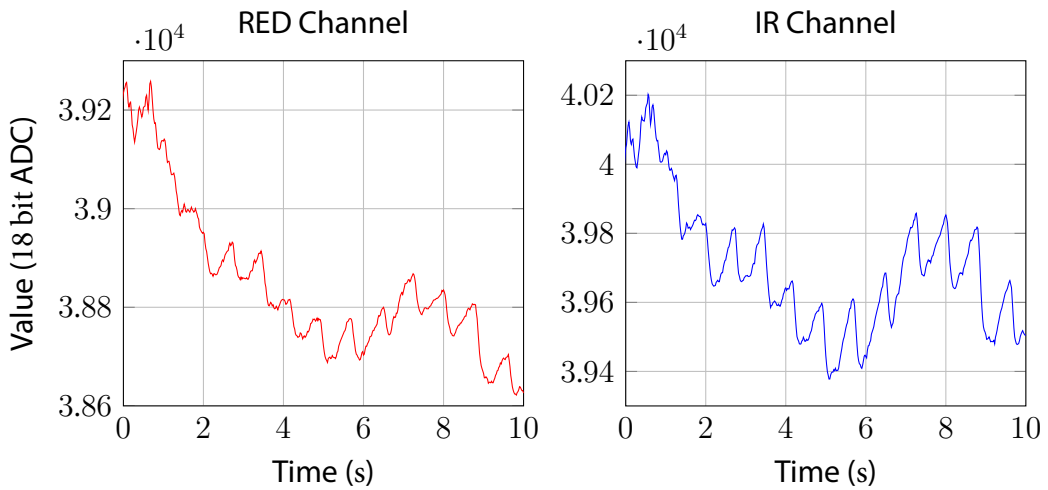


Figure 52: MAX30102 output. 10 s acquisition at 50 Hz (effective).

Due to the limited resources of TI CC2640R2FRGZ (30 kB of RAM overall), data acquisition and data processing phases have been separated. This only partially violates the real-time constraint of VITAL EKG (4). This requirement is relaxed by on-demand acquisitions, as explained in 4.1.

The DSP can be conceptually split in 2 distinct algorithms. The first algorithm allows the identification of both HR and SpO₂ by directly operating on RED and IR channels; the second allows only to find the HR and is used to improve the reliability of the first algorithm. In the following, they are identified as Time Domain (TD) processing and Frequency Domain (FD) processing, respectively.

At this point, it is useful to refer to a typical MAX30102 acquisition. RED and IR channels are shown in Fig. 52. The acquisition has been performed in typical conditions: 10 s at 50 Hz. More details about MAX30102 configuration are included in 4.3.1.

The channels are both characterized by an AC signal superimposed to a large DC signal. Furthermore, the first samples of any acquisition should not be considered because they are affected by artifacts introduced by the finger placed on the sensor. In the following, only effective samples are considered when referring to 10 s acquisitions. Generally, most acquisitions present a slowly-varying baseline signal in both channels. In other words, the DC signal (as defined in [44]) should not be considered constant during an acquisition.

Optimization of the RAM of ARM® CORTEX® M3 has required the DSP to be done few samples at a time. Nonetheless, the processing is not performed online because the acquisition is completed before starting the DSP on the first batch of samples. This kind of processing, easily adaptable to a strictly online scenario, will be called **quasi-online**.

TD processing

TD processing is based on the observation that both channels have a clearly periodic signal. In order to evaluate SpO₂, precise peaks and valleys locations and values must be estimated. Channels are processed sequentially in the same way. Thus, only one channel will be considered during in this Section.

The first step, after loading a few samples from flash memory, is to LPF the signal. Specifications are listed below:

- Butterworth;
- 4th order;
- 5 Hz cut-off frequency;
- unitary DC gain;
- 30 samples step response transient;
- 7 samples maximum group delay (close to 5 Hz).

This step is necessary to reduce high frequency components. It has been implemented as two second order sections Infinite Impulse Response (IIR) filter in Transposed Direct-Form II because of superior numerical stability in fixed point implementations. To minimize the effects of the step response transient, the filter internal state variables are initialized to a typical DC value. Clearly, this static choice does not eliminate the transient but an improvement has been observed. Furthermore, the first 7 samples are not considered in the following processing steps because of the delay introduced by the filter. Results are shown in Fig. 53.

The rest of the processing for main peaks and valleys detection is based on the observation that peaks represent systoles; as such, they are impulsive and after a peak the signal exhibits a large decrease in magnitude in short time. As a consequence, the discrete time derivative of the signal is expected to have large negative peaks right after a peak of the channel signal, as shown in Fig. 54. The differentiation performed according to 5.2 is far from optimal. Indeed, it greatly amplifies noise as well as high frequency useful signal components. However, in-depth testing has proved that a first order difference equation is enough and has the great advantage of being computationally extremely simple.

$$y[n] = x[n] - x[n - 1]. \quad (5.2)$$

After computing the derivative, a threshold value is calculated as a fraction of the minimum value in the time interval.

At this point, it is necessary to evaluate the locations at which the derivative is equal to the threshold. Two points, which are called *left and right threshold locations* in the

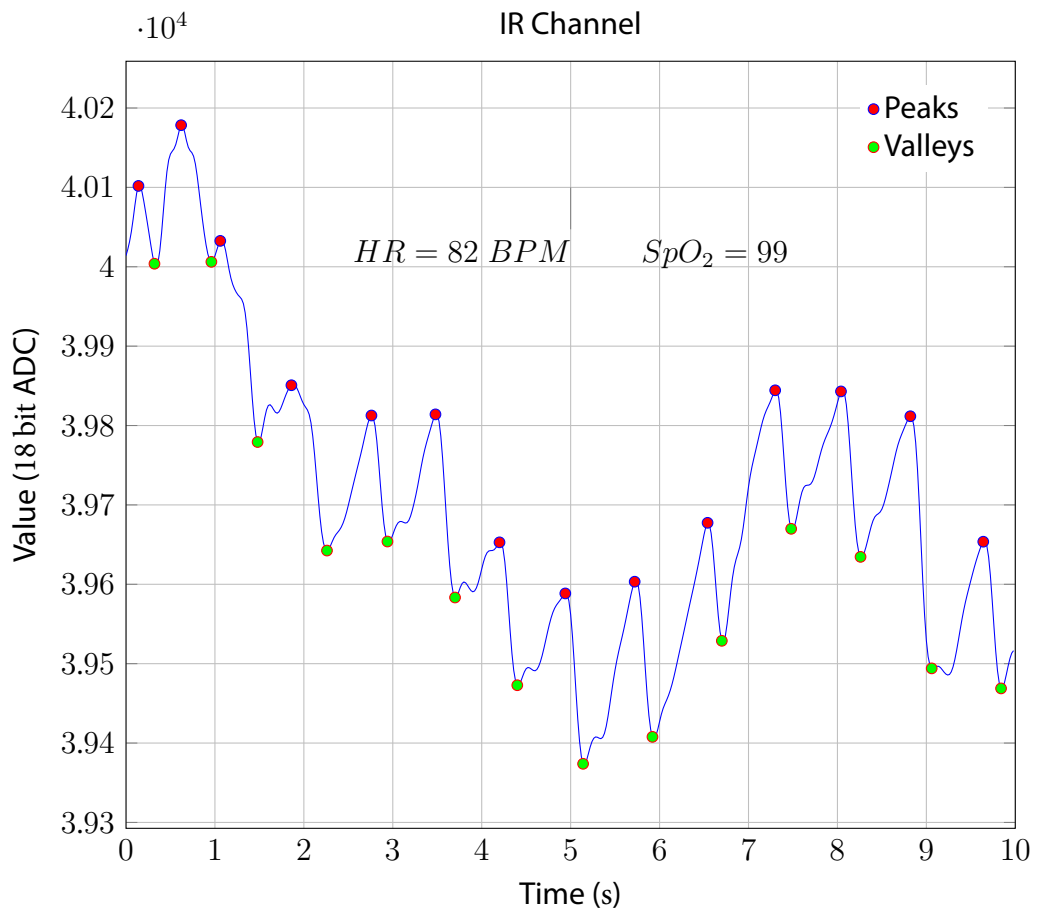


Figure 53: MAX30102 IR channel after Butterworth LPF filtering. Peaks and valleys detected by TD DSP are highlighted.

following, are expected for each peak of the derivative. Clearly, for a digital signal this step is a minimization problem: the pair of points for which the difference between the threshold and the derivative is lower is considered (for each peak).

This step is critical to correctly identify peaks and valleys. Indeed, if a threshold too close to the minimum value is chosen (threshold factor too close to 1), too few peaks might be detected and estimated HR will be too low. To minimize this problem, the threshold factor is initially set close to 1 and iteratively decreased by 10% until at least a pair of threshold locations is found; if no pair is found within the first 5 iterations, systole events are assumed to be absent in the time interval under analysis. If the number of iterations were not limited, threshold locations might be found were no systole event occurred, causing excessive HR estimation.

Since the search of threshold location pairs is performed by scanning linearly the

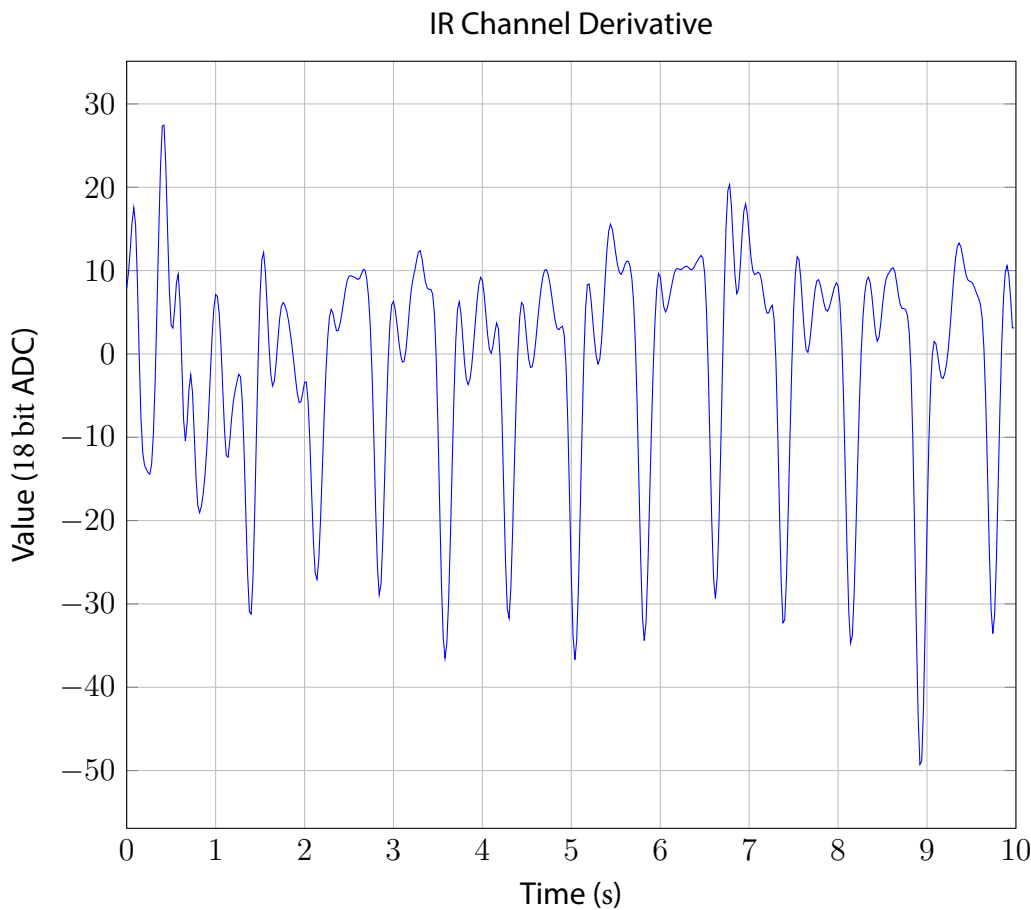


Figure 54: MAX30102 IR channel. First order discrete time differentiation.

sample interval (online detection), a few limit cases are considered below and illustrated in Fig. 55.

1. The first threshold location pair of a sample interval is detected but no peak is really associated to it because the sample interval begins between the peak (which is in the previous interval) and the left threshold location point; a specular case can be identified at the end of the sample interval.
2. Only the right threshold location point is detected at the beginning of a sample interval because the sample interval begins right in the middle of a threshold location pair; also in this situation, a specular case exists at the end of the sample interval.

These problems are solved by considering an adaptive size for the sample interval. More specifically, all the samples which follow the last right point threshold location

are prepended to the following sample interval. A key point to remember is that in a Butterworth filter current output depends on past inputs and past outputs. In other words, it is an IIR filter characterized by zeros and poles. This fact does not allow to perform double filtering of the same samples (the ones which must be prepended to the new sample interval) to avoid a modification of the state of the filter. The sample interval is composed of a variable number of past elements and a fixed number of new elements (50), which are linked together only after filtering.

Once that threshold location points have been identified, peaks and valleys locations can finally be estimated easily. Indeed, it can be assumed that no maxima and minima are present in the interval between a peak and a valley. Thus, for each couple of threshold location points, a peak location can be found by scanning the derivative signal backward starting from the left threshold location point; conversely, a valley can be found by scanning the same signal forward starting from the right threshold location point. In both case, the location of peak and valley is determined by the zero of the derivative signal (in wide sense: finding the zeros of a discrete signal is again a minimization problem).

During forward scanning to find a valley location, the end of the interval might be encountered before a zero is found in the derivative signal (for the last threshold location pair of the interval). In this case, the simplest approach to solve the problem is to modify the number of samples which must be processed again in the following interval. Specifically, it must be extended back up to the right threshold point of the last peak-valley pair successfully detected in the current interval.

The identification of peaks and valleys, along with their locations, concludes the quasi-online, channel-independent processing. The alignment of the channels is key point to successfully estimate SpO_2 : each peak-valley pair of the RED channel should be superimposed to a peak-valley pair of the IR channel. To make sure this happens, the lists of peaks and valleys of the 2 channels are analyzed with a peak-valley matching procedure which keeps only the peaks and valleys whose location differ by less than 5 samples across the channels. A tolerance of ± 5 samples means that RED and IR data can have a shift of no more than ± 100 ms at the typical sample rate of 50 Sa s^{-1} . At this point, HR, expressed in Beats per Minute (BPM), can be estimated easily using Eq. 5.3.

$$BPM = \frac{60f_s}{\overline{PP}}. \quad (5.3)$$

\overline{PP} is the average distance in samples between peaks after the application of the peak-valley matching procedure.

Estimation of SpO_2 is based on computation of RED:IR modulation ratio (Eq. 2.9). Maxim Integrated indicates a simple method for evaluation of DC and AC components [44]. The DC component is the value component of the projection of a peak on the straight line crossing its two adjacent valleys; the AC component is the distance between DC point and the peak used for the projection.

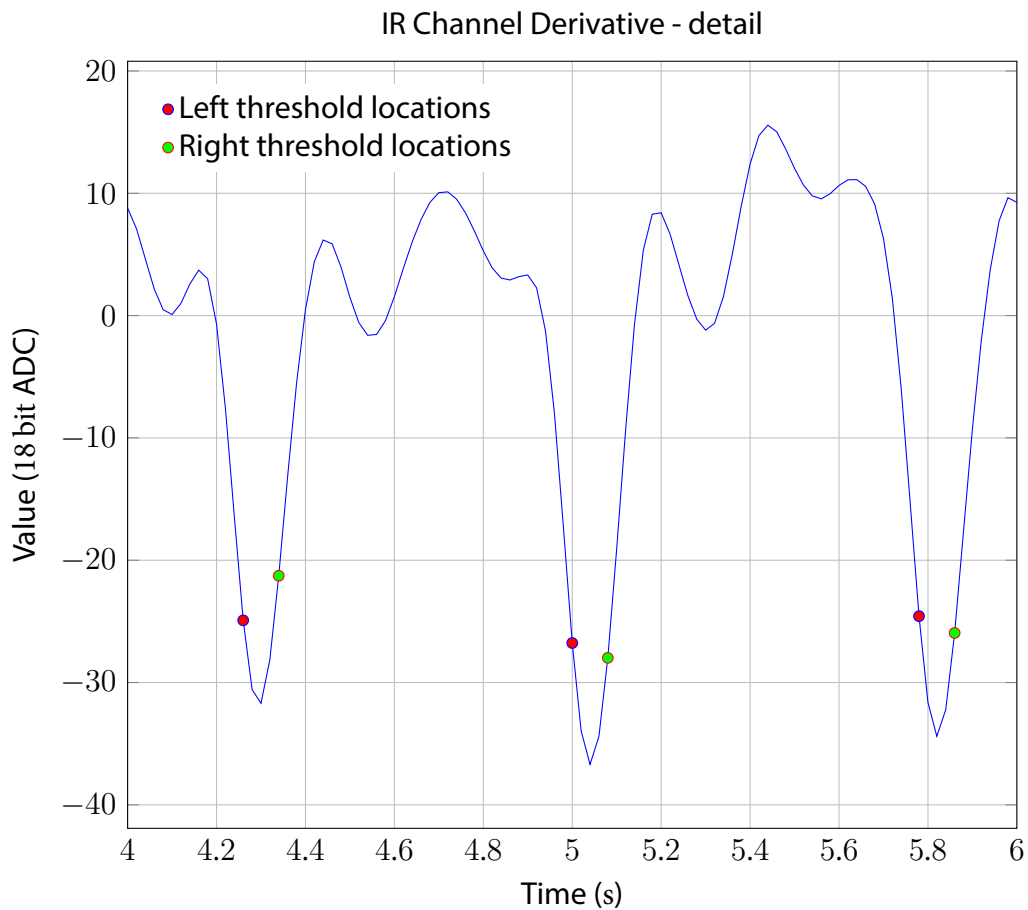


Figure 55: Evaluation of the threshold location pairs in MAX30102 channels.

Finally, the SpO_2 is linked to R by a relationship which strongly depends on the light sources and photodetectors. Maxim Integrated provides the following calibration relation:

$$\text{SpO}_2 = -45.060\bar{R}^2 + 30.354 * \bar{R} + 94.845, \quad (5.4)$$

where \bar{R} indicate the average R across the whole acquisition interval. Testing has underlined that Eq. 5.4 is a parabola which presents an excessive aperture. In practice, values in the range 99% to 100% were too common when compared to the fingerclip sensor used as a reference. For this reason, Eq. 5.5 has been derived experimentally and used instead as a calibration relation.

$$\text{SpO}_2 = -1\bar{R}^2 + 1 * \bar{R} + 1. \quad (5.5)$$

FD processing

FD processing has been implemented to confirm the results obtained with TD processing, thus increasing the reliability of the outputs. In particular, FD processing excels at estimating the HR.

Also this algorithm can be thought as quasi-online. However, since Discrete Fourier Transform (DFT) computation is required, the sample interval has to be larger to correctly locate the frequency components of the signal.

The processing is performed on the IR channel. Conceptually, it could also be done on the RED channel but in practice it works better on the IR channel because it is naturally less noisy (Fig. 52).

A sample interval of 100 samples has been considered. At the typical 50 Sa s^{-1} sample frequency, this translates to an observation of 2 s.

The first step is the removal of the mean. It is done online and in-place by applying equation 5.6. It is required to avoid long transients of the IIR filters which follow this step.

$$\begin{aligned} m &= m + \frac{x[i] - m}{i}, \\ y[i] &= x[i] - m. \end{aligned} \tag{5.6}$$

At this point, the channel signal is filtered with a simple 1st order IIR LPF described by the following difference equation (Fig. 56, ——):

$$y[n] = 0.2 \cdot x[n] + 0.8 \cdot y[n - 1]. \tag{5.7}$$

Then, the channel has been filtered with a Butterworth Band Pass Filter (BPF) with the following parameters:

- 4th order;
- 40 Hz to 200 Hz pass-band;
- unitary DC gain;

This filter has much longer step and impulse responses with respect to the LPF Butterworth which has been previously used for TD processing. However, in the previous case limitation of distortion was important because the value of the channels at peaks and valleys had to be preserved for correct SpO₂ estimation. In this case, however, the only aim is smoothing out the signal as much as possible to preserve only the main frequency component. Time delays introduced by causal filtering are not very important, as long as the relative distance among the peaks is preserved (Fig. 56, ——). Filtering results are

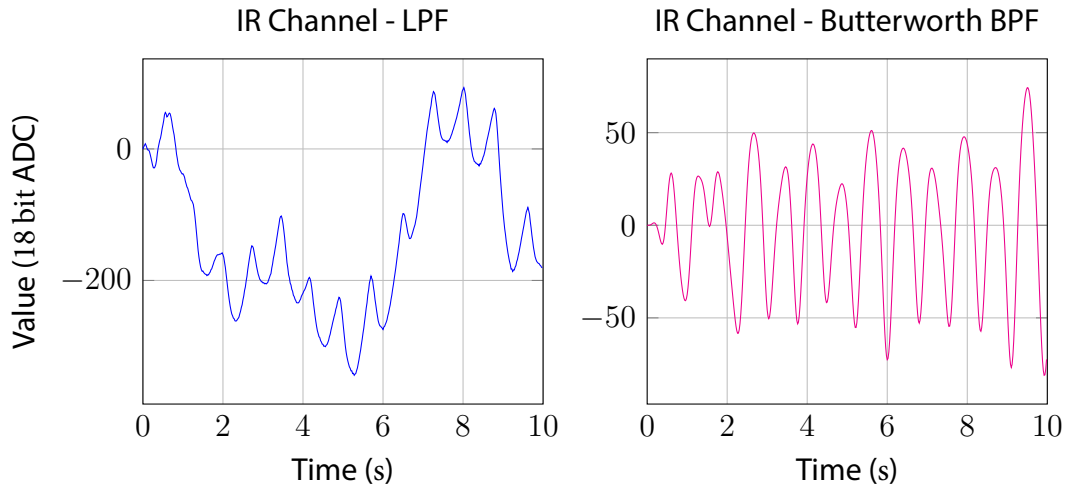


Figure 56: MAX30102 10 s acquisition at 50 Hz (effective). FD processing.

shown on the whole acquisition for presentation reasons. However, as long as the state of IIR filters is preserved during the transition from an interval to the next and no sample is filtered twice, the results are exactly the same.

At this point the channel signal is clean enough to continue the processing in the frequency domain. The HR can be estimated by computing the periodicity of the signal. A simple and reliable way to do that is to calculate the Autocorrelation Function (ACF), that is the correlation of a signal with a delayed copy of itself. The location of the first peak (excluding the one at 0 delay, which is the ACF of the signal with a non delayed version of itself and it's not informative), expressed in seconds, gives the periodicity of the original signal. The ACF for a discrete signal x is defined according to Eq. 5.8.

$$R_{xx}[\ell] = \sum_{i=0}^{N-1} x[i] \cdot x[i - \ell], \quad (5.8)$$

in which $\ell \in \mathbb{Z}$ is the delay of the copy. For a time limited signal of size N , $R_{xx}[\ell] = 0$ for $|\ell| > N$.

The computation of the ACF according to 5.8 has a quadratic complexity; that is not acceptable in most cases in which N is large. An efficient method to calculate the ACF is to use the DFT. Indeed, it turns out that:

$$R_{xx}[\ell] = IDFT \left\{ |DFT\{x[n]\}|^2 \right\}, \quad (5.9)$$

as a consequence of the Wiener-Khinchin theorem [45]. The advantage stems from the fact that the computation of DFT can be performed using Fast Fourier Transform

(FFT) algorithm if $N = 2^m$, reducing the complexity to $N \cdot \log(N)$. Given the size of the interval set to 100 samples, a FFT of size $N = 256$ has been chosen and the signal has been zero-padded to obtain the required length. Moreover, computation of the ACF using FFT requires N to be at least twice the signal length to avoid circular convolution introduced by FFT [46].

Further optimizations have been applied to reduce the memory footprint of the algorithm. In general, a N points FFT algorithm takes a complex sequence of length N and produces a complex sequence of the same length. However, if the input is real the output is guaranteed to be Hermitian. It can be proved that the FFT of a real sequence of length N can be obtained by rearranging the input into a complex sequence of length $N/2$, performing a FFT of length $N/2$ and a few additional computations. In this case, the output is a complex sequence of length $N/2$ which does not present any symmetry [47].

At this point, $|DFT\{x[n]\}|^2$ must be computed. A convenient way to do that is multiplying the complex FFT output of length $N/2$ just obtained by its complex conjugate to obtain a $N/2$ real signal. The optimization exploited earlier is useful again because the inverse FFT of a real sequence of length $N/2$ has to be computed. However, since the ACF is known to be real, it is convenient to mirror² the signal and produce a real even input signal of length N for the optimized inverse FFT algorithm³. Finally, the ACF can be truncated to the first 50 samples because it is even; furthermore, the last 156 samples (zero-padding) are zero (Eq. 5.8). The ACF has been normalized in the interval $[-1; 1]$, since the maximum is always at 0 lag.

The relation between the lags and the HR expressed in BPM is shown in Eq. 5.10. Note the similarity with Eq. 5.3.

$$BPM = \frac{60f_s}{\ell_{peak}}. \quad (5.10)$$

The ACF for 100 samples (from the 300th to the 399th of the IR channel is shown in Fig. 57.

5.3.2 EKG Digital Signal Processing

THE EKG DSP is performed for two reasons. Firstly, the raw signal, as acquired from the ADC, has large noise components which must be filtered in order to appreciate the waves of a typical EKG; secondly, the location of the R waves must be identified to

²When mirroring a signal of length N to produce an even sequence of length $2N$, it must be remembered that FFT algorithm expects a periodic input. As such, mirroring the sequence $\{4, 3, 2, 1\}$ produces $\{4, 3, 2, 1, 1, 2, 3\}$ which is even when extended to $[-\infty; +\infty]$.

³Alternatively, the (inverse) FFT of a real even sequence can be computed efficiently using a Discrete Cosine Transform (DCT). This step would further halve the complexity and the memory requirements. Efficient algorithms to compute the DCT based on FFT are documented in literature [48].

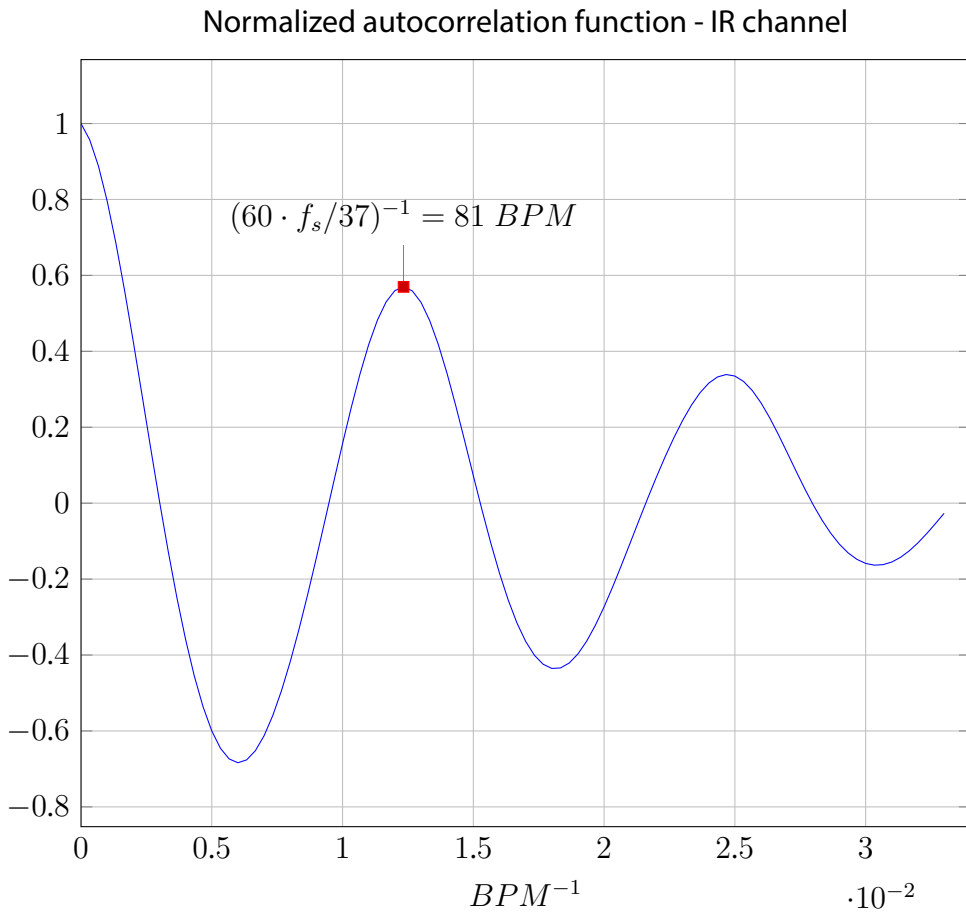


Figure 57: MAX30102 IR channel. ACF for 100 samples (from the 300th to the 399th). Acquisition at 50 Sa s^{-1} .

provide an estimation of the HR which has to be compared to the one obtained with PPG acquisition.

Denoising

The analog front end provides a signal with a useful bandwidth which ranges from 0.5 Hz to 100 Hz. To understand which filters are more suitable, it is useful to analyze both the raw signal and its spectrum. They are reported in Fig. 58 and 59. The acquisition has been performed at an effective frequency of 500 Sa s^{-1} for 10 s.

The spectrum provides some insights:

- Large DC component is expected and is due to the artificial offset of 1.65 V introduced by the differential section of the analog front end. It must be removed

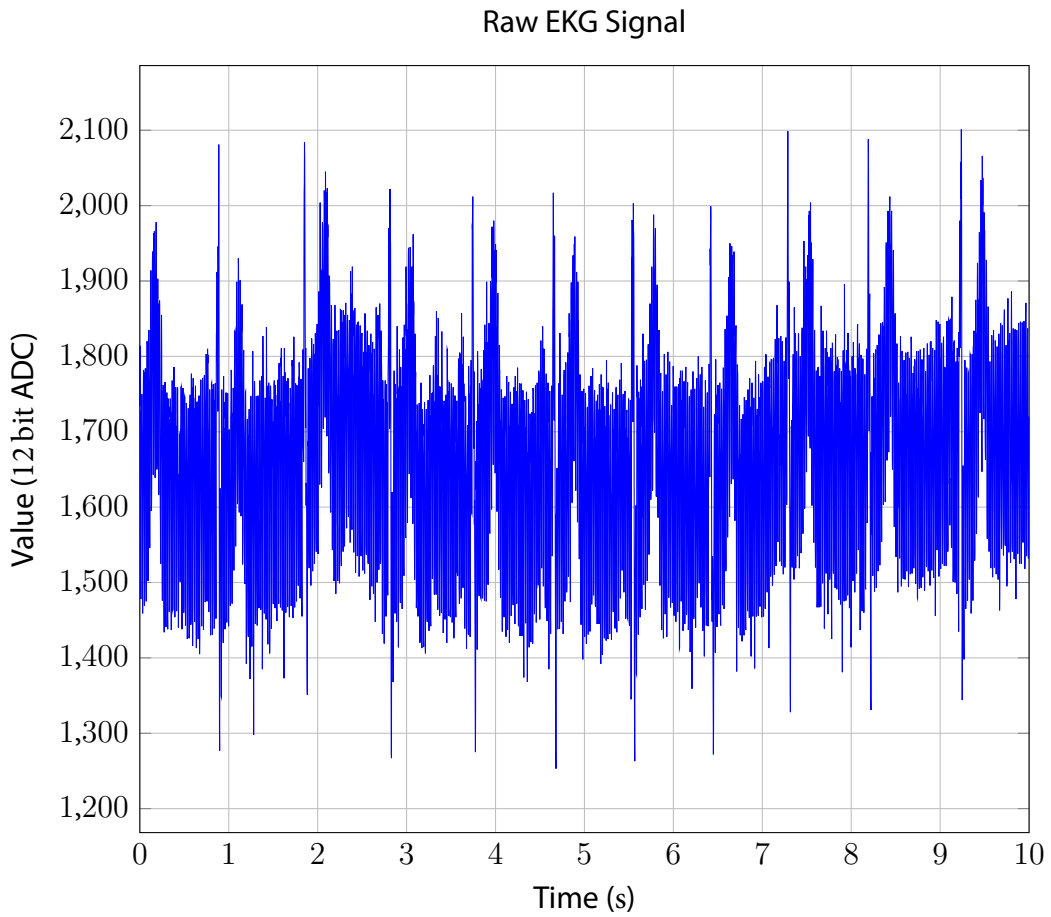


Figure 58: Raw EKG signal. Acquisition of 10 s at 500 Sa s^{-1} .

before processing to minimize the step response of IIR filters.

- There is a strong 50 Hz component (and multiples) due to mains. Upon careful inspection, the first peak in the spectrum occurs at 49.68 Hz. After exhaustive testing with a 50 Hz sinusoidal signal, it was found that the internal ADC of TI CC2640R2FRGZ introduces a systematic frequency shift. The simplest solution to this problem is to set the sampling frequency at 496 Sa s^{-1} . This value has been obtained experimentally.

The processing of raw EKG signal has been kept as simple as possible to preserve the features of the signal and avoid distortions. As a first operation, the artificial offset of 1.65 V has been removed sample by sample. This is possible because this offset has been intentionally introduced in the analog front-end to make the waveform compatible with single-rail supply voltage. The remaining DC component, along with 50 Hz and multiples

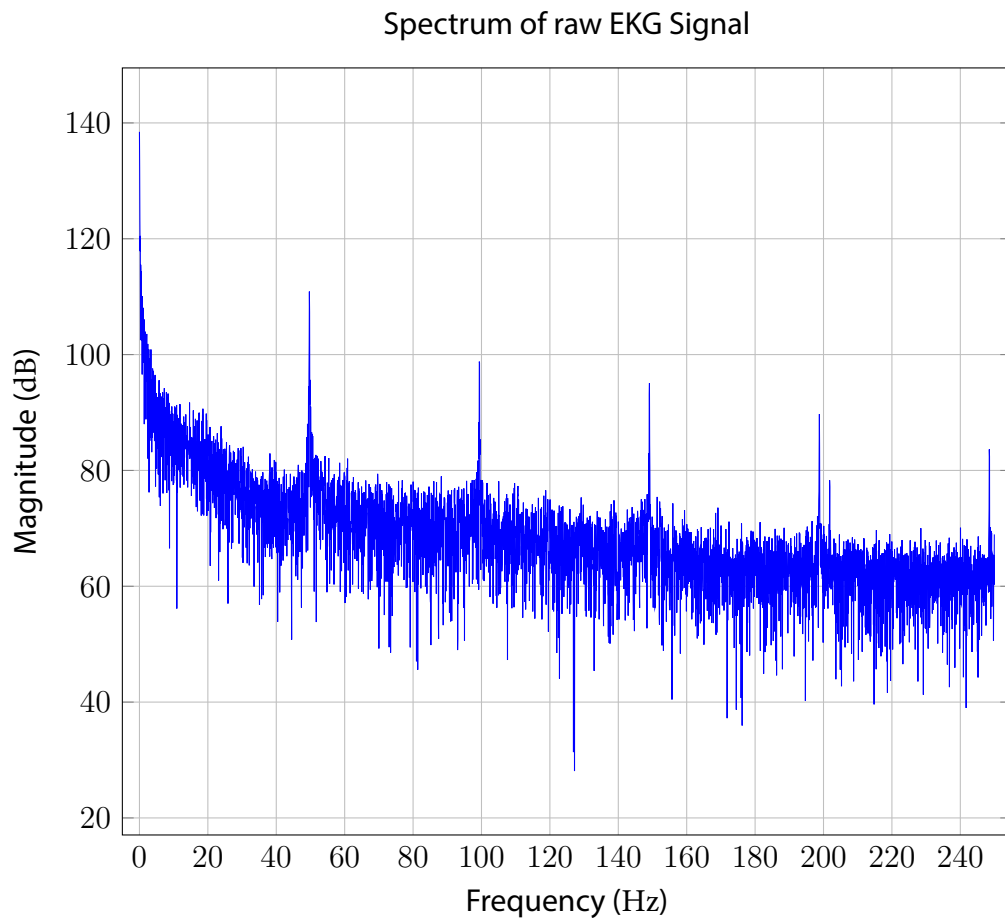


Figure 59: Spectrum of raw EKG signal computed with FFT of size 2^{13} .

and slowly-varying baseline components, has been removed using a **Comb Notch** filter with the following specifications:

- order $N = 10$;
- bandwidth $BW = 0.01$;
- unitary DC gain;
- 300 samples step response transient;
- 300 samples impulse response transient;
- 64 samples maximum group delay at notch frequencies.

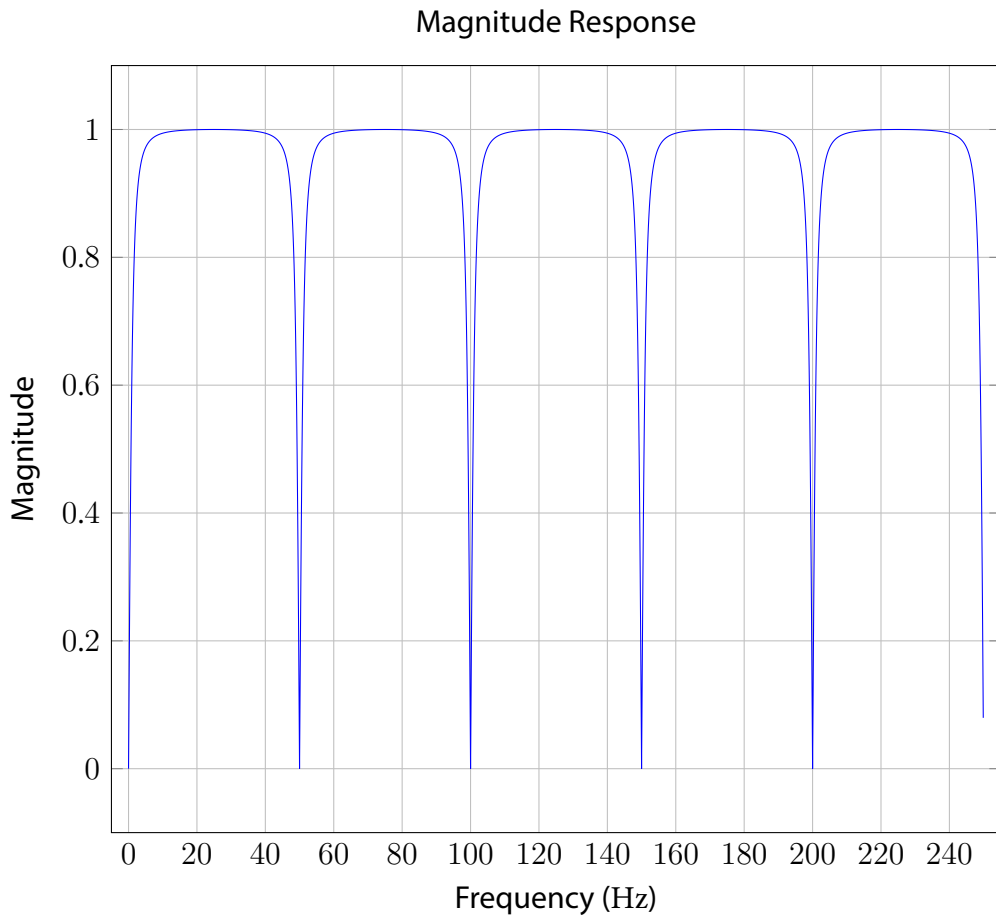


Figure 510: Magnitude response of 10th order Comb Notch filter.

The order is computed according to Eq. 5.11.

$$N = \frac{f_s}{f_f}, \quad (5.11)$$

where $f_s = 500 \text{ Sa s}^{-1}$ is the sampling frequency and $f_f = 50 \text{ Hz}$ is the center of the notch where the filter provides maximum attenuation. A 10th order comb notch exhibits 10 equally spaced notches in the range $-f_s/2$ to $f_s/2$. The bandwidth is computed at -3 dB and represents the width of the notch. The magnitude response is shown in Fig. 510.

The comb notch filter is the simplest approach to denoise a EKG signal. However, the 300 samples impulse response transient heavily affects the QRS complex, which behaves like an impulse. Furthermore, the group delay has peaks of 64 samples at multiples of 50 Hz. Significant distortion is introduced for these frequencies. To provide

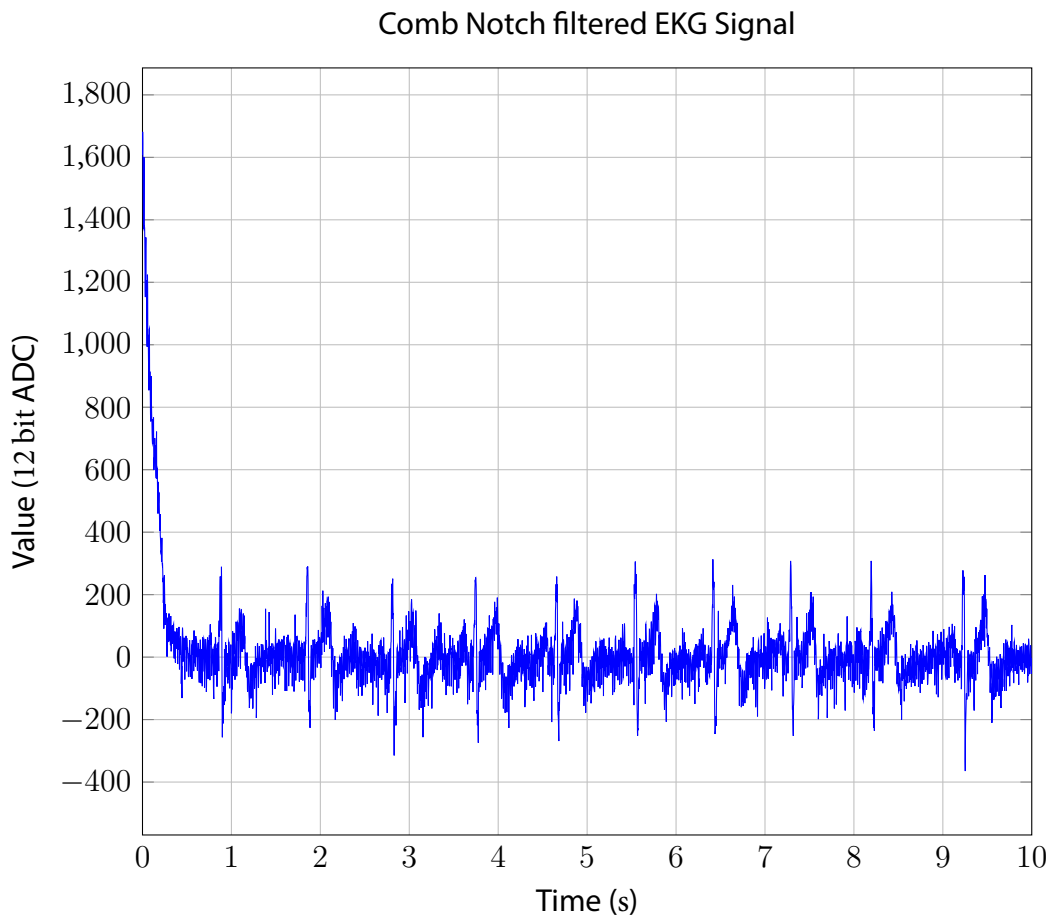


Figure 511: EKG signal after Comb Notch filtering.

a reference for these numbers, it's worth recalling that a typical QRS complex lasts from 60 ms to 100 ms, which corresponds to 30 and 50 samples, respectively, at 500 Sa s^{-1} . The first half second of acquisition turns out to be not usable due to the comb notch. Since synchronization with PPG signal is required, this is not a problem because PPG processing requires to discard a whole second to eliminate the transient linked to the positioning of the finger on the sensor. The output of the comb notch filter is shown in Fig. 511.

The QRS complexes are visible, even though further processing is required, especially to remove high frequency components. The spectrum of the comb notch filtered EKG signal shows that noise from mains is not really a narrow peak but spreads across several Hz. As a consequence, a narrow comb notch is not sufficient to remove these components. On the other hand, a comb notch with greater bandwidth would further worsen its performance with respect to impulse response transient length and group

delay. For these reasons, a 4th order Low-Pass Butterworth filter has been applied after the comb notch. Specifications are listed below.

- order $N = 4$;
- cut-off frequency $f_c = 40$ Hz;
- unitary DC gain;
- 30 samples step response transient;
- 30 samples impulse response transient;
- 8 samples maximum group delay at cut-off frequency.

This filter provides an attenuation of only 9 dB at 50 Hz; it is much more effective at its multiples, providing 36 dB attenuation at 100 Hz. Furthermore, introduced distortions are very modest with respect to the comb notch.

The filtering phase has been concluded with the application of 2 moving average filters of length 10 (also called box filters) to smooth out the signal. The use of moving average filters is controversial. Their response is Low-Pass but they have the downside of widening the QRS complexes. Further analyses of the signals cannot rely on typical QRS complex duration after the application of wide box filters.

The final result of the denoising filtering is shown in Fig. 512. The distortions introduced by the comb notch filter are clearly visible in increased S wave after the R wave and negative deflection after the T wave. Furthermore, the ST segment should be isoelectric and the increased S waves cause this feature not to be visible. Finally, 50 Hz noise components remain because Butterworth LPF is only moderately effective at this frequency.

5.3.3 QRS complexes identification

The identification of QRS complexes is in development on the Central device, after BLE transmission to the denoised EKG waveform. The employed procedure is a modified version of Pan-Tompkins algorithm, which is a classic QRS detection routine introduced in 1985 by J. Pan and W. Tompkins [48].

5.4 Android Application

An Android application is in development to pair VITAL EKG with a user-friendly visualization of acquisition results. A rendering of the interface is shown in Fig. 513.

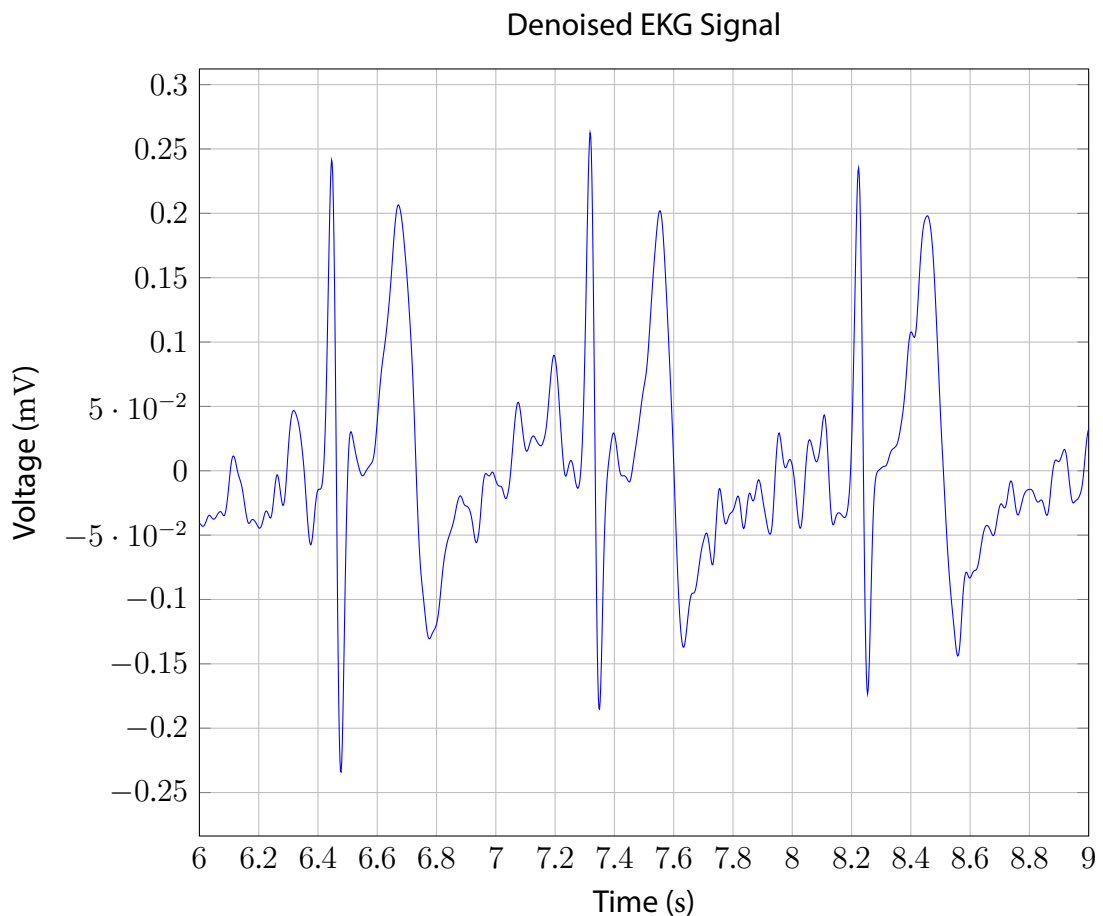


Figure 512: EKG signal after denoising filtering. Focus on 3 s. The signal is scaled by the total amplification of the analog front end (705).

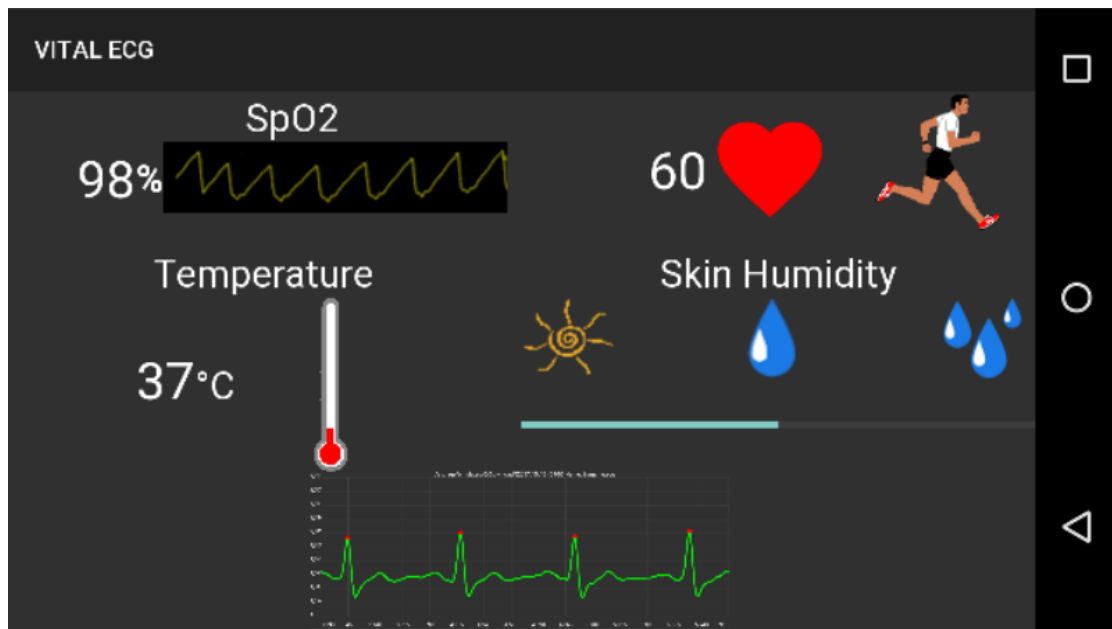


Figure 513: Android app rendering. Results window.

CHAPTER 6

Testing and Discussion

AFTER complete hardware testing, which highlighted a few pitfalls in the design which are described in all detail in Chapter 7.1, VITAL EKG's firmware has been verified to ensure correct behaviour in all circumstances without deadlocks and to assess correctness and accuracy of the algorithms discussed in 5.3.

6.1 Testing with Vital Sign Patient Simulator

ALL the algorithms described in 5.3 have been coded specifically for VITAL EKG. In some cases, such as TD PPG processing, the algorithms have been engineered from scratch; in other cases, such as FFT implementation, the coding phase has been limited to a translation of already existing Matlab code or pseudocode found in literature. To exclude potential pitfalls in the design phase of the algorithms, the initial testing has been performed with Fluke ProSim 3 Vital Sign and ECG Simulator.

6.1.1 EKG Acquisition System

The analog front end, along with the ADC configuration, has been tested using Fluke ProSim 3 Vital Sign and ECG Simulator. LA and RA terminals have been used and attached to VITAL EKG's electrodes. Several of the available configurations have been tested but only a few of them are included in this section for brevity. Unfortunately Fluke ProSim 3 Vital Sign and ECG Simulator does not allow to export data to assess numerically the acquisition system. For each test, both the raw (—) and denoised (—) signals are included. All the acquisitions have been performed for 10 s at an effective sampling frequency of 500 Sa s^{-1} (the ADC has been set to $16 \cdot 496 \text{ Sa s}^{-1}$ for an oversampling of 2 bit).

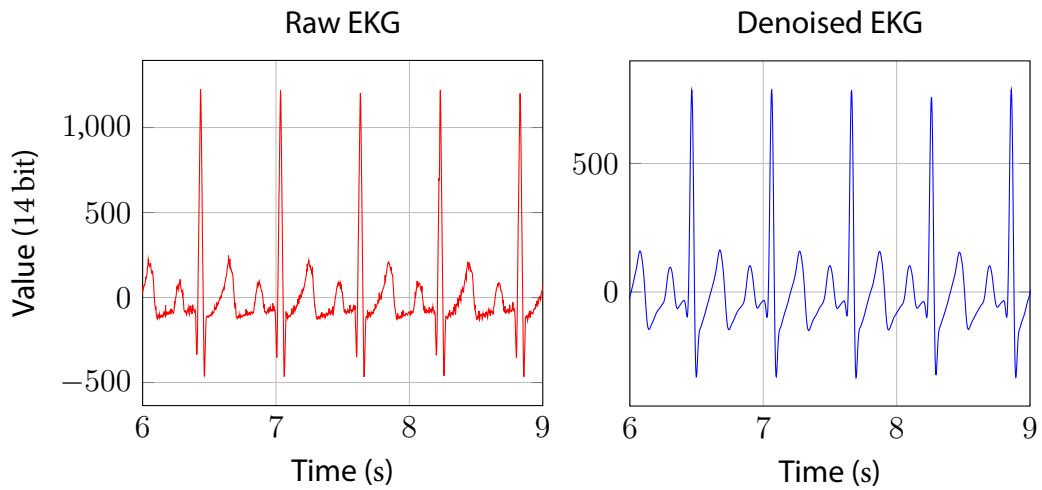


Figure 61: ProSim 3 waveform. 100 BPM, 1 mV, adult.

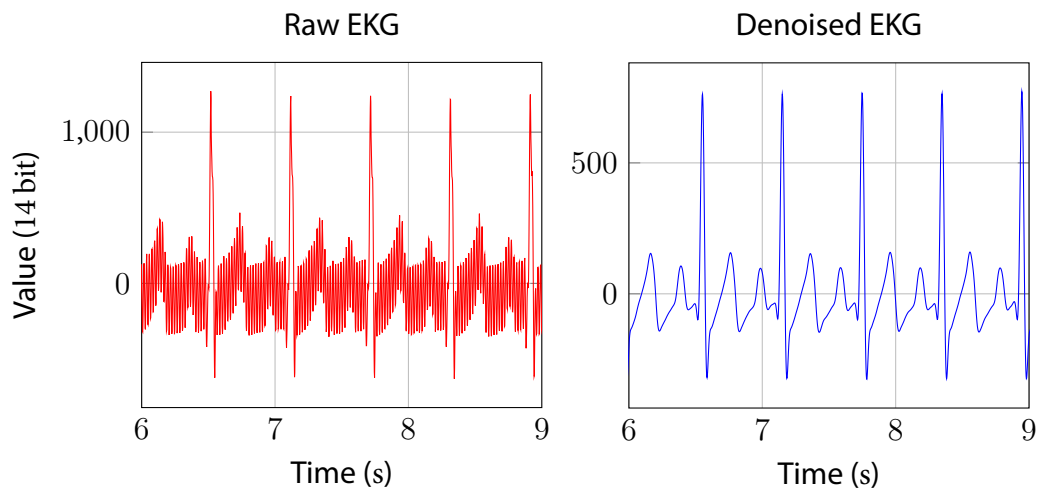


Figure 62: ProSim 3 waveform. 100 BPM, 1 mV, adult, 50 Hz noise.

Fig. 61 and 62 show a healthy heart with an accelerated heart rate of 100 BPM. Artificial mains noise at 50 Hz is added to the waveform in Fig. 62. In this case the filtering is effective, with two major drawbacks:

1. the short ST interval is not isoelectric, due to the strong distortion that the Comb Notch filter introduces. The effect worsens with accelerated heart rates.
2. Comb Notch aggressive filtering introduces an artificial negative deflection after

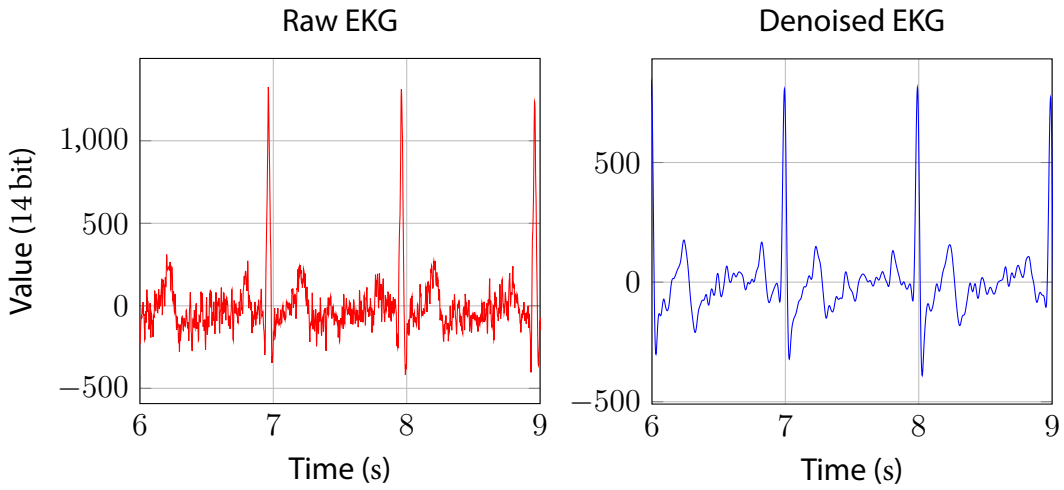


Figure 63: ProSim 3 waveform. 60 BPM, 1 mV, adult, muscular noise.

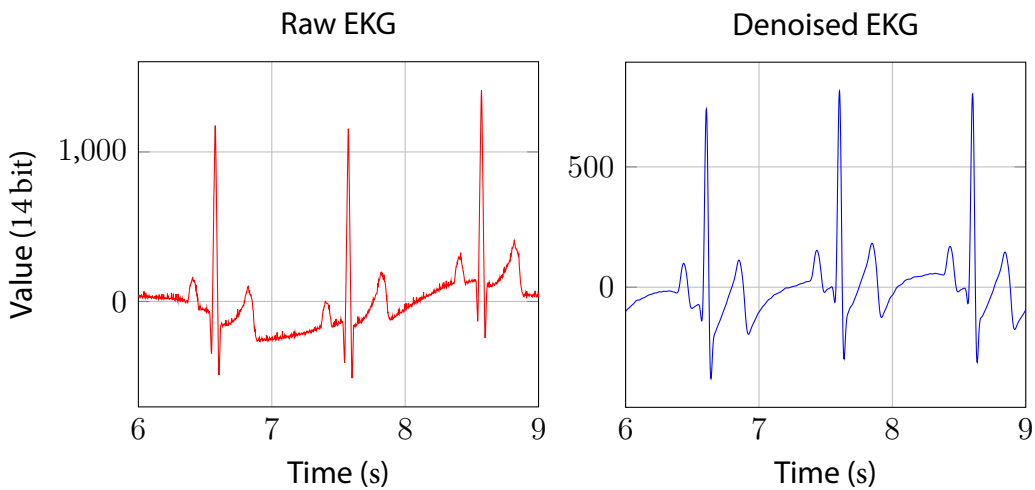


Figure 64: ProSim 3 waveform. 60 BPM, 1 mV, adult, breathing noise.

the T wave.

Fig. 63, 64 and 65 introduce artificial muscular noise, breathing and wandering effects, respectively. Muscular noise cannot really be removed completely because its frequency coincides with important frequency components of the EKG signal.

Breathing introduces a low frequency baseline in the signal around 0.3 Hz. The hardware 1st order High-Pass filter, realized by the feedback integrator network of the instrumentation amplifier, does not help in this case because it has been designed with

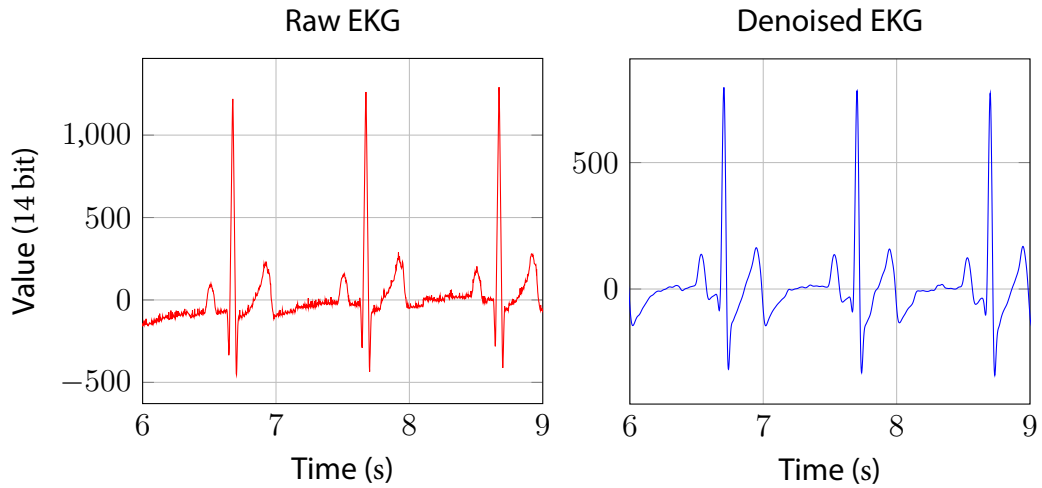


Figure 65: ProSim 3 waveform. 60 BPM, 1 mV, adult, wandering noise.

a cut-off frequency of 0.48 Hz.

The Comb Filter is instead effective. Indeed, it has been designed with a bandwidth $BW = 0.01 \cdot f_s/2 = 2.5$ Hz, which means only half of it lies in the positive frequency axis for the DC notch. The attenuation provided at 0.3 Hz is greater than 12 dB. The baseline is not completely removed and is still visible between the T wave and the P wave, where the signal presents an abnormally increasing segment.

The term wandering noise groups all the movements which modify the conduction paths during the acquisition. These includes, for example, small arm movements, which are very common in real EKG acquisition. The net effect is a denoised signal very similar to the previous case.

Fig. 66 depicts a simulation of atrial fibrillation condition. The atria contract autonomously and the ventricular systole is not regular. In this case, the oscillations which derive from atrial contractions are not removed by the denoising algorithm, potentially allowing correct identification of the condition.

Many other waveforms have been tested. However they are not included because the focus of this thesis work is not on the correct identification of cardiac abnormal rhythms.

6.2 Testing on Patients

A further validation phase was carried out with the help of generally healthy subjects. A few difficulties have been encountered and are presented in this section, along with relevant results.

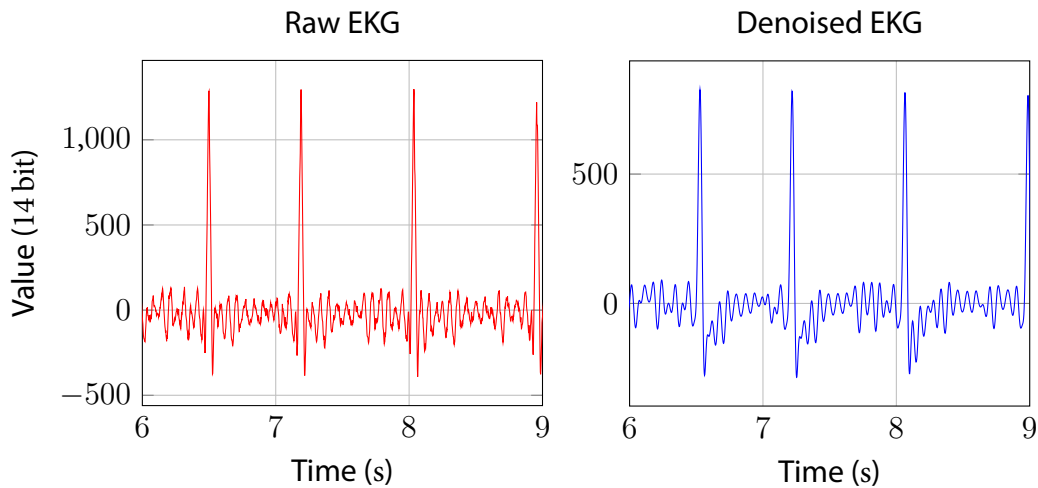


Figure 66: ProSim 3 waveform. 1 mV, adult, atrial fibrillation.

6.2.1 EKG Acquisition System

EKG acquisition system, as underlined already in previous Chapters, presents weak points in the DSP. Specifically, the step and impulse responses of the Comb Notch filter introduce deflections both after R waves and after T waves.

Furthermore, a meaningful validation of the analog front-end and digital filters would require a numerical comparison with a synchronized waveform acquired by a professional certified electrocardiograph. Unfortunately, such a system is not available at the time of writing.

6.2.2 Maxim Integrated MAX30102

The validation of Maxim Integrated MAX30102 with artificial PPG signals has been tried with Fluke SPOT Light SpO₂ FUNCTIONAL TESTER. Unfortunately this tool is only intended to test transmittance based devices, since it features photodetectors and LEDs on opposite sides. In order to generate a signal, two samples of MAX30102 were mounted on the tester. The first sample was positioned below the tester, in order to face the photodetectors and allow the generation of a suitable response, which was measured by the first sample. The system as whole did not produce intended results, probably as a consequence of misaligned emission and detection phases. Since MAX30102 only mounts one photodetector which is sensible to both RED and IR light, the acquisition circuitry of MAX30102 needs to be synchronized with the LEDs to save the values in the internal FIFO memory in the correct position. The synchronization was clearly not possible between two different MAX30102 devices.

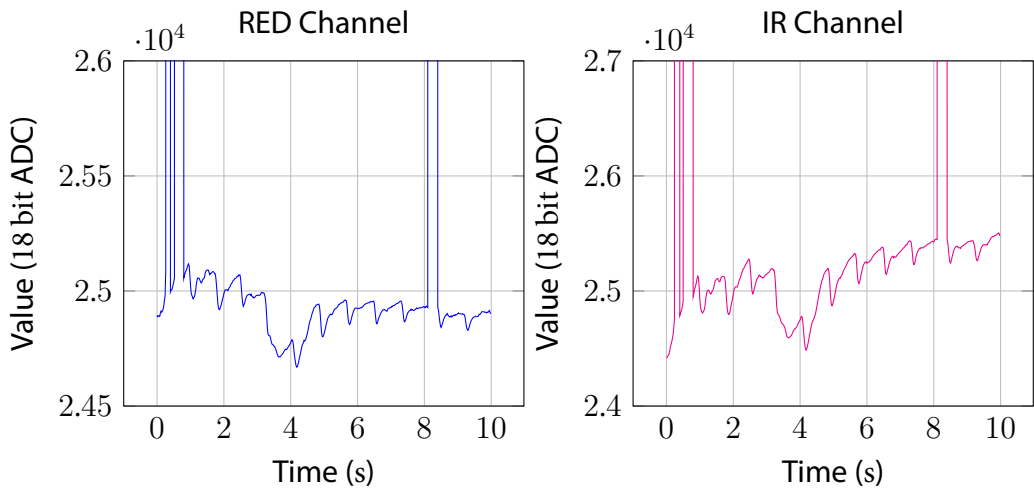


Figure 67: MAX30102 acquisition with a sensor with faulty FIFO memory

Testing of Maxim Integrated MAX30102 underlined a weakness of the internal FIFO memory. Five samples of MAXREFDES117 have been tested with the following results:

- sample 1: failure after 6 weeks;
- sample 2: failure after 4 weeks;
- sample 3: no failures;
- sample 4: failure from day 1;
- sample 5: no failures.

The sensor samples have been configured in the same way. The failure consisted in saturation of a random number of contiguous bytes. An example of such situation is shown in Fig. 67, where saturated samples have been cut to show the meaningful portion of the signal. Since a single sample is 3 B long, saturated samples have value 2^{24} . Several acquisitions have shown that the number of saturated samples tend to be small. More specifically, it has been noticed that replacing the saturated samples with constant values equal to the last non-saturated sample does not invalidate HR and SpO₂ estimation because the beat can still be identified in most of the cases.

HR and SpO₂ were estimated for 10 subjects using MAX30102 PPG waveforms with onboard processing. Results are compared with JPD-500E fingertip Pulse Oximeter and reported in Table 61.

In one case (subject 6), TD and FD gave compatible results only using the thumb. The subject was also wearing red nail polish. Since the nail polish was present on all the

Table 61: Comparison among VITAL EKG and JPD-500E fingertip Pulse Oximeter on HR and SpO₂.

Subject	Gender	VITAL EKG		JPD-500E	
		HR	SpO ₂	HR	SpO ₂
1	M	65	98	65	97
2	M	64	99	66	98
3	M	65	99	67	98
4	M	57	98	60	98
5	M	64	99	64	99
6	F	78	97	80	99
7	F	63	98	63	98
8	F	82	99	84	99
9	F	74	99	74	97
10	F	77	98	78	98

fingers but only the thumb allowed to complete the processing successfully, the reason lies in the particularly small size of the fingers. In order to obtain a significant SNR, the finger must cover completely the LEDs and photodetector and no light shall diffuse into the environment.

CHAPTER

7

Conclusions

THIS Chapter documents limitations of VITAL EKG, such as hardware errors which have been noticed during testing, bugs and potential weaknesses in the firmware; it also gives suggestions on possible improvements of DSP. Furthermore, it provides guidelines to improve VITAL EKG in future releases and implement new features.

7.1 Limitations and Future Work

DURING the electrical and functional testing of VITAL EKG PCB, a few design errors in the schematic have been discovered. They are documented here such that a future version of VITAL EKG can correct them.

7.1.1 Pull-up Resistors

Pull-up resistors should have been included for TI HDC2010 temperature and humidity sensor and Micro-SD card interrupt traces. For TI HDC2010 a polling technique has been used to read data, as described in 5.2.4; the Micro-SD card interrupt functionality would have allowed to understand when a card is inserted and ejected. Since this first version of VITAL EKG does not offer firmware support for the Micro-SD card, this problem remains open.

7.1.2 Micro SD card Support

A number of solutions have been explored to include the micro SD already in this first version of the firmware, including raw use of the card and a FAT32 filesystem. Raw

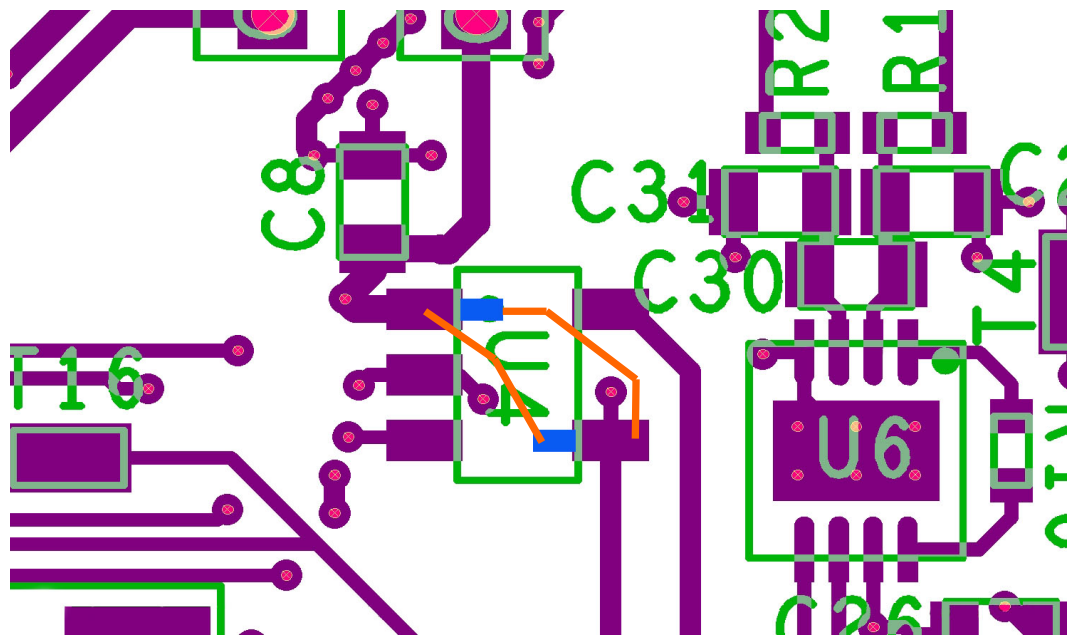


Figure 71: Correction of TI REF2033 (U4) schematic symbol error in PCB. bent pins are in blue. Orange lines are wires.

reading and writing operations, despite straightforward from the implementation point of view, are not an optimal solution because VITAL EKG was designed with hardware support for a Micro-SD card to be able to offload old acquisitions quickly, eventually enabling post processing of raw data with a desktop application and relaxing the real-time requirements. Clearly, raw use of the card forces the desktop application to be aware of the exact location of the data.

TI provides a third-party FAT32 implementation, adapted from an open source project to use TI CC2640R2FRGZ peripherals and TI's drivers. However, the memory footprint of the filesystem library is too large and a successfull integration has not been possible.

7.1.3 TI REF2033 Symbol Error

TI REF2033 feature a 5-pin SOT-23 package. During the creation of the schematic symbol for this component, pin 1 (VIN) and 4 (BIAS) were inverted. The problem was discovered during electrical testing of the PCB. The fix consisted in bending the pins such that wires could be hand soldered from the bent pins to the correct pads. The operation is documented in Fig. 71.

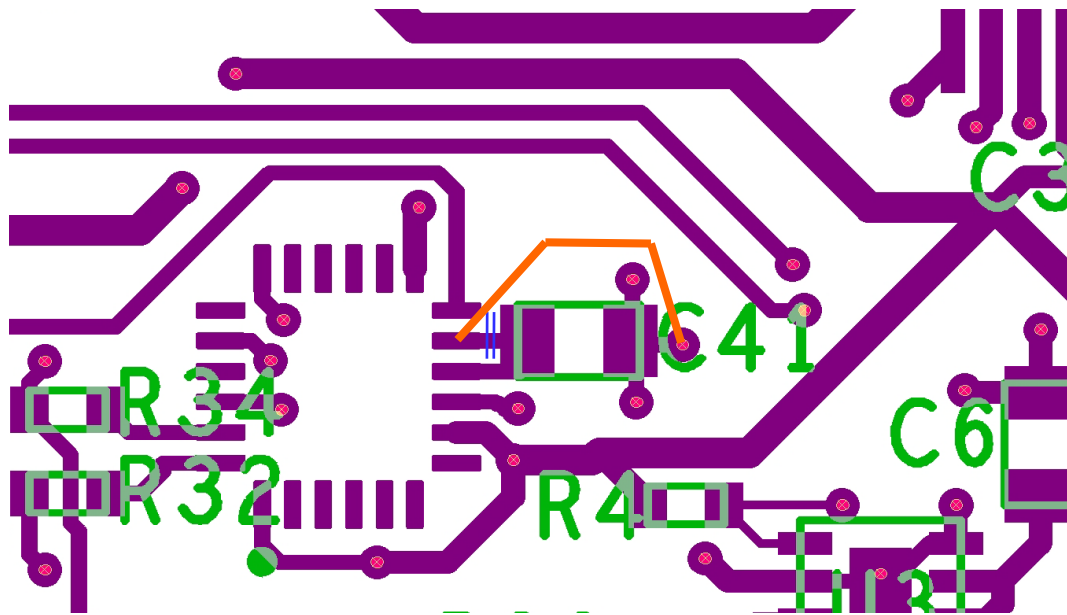


Figure 72: Correction of TDK Invensense MPU-9250 (U9) schematic connection error in PCB. The trace cut is represented by 2 parallel blue lines. Orange line is the wire which needs to be soldered.

7.1.4 TDK Invensense MPU-9250 Connection Error

A schematic mistake about TDK Invensense MPU-9250 9-axis motion-tracking unit was discovered during functional testing. Also in this case, a modification of PCB was necessary to correct the error. More specifically, FSYNC (pin 11) needed to be connected to ground and was instead connected to pin 10 (the schematic in Fig. 49 is already correct). To fix the problem, the trace was cut and a wire has been soldered from pin 11 to ground. The operation is documented in Fig. 72.

7.1.5 MAX30102 Errors

Maxim Integrated MAX30102 pulse oxymetry sensor appeared to present a weakness in the management of the FIFO. Indeed, even though it features a 18 bit ADC, saturation to $0xFFFFFFF$ happened randomly during an acquisition for a random number of samples. The weakness is thought to be related to the FIFO, since the saturation occurs for both channels at the same time.

Moreover, the FIFO turned out to be unable to receive samples from the ADC at a rate greater than 50 Sa s^{-1} . Several combinations of ADC sampling rate and onboard averaging were tested to debug this problem, which did not occur when the sampling frequency was set at 400 Sa s^{-1} with averaging of 8 consecutive samples. Increasing the effective rate

at which the FIFO received samples caused FIFO almost full interrupts to be generated randomly even though the sensor was configured properly. Possible solutions include using a more recent version of the IC (e.g., MAX30110, MAX30112, which are described by Maxim Integrated as optimized versions of basic MAX30102).

7.1.6 Acquisition and Processing Global Buffer

TI CC2640R2FRGZ features an ultra low-leakage RAM which is barely enough to support basic functionalities of VITAL EKG. In order to optimize the memory usage at all times and minimize deadlocks caused by failed memory allocations, dynamic memory usage has been limited to short messages for inter-task communication. Large arrays for data acquisition and processing were initially allocated from the stack of the tasks. This approach caused large portion of RAM to be used only rarely. The problem was solved by noticing that a unique large memory buffer could be used for all operations which could be time-multiplexed. Great care has been taken to ensure thread-safety, even though using a globally allocated buffer leads to code which is hard to be maintained because it is difficult to remember which portion of the array is used in which task at any given time.

A possible solution would be to move the array in the Flash Memory Manager. Tasks which intend to use the memory buffer would need to register with the Flash Memory Manager; messages would be used to request a portion of memory and return the same memory after use. The Flash Memory Buffer could ensure thread safety by book keeping all requests.

This approach apparently looks similar to using a heap memory manager. However, the memory buffer would still be allocated on the stack, thus avoiding potential dynamic memory allocation failures.

7.1.7 EKG Processing

The EKG processing has been intentionally kept simple to provide a proof of concept for VITAL EKG. DSP clearly showed that a Comb Notch filter should not be used for this application because it introduces artifacts in the signal due to its long impulse response. Many more advanced techniques are described in literature, such as adaptive filters and processing based on wavelet transforms [49].

7.1.8 Calibration of TI HDC2010

TI HDC2010 temperature and humidity sensor allows onboard offset compensation by setting specific registers. More complex errors, like gain and hysteresis, can be corrected using a look-up table. Clearly, the look-up table needs to include many values in order to

provide high accuracy. Given the limited non-volatile flash memory to store such table, the best approach would probably be to perform the correction on the Central device.

7.1.9 TDK Invensense MPU-9250 Motion Tracking Algorithm

TDK Invensense MPU-9250 is fundamental for VITAL EKG because a motion tracking unit can provide additional information which are required to filter out wandering and muscular noises from EKG signal. Furthermore, many studies (such as [50]) are devoted to the development of algorithms to detect several types of motion, such as walking, running, phoning statically. A library to configure MPU-9250 and read output data has been written and can be used as a basis for a development of motion tracking algorithms.

7.1.10 Blood Pressure Estimation

Recent works have shown that synchronized EKG and PPG waveforms can provide an estimation of systolic blood pressure [51]. The method is extremely promising to replace cuff-based blood pressure measurements and enable continuous monitoring of this important vital sign.

The **pulse transit time**, which is the time elapsed from an R wave to the fingertip PPG waveform peak, is believed to be related to the systolic blood pressure through arterial stiffness. Diastolic blood pressure estimation poses more challenges. Indeed, while the beginning of a ventricular systole can be easily detected because it is marked by a R wave, diastole detection algorithms cannot rely on clear fiducial marks.

7.2 Concluding Remarks

A first proof of concept of a wrist-worn PHS device has been designed. VITAL EKG only partially fulfills the requirements due to technological limitations related to the positioning of the electrodes for *LEAD-I* EKG. Moreover, a novel set of algorithms have been designed to process PPG signals, despite a few problems with the specific sensor employed in this first hardware revision have been encountered. The presence of temperature and humidity sensors, as well as a motion-tracking unit, potentially allows to correlate HR and SpO₂ with the daily activities of the user, thus providing more accurate estimation of general health conditions. Low-power Bluetooth v4.2 communication provides nearly infinite possibilities to connect VITAL EKG with the Internet of Things. Finally, this work sets the basis for more advanced studies using the same hardware. A general firmware and software framework, composed by interface libraries to communicate with sensors and an Android application, have been designed specifically to ease customization and documented thoroughly to guide the developer and provide a steep learning curve.

APPENDIX A

PCB Design Material

A.1 Gerber Files

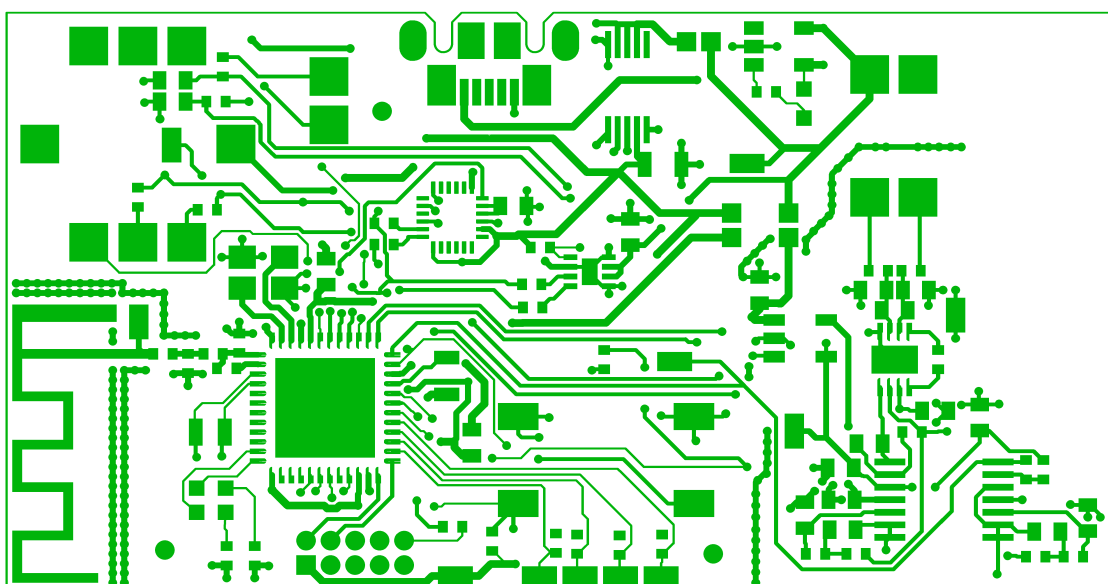


Figure A1: VITAL EKG: Top Layer.

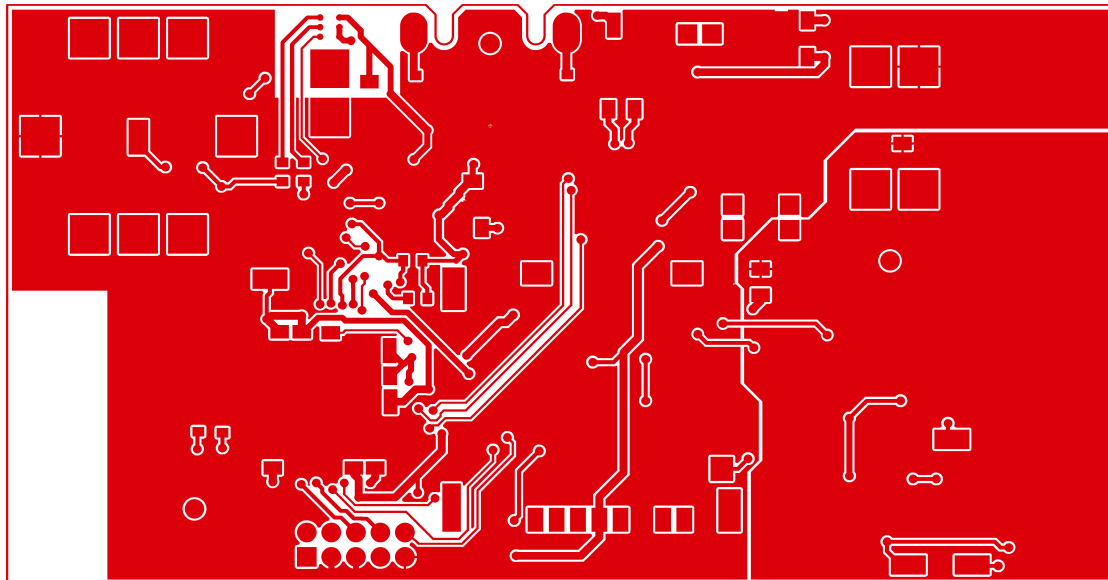


Figure A2: VITAL EKG: Bottom Layer.

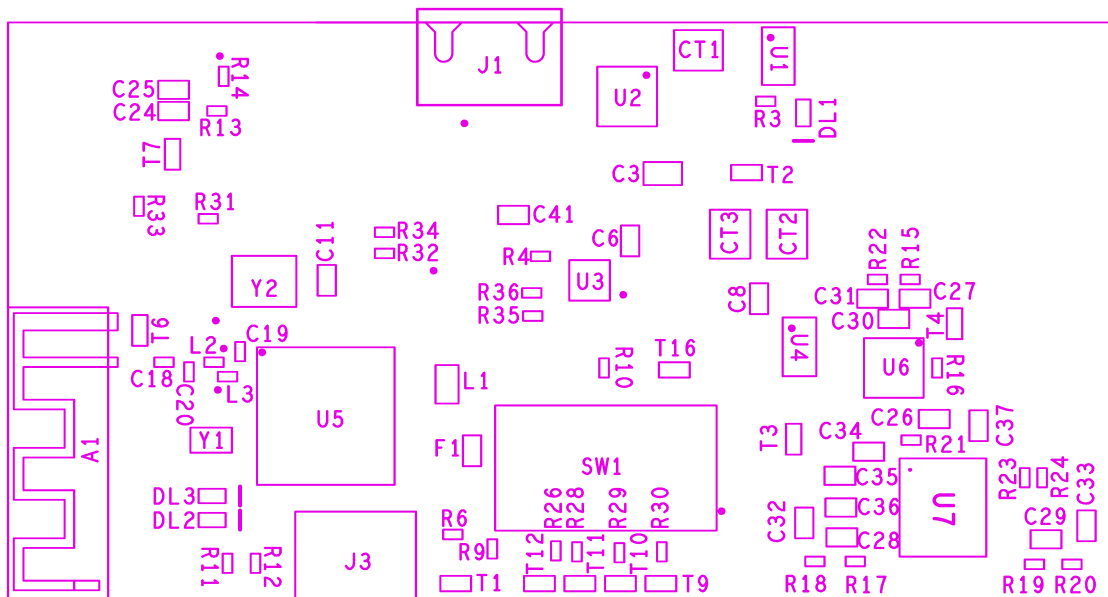


Figure A3: VITAL EKG: Assembly Top Layer.

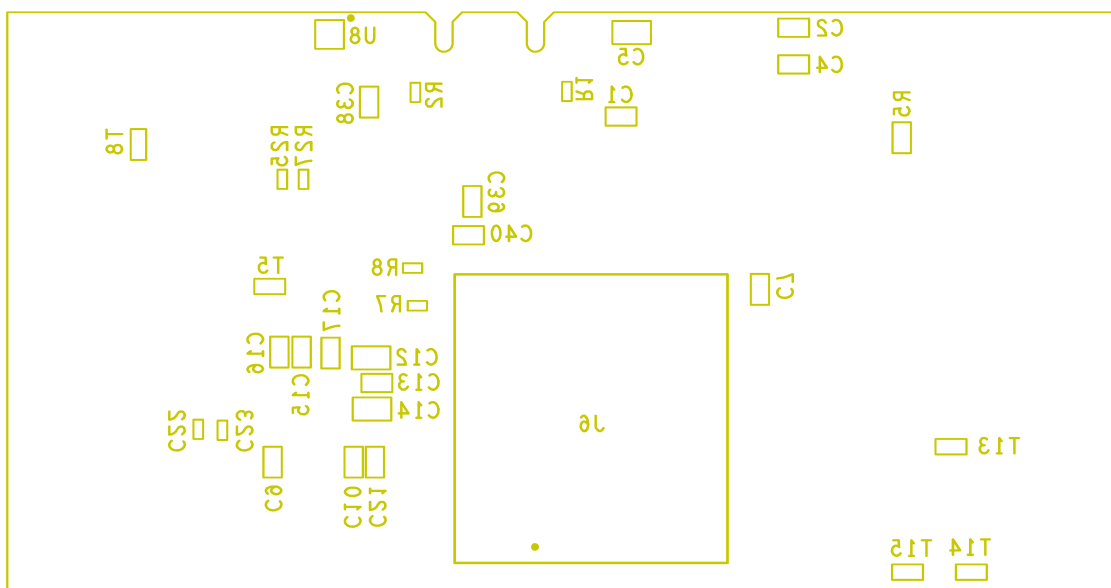


Figure A4: VITAL EKG: Assembly Bottom Layer.

B APPENDIX

Events Reference, BLE Dispatcher Commands and Status Codes

B.1 BLE Dispatcher Commands

The following commands are sent by Central device to BLE Dispatcher.

CMD_START_ACQ

- Value : 0x03
- Start PPG and EKG acquisitions.

B.2 BLE Dispatcher Status Codes

The following status codes are sent by BLE Dispatcher to Central device on STATUS characteristic of Misc Service.

STATUS_MAX30102_ACQ_STARTED

- Value : 0x10
- MAX30102 acquisition started.

STATUS_ECG_ACQ_STARTED

- Value : 0x20
- EKG acquisition started.

STATUS_MAX30102_ACQ_DONE

- Value : 0x11
 - MAX30102 acquisition completed.
STATUS_ECG_ACQ_STARTED
- Value : 0x21
 - EKG acquisition completed.
STATUS_MAX30102_ACQ_FAILED
- Value : 0x12
 - MAX30102 acquisition failed. This is likely due to sensor FIFO failure.
STATUS_ECG_ACQ_FAILED
- Value : 0x22
 - EKG acquisition failed.
STATUS_HDC2010_ACQ_FAILED
- Value : 0x32
 - HDC2010 acquisition failed.
STATUS_MAX17048_ACQ_FAILED
- Value : 0x42
 - MAX17048 acquistion failed.
STATUS_MAX30102_FD_PROCESSING_DONE
- Value : 0x14
 - MAX30102 frequency domain processing completed.
STATUS_MAX30102_TD_PROCESSING_DONE
- Value : 0x13
 - MAX30102 time domain processing completed.
STATUS_RESULT_NON_VALID
- Value : 0x19

- MAX30102 time domain and frequency domain processing gave non compatible results. Processing is not valid.

STATUS_ECG_PROCESSING_DONE

- Value : 0x23
- EKG processing completed. All the packets have been transmitted.

STATUS_ECG_PAYLOAD_RDY

- Value : 0x2A
- EKG packet is ready to be read.

STATUS_ECG_PROCESSING_FAILED

- Value : 0x25
- Processing of EKG waveform failed.

STATUS_MAX17048_OVERVOLTAGE

- Value : 0x4C
- Device is fully charged. Battery voltage is greater than 4.0 V.

STATUS_MAX17048_UNDERVOLTAGE

- Value : 0x4D
- Device needs to be recharged. Battery voltage is lower than 3.4 V. No acquisition is possible until battery voltage gets back in the normal range.

STATUS_MAX30102_MEM_ALLOC_ERR

- Value : 0x17
- A memory allocation error occurred in MAX30102 Manager.

STATUS_ECG_MEM_ALLOC_ERR

- Value : 0x27
- A memory allocation error occurred in EKG Manager.

STATUS_MAX30102_NV_TIMEOUT

- Value : 0x17

- Flash Memory Manager message Mailbox timed out while MAX30102 Manager was requesting a flash memory operation.

STATUS_ECG_NVS_TIMEOUT

- Value : 0x28
- Flash Memory Manager message Mailbox timed out while BLE Manager was requesting a flash memory operation.

B.3 I²C Events

I2C_TRANSFER_SUCCESS_EVT

- Value : Event_Id_01
- Description : this event is returned when a I²C transfer succeeds. The event variable must be provided by the calling task. The event is posted in the callback function of I²C.

I2C_TRANSFER_ERROR_EVT

- Value : Event_Id_01
- Description : this event is returned when a I²C transfer succeeds. The event variable must be provided by the calling task. The event is posted in the callback function of I²C.

B.4 Non-Volatile Memory Events

NVS_WR_ERROR_EVT

- Value : Event_Id_21
- Description : this event is posted by Flash Memory Manager on the event variable provided as arg2 by the calling task message of type NvsMsg. This event signals that a write operation to internal flash memory failed. Possible causes includes writing a non-erased page or writing outside the boundaries of memory associated to NVS Driver.

NVS_RD_ERROR_EVT

- Value : Event_Id_22

- Description : this event is posted by Flash Memory Manager on the event variable provided as arg2 by the calling task message of type NvsMsg. This event signals that a read operation to internal flash memory failed. Possible causes includes reading from a location not associated to NVS Driver.

B.5 BLE Dispatcher Response Messages

The messages included in this sections are really just status codes included in the payload of a queue message delivered to BLE Dispatcher. The event variable associated to all these codes is syncEvent. The event which is posted is APP_QUEUE_EVT. A convention is followed for message values:

- bit 0 to 7 encode the proper message code;
- bit 8 to 11 encode the entity which generated the message (e.g., MAX30102 Manager, EKG Manager, Monitoring Task);
- bit 12 to 15 are reserved for future use.

B.5.1 Profile Messages

ECG_CHAR_CHANGE_EVT

- Value : 0x0001
- Description : this code is posted in EKG profile callback function whenever a characteristic changes.
This is done to handle the change in BLE Dispatcher task context.

MISC_CHAR_CHANGE_EVT

- Value : 0x0002
- Description : this code is posted in Misc profile callback function whenever a characteristic changes.
This is done to handle the change in BLE Dispatcher task context.

HDC2010_CHAR_CHANGE_EVT

- Value : 0x0003
- Description : this code is posted in HDC2010 profile callback function whenever a characteristic changes.
This is done to handle the change in BLE Dispatcher task context.

B.5.2 EKG Messages

ECG_INT_ACQ_STARTED_EVT_R

- Value : 0x0101
- Description : this code is posted by EKG Manager to BLE Dispatcher to signal that the acquisition was started correctly. The final R indicates that the receiver of the message is BLE Dispatcher.

ECG_INT_ACQ_DONE_EVT_R

- Value : 0x0102
- Description : this code is posted by EKG Manager to BLE Dispatcher to signal that the acquisition was completed successfully. The final R indicates that the receiver of the message is BLE Dispatcher.

ECG_INT_ACQ_FAILED_EVT_R

- Value : 0x0105
- Description : this code is posted by EKG Manager to BLE Dispatcher to signal that the acquisition failed for unspecified reasons. The final R indicates that the receiver of the message is BLE Dispatcher.

ECG_INT_SECTOR_RDY_EVT_R

- Value : 0x0103
- Description : this code is posted by EKG Manager to BLE Dispatcher to signal that the processing of a portion of the signal has been completed and is ready for transmission. When this message is received, the payload contains 204 B of data. The first 200 B contain 100 samples arranged on 2 B; the last 2 B contain the progressive number of the transmission packet. The payload must not be freed because it is allocated on the stack. The final R indicates that the receiver of the message is BLE Dispatcher.

ECG_INT_PROCESSING_DONE_EVT_R

- Value : 0x0104
- Description : this code is posted by EKG Manager to BLE Dispatcher to signal that the processing has been completed. The final R indicates that the receiver of the message is BLE Dispatcher.

ECG_INT_PROCESSING_FAILED_EVT_R

- Value : *0x0106*
- Description : this code is posted by EKG Manager to BLE Dispatcher to signal that the processing failed for unspecified reasons. The final R indicates that the receiver of the message is BLE Dispatcher.

`ECG_INT_MEMORY_ALLOC_ERR_EVT_R`

- Value : *0x0107*
- Description : this code is posted by EKG Manager to BLE Dispatcher to signal that a memory allocation error occurred. The only memory allocations which can fail are associated to inter-task communication messages, since data processing uses memory allocated on the stack. The final R indicates that the receiver of the message is BLE Dispatcher.

`ECG_INT_NVS_TIMEOUT_EVT_R`

- Value : *0x0108*
- Description : this code is posted by EKG Manager to BLE Dispatcher to signal that the caller task was unable to enqueue a message in Flash Memory Manager mailbox within specified time. The final R indicates that the receiver of the message is BLE Dispatcher.

B.5.3 MAX30102 Messages

`MAX30102_INT_ACQ_STARTED_EVT_R`

- Value : *0x0201*
- Description : this code is posted by MAX30102 Manager to BLE Dispatcher to signal that the acquisition was started correctly. The final R indicates that the receiver of the message is BLE Dispatcher.

`MAX30102_INT_ACQ_DONE_EVT_R`

- Value : *0x0202*
- Description : this code is posted by MAX30102 Manager to BLE Dispatcher to signal that the acquisition was completed successfully. The final R indicates that the receiver of the message is BLE Dispatcher.

`MAX30102_INT_ACQ_FAILED_EVT_R`

- Value : *0x0203*

- Description : this code is posted by MAX30102 Manager to BLE Dispatcher to signal that the acquisition failed for unspecified reasons. The final R indicates that the receiver of the message is BLE Dispatcher.

`MAX30102_INT_MEMORY_ALLOC_ERR_EVT_R`

- Value : `0x0204`
- Description : this code is posted by MAX30102 Manager to BLE Dispatcher to signal that a memory acquisition error occurred.
See `ECG_INT_MEMORY_ALLOC_ERR_EVT_R` for further details. The final R indicates that the receiver of the message is BLE Dispatcher.

`MAX30102_INT_NVS_TIMEOUT_EVT_R`

- Value : `0x0205`
- Description : this code is posted by MAX30102 Manager to BLE Dispatcher to signal that the caller task was unable to enqueue a message in Flash Memory Manager mailbox within specified time. The final R indicates that the receiver of the message is BLE Dispatcher.

`MAX30102_INT_FD_PROCESSING_DONE_EVT_R`

- Value : `0x0206`
- Description : this code is posted by MAX30102 Manager to BLE Dispatcher to signal that the frequency domain processing has terminated. The final R indicates that the receiver of the message is BLE Dispatcher.

`MAX30102_INT_TD_PROCESSING_DONE_EVT_R`

- Value : `0x0207`
- Description : this code is posted by MAX30102 Manager to BLE Dispatcher to signal that the time domain processing has terminated. The final R indicates that the receiver of the message is BLE Dispatcher.

`MAX30102_INT_FD_PROCESSING_FAILED_EVT_R`

- Value : `0x0208`
- Description : this code is posted by MAX30102 Manager to BLE Dispatcher to signal that the frequency domain processing failed. The final R indicates that the receiver of the message is BLE Dispatcher.

MAX30102_INT_TD_PROCESSING_FAILED_EVT_R

- Value : 0x0209
- Description : this code is posted by MAX30102 Manager to BLE Dispatcher to signal that the time domain processing failed. The final R indicates that the receiver of the message is BLE Dispatcher.

MAX30102_INT_RESULT_NON_VALID_EVT_R

- Value : 0x020A
- Description : this code is posted by MAX30102 Manager to BLE Dispatcher to signal that frequency domain processing and time domain processing produces HR which are not equal, within specified tolerance. The final R indicates that the receiver of the message is BLE Dispatcher.

B.5.4 Other Messages

HDC2010_INT_RD_ERROR_EVT_R

- Value : 0x0303
- Description : this code is posted by Monitoring Task to BLE Dispatcher to signal that reading HDC2010 failed. The final R indicates that the receiver of the message is BLE Dispatcher.

MAX17048_INT_RD_ERROR_EVT_R

- Value : 0x0403
- Description : this code is posted by Monitoring Task to BLE Dispatcher to signal that reading MAX17048 failed. The final R indicates that the receiver of the message is BLE Dispatcher.

HDC2010_INT_DATA_RDY_EVT_R

- Value : 0x0307
- Description : this code is posted by Monitoring Task to BLE Dispatcher to signal that HDC2010 temperature and humidity values are ready to be transmitted. This message has an associated 4 B payload. The first 2 B encode the temperature value; the last 2 B the relative humidity. For each quantity, the first byte encodes the integer part and the last byte the fractional part. The payload must not be freed. The final R indicates that the receiver of the message is BLE Dispatcher.

MAX17048_INT_DATA_RDY_EVT_R

- Value : 0x0407
- Description : this code is posted by Monitoring Task to BLE Dispatcher to signal that MAX17048 voltage level has been read. This message has an associated 1 B payload representing the voltage level, where value 0 is 0 V and 255 is 5.20 V. The payload must not be freed. The final R indicates that the receiver of the message is BLE Dispatcher.

B.6 MAX30102 Events

These events are posted to `max30102Event` variable and deliver messages to MAX30102 Manager.

MAX30102_INT_START_ACQ_EVT

- Value : Event_Id_01
- Description : this event is posted by BLE Dispatcher to forward to MAX30102 Manager the start acquisition command received from the Central device.

MAX30102_INT_INTERRUPT_EVT

- Value : Event_Id_02
- Description : this event is posted in the callback function registered with Maxim Integrated MAX30102 FIFO interrupt to manage the reading from the FIFO in task context.

MAX30102_INT_START_PROCESSING_EVT

- Value : Event_Id_03
- Description : this event is posted by EKG Manager when its acquisition phase is completed to allow MAX30102 Manager to start MAX30102 processing. This inter-task synchronization is required because MAX30102 processing and EKG acquisition use the same automatic memory. Since in general this event might be generated before MAX30102 Manager completed its own acquisition, it is saved in a boolean variable (`ecgAcqDone`) and consumed whenever MAX30102 Manager is ready.

MAX30102_INT_NEXT_STATE_EVT

- Value : Event_Id_04

- Description : this event is posted at the end of each state handler function each time the FSM must change state without waiting for external events. This is analogous to the clock signal for hardware FSMs.

MAX30102_INT_BATTERY_DEAD_EVT

- Value : Event_Id_05
- Description : this event is posted by the Monitoring Task when the battery level falls below 3.4 V. This event is saved in a boolean variable (batteryOK). No acquisitions are possible until MAX30102_INT_BATTERY_OK_EVT is posted by the Monitoring Task.

MAX30102_INT_BATTERY_OK_EVT

- Value : Event_Id_06
- Description : this event is posted by the Monitoring Task when the battery voltage level returns within normal range. batteryOK boolean variable is reset and acquisitions are enabled.

ECG_INT_PROCESSING_DONE_EVT

- Value : Event_Id_07
- Description : this event is posted by the EKG Manager when the processing is finished. This is required because MAX30102 Manager needs to know if all EKG values have been read before a new acquisition is requested from Central device. If this is not the case (that is, this event is not detected), MAX30102 Manager needs to cancel ongoing EKG processing the battery voltage level returns within normal range. batteryOK boolean variable is reset and acquisitions are enabled.

ECG_INT_CANCEL_ACK_EVT

- Value : Event_Id_08
- Description : this event is posted by the EKG Manager when an ongoing processing cancel request is acknowledged. This is required because EKG Manager needs to be in idle state before a new acquisition can start.

B.7 EKG Events

These events are posted to `ecgEvent` variable and deliver messages to EKG Manager.

`ECG_INT_START_ACQ_EVT`

- Value : `Event_Id_01`
- Description : this event is posted by MAX30102 Manager to forward the start acquisition command from the Central device to EKG Manager.

`ECG_INT_BUFFER_FULL_EVT`

- Value : `Event_Id_02`
- Description : this event is posted by ADCBuf callback function whenever an acquisition buffer is full and ready to be stored in memory. This event is necessary to perform the operations in task context.

`ECG_INT_START_PROCESSING_EVT`

- Value : `Event_Id_02`
- Description : this event is posted by MAX30102 Manager when it finishes its processing and only in case frequency domain processing and time domain processing results are in accordance. In case they are not, there is clearly no need to waste resources doing EKG processing and transmission.

`ECG_INT_CANCEL_EVT`

- Value : `Event_Id_04`
- Description : this event is posted by MAX30102 Manager when it receives a start acquisition command from Central device before EKG Manager processing is finished. Note that this situation might happen each time Central device does not read all the packets, since processing of a batch is started only when the previous batch has been read. This is necessary to allow EKG Manager to get back to idle state before its acquisition starts. MAX30102 Manager forwards the start acquisition command to EKG Manager only when it receives the event `ECG_INT_CANCEL_ACK_EVT`, which means EKG Manager has acknowledged the command.

`ECG_INT_PROCESS_SECTOR_EVT`

- Value : `Event_Id_05`

- Description : this event is posted by BLE Dispatcher when the Central device reads a EKG packet. In this case, a new series of samples can be loaded from internal flash memory and processed.

ECG_INT_NEXT_STATE_EVT

- Value : Event_Id_07
- Description : this event is posted at the end of each state handler function each time the FSM must change state without waiting for external events. This is analogous to the clock signal for hardware FSMs.

B.8 Monitoring Task Events

These events are posted to monitEvent variable and deliver messages to Continuous Monitoring Manager.

HDC2010_INT_DATA_RDY_EVT

- Value : Event_Id_01
- Description : this event is posted by HDC2010 timer callback function to manage in task context the reading of temperature and humidity data.

MAX17048_INT_INTERRUPT_EVT

- Value : Event_Id_02
- Description : this event is posted by MAX17048 interrupt callback function to handle in task context a detection of out of normal range battery voltage.

MAX17048_INT_DATA_RDY_EVT

- Value : Event_Id_03
- Description : this event is posted by MAX17048 timer callback function to handle in task context the reading of battery voltage.

MAX17048_INT_DATA_RDY_EVT

- Value : Event_Id_04
- Description : this event is posted by MAX30102 Manager when the Central device requests an acquisition. This is done to provide updated temperature and humidity readings.

C APPENDIX

MAX30102 Manager

Listing C.0.1: MAX30102 Manager finite state machine.

```
1  /*************************************************************************/
2  static void MAX30102_taskInit(MAX30102 * max30102,
3                                MAX30102Params * params)
4  {
5    /* Create an Event to notify the task of I2C Transfer outcome */
6    Event_construct(&i2cTransferEventStruct, NULL);
7    i2cTransferEvent = Event_handle(&i2cTransferEventStruct);
8
9    /* Create a Mailbox to read from NVS */
10   Mailbox_Parms mbxParams;
11   Mailbox_Parms_init(&mbxParams);
12   mbxParams.buf = (Ptr)max30102NvsReadMbxBuffer;
13   mbxParams.bufSize = sizeof(max30102NvsReadMbxBuffer);
14   Mailbox_construct(&max30102NvsReadMbxStruct,
15                     sizeof(NvsMsg),
16                     MAX30102_NVS_READ_MBX_MAX_NUM_MSG,
17                     &mbxParams,
18                     NULL);
19   max30102NvsReadMbx = Mailbox_handle(&max30102NvsReadMbxStruct);
20
21   /* Allocate a pin for MAX30102 interrupts and link a ISR */
22   if(!(max30102Int = PIN_open(&max30102IntState, max30102IntTable)))
23   {
24     while(1);
25   }
26
27   if (PIN_registerIntCb(max30102Int, &MAX30102_intCallbackFxn) != 0)
28   {
```

```
29     while(1);
30 }
31
32 /* Set MAX30102 parameters */
33 params->interruptEnable1 = 0x00;
34 params->interruptEnable2 = 0x00;
35 params->FIFOConfig = SMP_AVE_8Sa |  
    FIFO_ROLLOVER_EN |  
    FIFO_A_FULL_12Sa;  
36 params->modeConfig = SHDN;  
37 params->SP02Config = SP02_ADC_RGE_16384nA |  
    SP02_SR_400SaS |  
    LED_PW_411us;  
38 params->ledRedPulseAmplitude = 0x2F;  
39 params->ledIRPulseAmplitude = 0x2F;  
40 params->proxModeLed2PulseAmplitude = 0x7F;  
41 params->multiLedModeCtrl1 = SLOT_disabled;  
42 params->multiLedModeCtrl2 = SLOT_disabled;  
43 params->proxModeInterruptThreshold = 0x1F;  
44
45
46
47
48
49
50 if(!MAX30102_init(max30102,
51                     i2c,
52                     i2cTransferEvent,
53                     params,
54                     MAX30102_DEFAULT_SLAVE_ID))
55 {
56     while(1);
57 }
58
59 if (!MAX30102_reset(max30102))
60 {
61     while(1);
62 }
63 Task_sleep(1000 / Clock_tickPeriod);
64
65 if (!MAX30102_open(max30102))
66 {
67     while(1);
68 }
69 }
70
71 ****
72 static void MAX30102_taskFxn(UArg a0, UArg a1)
73 {
74     MAX30102 max30102;
75     MAX30102Params params;
```

```
77     MAX30102_taskInit(&max30102, &params);
78
79     /* FSM state variable */
80     MAX30102_state_t state = state_MAX30102_IDLE;
81
82     /* Asynchronous FSM inputs */
83     unsigned char batteryOK = 1;
84     unsigned char startRequested = 0;
85     unsigned char ecgAcqDone = 0;
86     unsigned char ecgReady = 1;
87
88     /* Allocate 5 biquads for processing */
89     iir_biquad_t biquads[5];
90
91     /* Frequency domain processing */
92     MAX30102_processing_t dsp;
93
94     /* Time domain processing */
95     MAX30102_channel_dsp_t td_dsp;
96     MAX30102_results_t red_results;
97     MAX30102_results_t ir_results;
98
99     /* Infinite Loop */
100    for (;;)
101    {
102        uint32_t events;
103
104        /* Wait for an event */
105        events = Event_pend(max30102Event,
106                            Event_Id_NONE,
107                            MAX30102_ALL_EVENTS,
108                            BIOS_WAIT_FOREVER);
109
110        if (events & MAX30102_INT_BATTERY_DEAD_EVT)
111        {
112            batteryOK = 0;
113        }
114
115        if (events & MAX30102_INT_BATTERY_OK_EVT)
116        {
117            batteryOK = 1;
118        }
119
120        if (events & MAX30102_INT_START_PROCESSING_EVT)
121        {
122            ecgAcqDone = 1;
123        }
124
```

```
125     /* ECG finished the processing or acknowledged
126      * a cancelled processing
127      */
128     if (events & ECG_INT_CANCEL_ACK_EVT || 
129         events & ECG_INT_PROCESSING_DONE_EVT)
130     {
131         ecgReady = 1;
132     }
133
134     switch (state)
135     {
136         /* Default IDLE state */
137         case state_MAX30102_IDLE :
138         {
139             /* Prevent acquisition if battery is dead */
140             if (batteryOK)
141             {
142                 if (events & MAX30102_INT_START_ACQ_EVT)
143                 {
144                     /* Remember that a start was sent */
145                     startRequested = 1;
146                 }
147             }
148
149             if (startRequested)
150             {
151                 if (ecgReady)
152                 {
153                     state = state_MAX30102_IDLE_handler(
154                         &max30102,
155                         memoryBuffer);
156
157                     startRequested = 0;
158                     ecgAcqDone = 0;
159                     ecgReady = 0;
160                 } else
161                 {
162                     /* Cancel ongoing ECG processing */
163                     Event_post(ecgEvent, ECG_INT_CANCEL_EVT);
164                 }
165             }
166             break;
167         }
168
169         /* Proximity sensor feature:
170          * proceed to acquisition
171          */
172         case state_MAX30102_START_ACQ :
```

```
173     {
174         if (events & MAX30102_INT_INTERRUPT_EVT)
175         {
176             state = state_MAX30102_START_ACQ_handler(
177                 &max30102,
178                 &dsp);
179         }
180         break;
181     }
182
183     /* Fifo full:
184      * Discard the first samples
185      * to avoid the transient due to
186      * the placing of the finger
187      */
188     case state_MAX30102_TRANSIENT_READ :
189     {
190         /* Interrupt from MAX30102*/
191         if (events & MAX30102_INT_INTERRUPT_EVT)
192         {
193             state = state_MAX30102_TRANSIENT_READ_handler(
194                 &max30102,
195                 &dsp);
196         }
197         break;
198     }
199
200     /* Fifo full:
201      * save data and get back here
202      * unless enough samples were
203      * collected
204      */
205     case state_MAX30102_FIFO_READ :
206     {
207         if (events & MAX30102_INT_INTERRUPT_EVT)
208         {
209             state = state_MAX30102_FIFO_READ_handler(
210                 &max30102,
211                 &dsp);
212         }
213         break;
214     }
215
216
217     /* Acquisition is finished:
218      * notify Central device
219      */
220     case state_MAX30102_ACQ_DONE :
```

```
221 |     {
222 |         if  (events & MAX30102_INT_NEXT_STATE_EVT)
223 |         {
224 |             state = state_MAX30102_ACQ_DONE_handler(
225 |                 &max30102);
226 |             }
227 |             break;
228 |     }
229 |
230 |     /* Processing can start only when ECG
231 |      * finishes its acquisition
232 |      * because we need the same memory buffer.
233 |      * Initialize filters and buffers here
234 |      */
235 |     case state_MAX30102_FD_PROCESS_INIT :
236 |     {
237 |         if  (ecgAcqDone)
238 |         {
239 |             state = state_MAX30102_FD_PROCESS_INIT_handler(
240 |                 &dsp,
241 |                 biquads,
242 |                 (float*) (memoryBuffer + 300),
243 |                 memoryBuffer);
244 |             ecgAcqDone = 0;
245 |         }
246 |         break;
247 |     }
248 |
249 |
250 |     /* Perform Quasi-online
251 |      * Frequency Domain
252 |      * processing
253 |      */
254 |     case state_MAX30102_FD_PROCESS :
255 |     {
256 |         if  (events & MAX30102_INT_NEXT_STATE_EVT)
257 |         {
258 |             state = state_MAX30102_FD_PROCESS_handler(
259 |                 &dsp);
260 |             }
261 |             break;
262 |     }
263 |
264 |     /* Frequency domain processing
265 |      * failed
266 |      */
267 |     case state_MAX30102_FD_PROCESS_FAILED :
268 |     {
```

```
269     if (events & MAX30102_INT_NEXT_STATE_EVT)
270     {
271         state = state_MAX30102_FD_PROCESS_FAILED_handler();
272     }
273     break;
274 }
275
276 /* Frequency domain processing
277 * completed successfully
278 */
279 case state_MAX30102_FD_PROCESS_DONE :
280 {
281     if (events & MAX30102_INT_NEXT_STATE_EVT)
282     {
283         state = state_MAX30102_FD_PROCESS_DONE_handler(
284             &dsp);
285     }
286     break;
287 }
288
289 /* Initialize Time Domain processing
290 * of red channel
291 */
292 case state_MAX30102_TD_RED_PROCESS_INIT :
293 {
294     if (events & MAX30102_INT_NEXT_STATE_EVT)
295     {
296         state = state_MAX30102_TD_RED_PROCESS_INIT_handler(
297             &td_dsp,
298             (float*) (memoryBuffer + 300),
299             memoryBuffer,
300             biquads,
301             &red_results);
302     }
303     break;
304 }
305
306 /* Quasi online time domain
307 * processing of red channel
308 */
309 case state_MAX30102_TD_RED_PROCESS :
310 {
311     if (events & MAX30102_INT_NEXT_STATE_EVT)
312     {
313         state = state_MAX30102_TD_RED_PROCESS_handler(
314             &td_dsp,
315             &red_results);
316 }
```

```
317     break;
318 }
319
320 /* Initialize Time Domain processing
321 * of ir channel
322 */
323 case state_MAX30102_TD_IR_PROCESS_INIT :
324 {
325     if (events & MAX30102_INT_NEXT_STATE_EVT)
326     {
327         state = state_MAX30102_TD_IR_PROCESS_INIT_handler(
328             &td_dsp,
329             (float*) (memoryBuffer + 300),
330             memoryBuffer,
331             biquads,
332             &ir_results);
333     }
334     break;
335 }
336
337 /* Quasi online time domain
338 * processing of red channel
339 */
340 case state_MAX30102_TD_IR_PROCESS :
341 {
342     if (events & MAX30102_INT_NEXT_STATE_EVT)
343     {
344         state = state_MAX30102_TD_IR_PROCESS_handler(
345             &td_dsp,
346             &ir_results);
347     }
348     break;
349 }
350
351 /* Time domain processing
352 * failed
353 */
354 case state_MAX30102_TD_PROCESS_FAILED :
355 {
356     if (events & MAX30102_INT_NEXT_STATE_EVT)
357     {
358         state = state_MAX30102_TD_PROCESS_FAILED_handler();
359     }
360     break;
361 }
362
363 /* Post processing:
364 * verify if the 2 processing methods
```

```
365     * gave compatible results
366     */
367 case state_MAX30102_TD_POST_PROCESS :
368 {
369     if (events & MAX30102_INT_NEXT_STATE_EVT)
370     {
371         state = state_MAX30102_TD_POST_PROCESS_handler(
372             &red_results,
373             &ir_results,
374             &dsp);
375     }
376     break;
377 }
378
379 /* Notify Central device and allow ECG
380  * to start its processing
381  */
382 case state_MAX30102_TD_PROCESS_DONE :
383 {
384     if (events & MAX30102_INT_NEXT_STATE_EVT)
385     {
386         state = state_MAX30102_TD_PROCESS_DONE_handler(
387             &dsp);
388     }
389     break;
390 }
391
392 /* MAX30102 Fifo failed */
393 case state_MAX30102_FIFO_ERR :
394 {
395     if (events & MAX30102_INT_NEXT_STATE_EVT)
396     {
397         state = state_MAX30102_FIFO_ERR_handler(
398             &max30102);
399     }
400     break;
401 }
402
403 /* Memory allocation failed */
404 case state_MAX30102_MEMORY_ALLOC_ERR :
405 {
406     if (events & MAX30102_INT_NEXT_STATE_EVT)
407     {
408         state = state_MAX30102_MEMORY_ALLOC_ERR_handler();
409     }
410     break;
411 }
412 }
```

```
413     /* Flash Memory Manager communication
414      * took longer than expected
415      */
416     case state_MAX30102_NVS_TIMEOUT :
417     {
418         if (events & MAX30102_INT_NEXT_STATE_EVT)
419         {
420             state = state_MAX30102_NVS_TIMEOUT_handler();
421         }
422         break;
423     }
424
425     default :
426         state = state_MAX30102_IDLE;
427     }
428
429     /* Error during NVS_operation
430      * Terminate execution and restore IDLE state
431      * asynchronously
432      */
433     if (events & NVS_WR_ERROR_EVT)
434     {
435         MAX30102_changeMode(&max30102, SHDN);
436         enqueueMsg(MAX30102_INT_NVS_TIMEOUT_EVT_R,
437                     0, NULL, 0, BLEsyncEvent, BLEappMsgQueue);
438         state = state_MAX30102_IDLE;
439     }
440
441     /* Error during NVS_read */
442     if (events & NVS_RD_ERROR_EVT)
443     {
444         enqueueMsg(MAX30102_INT_NVS_TIMEOUT_EVT_R,
445                     0, NULL, 0, BLEsyncEvent, BLEappMsgQueue);
446         state = state_MAX30102_IDLE;
447     }
448 }
449 }
```

D APPENDIX

EKG Manager

Listing D.0.1: EKG Manager finite state machine.

```
1  /*************************************************************************/
2  static void ECG_taskInit(ECG * ecg,
3  	(unsigned short * sampleBufferOne,
4  	(unsigned short * sampleBufferTwo,
5  	(unsigned short * supportBuffer,
6  	(unsigned short * nvsBuffer)
7  {
8
9  /* REF2033 enable */
10 if(!(ref2033En = PIN_open(&ref2033EnState, ref2033EnTable)))
11 {
12     while(1);
13 }
14
15 /* Initialize ADCBuf driver */
16 ADCBuf_init();
17
18 /* Set up ADCBuf */
19 ADCBuf_Params adcBufParams;
20 ADCBuf_Params_init(&adcBufParams);
21 adcBufParams.callbackFxn = adcBufCallback;
22 adcBufParams.recurrenceMode = ADCBuf_RECURRENCE_MODE_CONTINUOUS;
23 adcBufParams.returnMode = ADCBuf_RETURN_MODE_CALLBACK;
24 adcBufParams.samplingFrequency = ECG_SAMPLING_FREQUENCY;
25 ecg->adcBuf = ADCBuf_open(CC2640R2_LAUNCHXL_ADCBUF0, &adcBufParams);
26
27 /* Make sure ADCBuf opened correctly. */
28 if (!ecg->adcBuf){
```

```
29     while(1);
30 }
31
32 /* Set up adc buffers */
33 ecg->sampleBufferOne = sampleBufferOne;
34 ecg->sampleBufferTwo = sampleBufferTwo;
35 ecg->supportBuffer = supportBuffer;
36 ecg->nvsBuffer = nvsBuffer;
37
38 /* Set up ADCBuf conversion structure */
39 ecg->continuousConversion.arg =
40     ecg->supportBuffer;
41 ecg->continuousConversion.adcChannel =
42     CC2640R2_LAUNCHXL_ADCBUF0CHANNEL0;
43 ecg->continuousConversion.sampleBuffer =
44     ecg->sampleBufferOne;
45 ecg->continuousConversion.sampleBufferTwo =
46     ecg->sampleBufferTwo;
47 ecg->continuousConversion.samplesRequestedCount =
48     ECG_SAMPLES_PER_BUFFER;
49
50 /* Create a Mailbox to read from NVS */
51 Mailbox_Parms mbxParams;
52 Mailbox_Parms_init(&mbxParams);
53 mbxParams.buf = (Ptr)ecgNvsReadMbxBuffer;
54 mbxParams.bufSize = sizeof(ecgNvsReadMbxBuffer);
55 Mailbox_construct(&ecgNvsReadMbxStruct,
56                 sizeof(NvsMsg),
57                 ECG_NVS_READ_MBX_MAX_NUM_MSG,
58                 &mbxParams, NULL);
59 ecgNvsReadMbx = Mailbox_handle(&ecgNvsReadMbxStruct);
60 }
61
62 ****
63 static void ECG_taskFxn(UArg a0, UArg a1)
64 {
65     ECG ecg;
66
67     /* Initialize application */
68     ECG_taskInit(&ecg,
69     (unsigned short*) (memoryBuffer+300),
70     (unsigned short*) (memoryBuffer+300
71     +1*(ECG_SAMPLES_PER_BUFFER*ECG_MEM_SAMPLE_SIZE)),
72     (unsigned short*) (memoryBuffer+300
73     +2*(ECG_SAMPLES_PER_BUFFER*ECG_MEM_SAMPLE_SIZE)),
74     (unsigned short*) (memoryBuffer+300
75     +3*(ECG_SAMPLES_PER_BUFFER*ECG_MEM_SAMPLE_SIZE)));
76 }
```

```
77  /* FSM State variable */
78  ECG_state_t state = state_ECG_IDLE;
79
80  /* Processing structs */
81  ECG_processing_t dsp;
82  iir_biquad_fixed_t biquads[7];
83  movmean_t movmean[2];
84
85
86  /* Application main loop */
87  for (;;)
88  {
89      uint32_t events;
90
91      events = Event_pend(ecgEvent,
92                           Event_Id_NONE,
93                           ECG_ALL_EVENTS,
94                           BIOS_WAIT_FOREVER);
95
96  /* Next state computation logic */
97  switch (state)
98  {
99      /* Idle state */
100     case state_ECG_IDLE :
101     {
102         if  (events & ECG_INT_START_ACQ_EVT)
103         {
104             state = state_ECG_IDLE_handler(&ecg, &dsp);
105         }
106         break;
107     }
108
109    /* Consume samples to take care of initial transient */
110    case state_ECG_TRANSIENT_READ :
111    {
112        if  (events & ECG_INT_BUFFER_FULL_EVT)
113        {
114            state = state_ECG_TRANSIENT_READ_handler(&ecg, &dsp);
115        }
116        break;
117    }
118
119    /* Buffer full: perform oversampling processing */
120    case state_ECG_READ :
121    {
122        if  (events & ECG_INT_BUFFER_FULL_EVT)
123        {
124            state = state_ECG_READ_handler(&ecg, &dsp);
```

```
125     }
126     break;
127 }
128
129 /* Transfer the samples to Flash Memory Manager for
130 * non-volatile storage
131 */
132 case state_ECG_NVS_WRITE :
133 {
134     if (events & ECG_INT_NEXT_STATE_EVT)
135     {
136         state = state_ECG_NVS_WRITE_handler(&ecg, &dsp);
137     }
138     break;
139 }
140
141 /* Acquisition is finished: notify MAX30102 Manager */
142 case state_ECG_ACQ_DONE :
143 {
144     if (events & ECG_INT_NEXT_STATE_EVT)
145     {
146         state = state_ECG_ACQ_DONE_handler(&ecg);
147     }
148     break;
149 }
150
151 case state_ECG_PROCESS_INIT :
152 {
153     /* MAX30102 Manager requested to cancel the processing.
154      * Send the acknowledge and proceed to idle state.
155      */
156     if (events & ECG_INT_CANCEL_EVT)
157     {
158         Event_post(max30102Event, ECG_INT_CANCEL_ACK_EVT);
159         state = state_ECG_PROCESSING_FAILED_handler();
160         break;
161     }
162
163     /* Initialize the processing. This event is sent by MAX30102
164      * Manager when its processing is finished
165      */
166     if (events & ECG_INT_START_PROCESSING_EVT)
167     {
168         state = state_ECG_PROCESS_INIT_handler(&dsp,
169             (int*) (memoryBuffer),
170             (int*) (memoryBuffer + ECG_SAMPLES_PER_PROCESSING_BUFFER *
171                     ECG_PROC_SAMPLE_SIZE),
172             biquads,
```

```
173         movmean);
174     }
175     break;
176 }
177
178 case state_ECG_PROCESS :
179 {
180     /* MAX30102 Manager requested to cancel the processing.
181      * Send the acknowledge and proceed to idle state.
182      */
183     if (events & ECG_INT_CANCEL_EVT)
184     {
185         Event_post(max30102Event, ECG_INT_CANCEL_ACK_EVT);
186         state = state_ECG_PROCESSING_FAILED_handler();
187         break;
188     }
189
190     /* Continue the processing by loading samples from flash memory.
191      * This event is posted by BLE Dispatcher when previous
192      * packet of processed samples is read from Central device.
193      */
194     if (events & ECG_INT_PROCESS_SECTOR_EVT)
195     {
196         state = state_ECG_PROCESS_handler(&dsp);
197     }
198     break;
199 }
200
201 /* Buffer state to handle clean up before getting back to idle. */
202 case state_ECG_PROCESSING_FAILED :
203 {
204     /* MAX30102 Manager requested to cancel the processing.
205      * Send the acknowledge and proceed to idle state.
206      */
207     if (events & ECG_INT_CANCEL_EVT)
208     {
209         Event_post(max30102Event, ECG_INT_CANCEL_ACK_EVT);
210     }
211
212     state = state_ECG_PROCESSING_FAILED_handler();
213     break;
214 }
215
216 case state_ECG_SEND_FIRST :
217 {
218     /* MAX30102 Manager requested to cancel the processing.
219      * Send the acknowledge and proceed to idle state.
220      */
```

```
221     if (events & ECG_INT_CANCEL_EVT)
222     {
223         Event_post(max30102Event, ECG_INT_CANCEL_ACK_EVT);
224         state = state_ECG_PROCESSING_FAILED_handler();
225         break;
226     }
227
228     /* Send first half of processed samples as a packet */
229     if (events & ECG_INT_NEXT_STATE_EVT)
230     {
231         state = state_ECG_SEND_FIRST_handler(&dsp);
232     }
233     break;
234
235 case state_ECG_SEND_SECOND :
236 {
237     if (events & ECG_INT_CANCEL_EVT)
238     {
239         /* MAX30102 Manager requested to cancel the processing.
240          * Send the acknowledge and proceed to idle state.
241          */
242         Event_post(max30102Event, ECG_INT_CANCEL_ACK_EVT);
243         state = state_ECG_PROCESSING_FAILED_handler();
244         break;
245     }
246
247     /* Send second half of processed samples as a packet */
248     if (events & ECG_INT_PROCESS_SECTOR_EVT)
249     {
250         state = state_ECG_SEND_SECOND_handler(&dsp);
251     }
252     break;
253 }
254
255 case state_ECG_PROCESS_DONE :
256 {
257     /* MAX30102 Manager requested to cancel the processing.
258      * Send the acknowledge and proceed to idle state.
259      */
260     if (events & ECG_INT_CANCEL_EVT)
261     {
262         Event_post(max30102Event, ECG_INT_CANCEL_ACK_EVT);
263         state = state_ECG_PROCESSING_FAILED_handler();
264         break;
265     }
266
267     /* Processing is finished. Notify MAX30102 Manager */
268     if (events & ECG_INT_NEXT_STATE_EVT)
```

```
269     {
270         state = state_ECG_PROCESS_DONE_handler(&dsp);
271     }
272     break;
273 }
274
275
276 /* An error occurred during ADCBuf operations */
277 case state_ECG_READ_ERR :
278 {
279     if (events & ECG_INT_NEXT_STATE_EVT)
280     {
281         state = state_ECG_READ_ERR_handler(&ecg);
282     }
283     break;
284 }
285
286 /* An error occurred during memory allocation */
287 case state_ECG_MEMORY_ALLOC_ERR :
288 {
289     if (events & ECG_INT_NEXT_STATE_EVT)
290     {
291         state = state_ECG_MEMORY_ALLOC_ERR_handler(&ecg);
292     }
293     break;
294 }
295
296 /* Flash Memory Manager did not accept the message */
297 case state_ECG_NVS_TIMEOUT :
298 {
299     if (events & ECG_INT_NEXT_STATE_EVT)
300     {
301         state = state_ECG_NVS_TIMEOUT_handler(&ecg);
302     }
303     break;
304 }
305
306 default :
307     state = state_ECG_IDLE;
308 }
309
310
311 /* Error during NVS_operation
312 * Terminate execution and restore IDLE state
313 * asynchronously
314 */
315 if (events & NVS_WR_ERROR_EVT)
316 {
```

```
317     enqueueMsg(ECG_INT_NVS_TIMEOUT_EVT_R,
318                 0, NULL, 0, BLEsyncEvent, BLEappMsgQueue);
319     state = state_ECG_IDLE;
320 }
321
322 /* Error during NVS_read */
323 if (events & NVS_RD_ERROR_EVT)
324 {
325     enqueueMsg(ECG_INT_NVS_TIMEOUT_EVT_R,
326                 0, NULL, 0, BLEsyncEvent, BLEappMsgQueue);
327     state = state_ECG_IDLE;
328 }
329
330 /* Error during SD create new file
331 * SD operations are not supported at this point
332 */
333 if (events & SD_FILE_CREATION_ERR_EVT)
334 {
335     enqueueMsg(ECG_INT_SD_FILE_CREATION_ERR_EVT_R,
336                 0, NULL, 0, BLEsyncEvent, BLEappMsgQueue);
337     state = state_ECG_IDLE;
338 }
339 }
340 }
```

Bibliography

- [1] “Troppi esami diagnostici prescritti inutilmente: i medici lo ammettono,” May 2016. [Online]. Available: <https://federproprieta.it/2499-2/>
- [2] E. Guirguis, “Holter Monitoring,” *Canadian Family Physician*, vol. 33, pp. 985–992, Apr. 1987. [Online]. Available: <https://www.ncbi.nlm.nih.gov/pmc/articles/PMC2218473/>
- [3] R. R. Kroll, E. D. McKenzie, J. G. Boyd, P. Sheth, D. Howes, M. Wood, and D. M. Maslove, “Use of wearable devices for post-discharge monitoring of ICU patients: a feasibility study,” *Journal of Intensive Care*, vol. 5, Nov. 2017. [Online]. Available: <https://www.ncbi.nlm.nih.gov/pmc/articles/PMC5698959/>
- [4] A. Pantelopoulos and N. Bourbakis, “A survey on wearable biosensor systems for health monitoring,” in *2008 30th Annual International Conference of the IEEE Engineering in Medicine and Biology Society*, Aug. 2008, pp. 4887–4890.
- [5] R. M. Anderson, J. M. Fritz, and J. E. O’Hare, “The mechanical nature of the heart as a pump,” *American Heart Journal*, vol. 73, no. 1, pp. 92–105, Jan. 1967. [Online]. Available: <http://www.sciencedirect.com/science/article/pii/0002870367903134>
- [6] H. Lodish, A. Berk, S. L. Zipursky, P. Matsudaira, D. Baltimore, and J. Darnell, *Molecular Cell Biology*, 4th ed. W. H. Freeman, 2000.
- [7] I. P. Temple, S. Inada, H. Dobrzynski, and M. R. Boyett, “Connexins and the atrioventricular node,” *Heart Rhythm*, vol. 10, no. 2, pp. 297–304, Feb. 2013. [Online]. Available: <https://www.ncbi.nlm.nih.gov/pmc/articles/PMC3572393/>
- [8] P. Schweitzer and S. Keller, “Willem Einthoven—inventor of electrocardiography,” *Vnitřní Lekarství*, vol. 48 Suppl 1, pp. 20–23, Dec. 2002.
- [9] “EKG/ECG Machine Buyers Guide.” [Online]. Available: <https://www.usamedicalsurgical.com/blog/ekg-ecg-machine-buyers-guide/>

- [10] J. Crawford and L. Doherty, "Ten steps to recording a standard 12-lead ECG," *Practice Nursing*, vol. 21, no. 12, pp. 622–630, Dec. 2010. [Online]. Available: <http://www.magonlinelibrary.com/doi/10.12968/pnur.2010.21.12.622>
- [11] M. B. Conover, *Understanding Electrocardiography*. Elsevier Health Sciences, Jan. 2002, google-Books-ID: pcPekl1Q1cAC.
- [12] J. E. Madias, "On Recording the Unipolar ECG Limb Leads via the Wilson's vs the Goldberger's Terminals: aVR, aVL, and aVF Revisited," *Indian Pacing and Electrophysiology Journal*, vol. 8, no. 4, pp. 292–297, Nov. 2008. [Online]. Available: <https://www.ncbi.nlm.nih.gov/pmc/articles/PMC2572021/>
- [13] "Cardiovascular Lab: Electrocardiogram: Basics." [Online]. Available: <https://www.medicine.mcgill.ca/physio/vlab/cardio/ECGbasics.htm>
- [14] T. A. Neff, "Routine Oximetry: A Fifth Vital Sign?" *CHEST*, vol. 94, no. 2, p. 227, Aug. 1988. [Online]. Available: [https://journal.chestnet.org/article/S0012-3692\(16\)33429-8/fulltext](https://journal.chestnet.org/article/S0012-3692(16)33429-8/fulltext)
- [15] J. W. Severinghaus and Y. Honda, "History of blood gas analysis. VII. Pulse oximetry," *Journal of Clinical Monitoring*, vol. 3, no. 2, pp. 135–138, Apr. 1987. [Online]. Available: <https://doi.org/10.1007/BF00858362>
- [16] C. P. Criée, S. Sorichter, H. J. Smith, P. Kardos, R. Merget, D. Heise, D. Berdel, D. Köhler, H. Magnussen, W. Marek, H. Mitfessel, K. Rasche, M. Rolke, H. Worth, and R. A. Jörres, "Body plethysmography – Its principles and clinical use," *Respiratory Medicine*, vol. 105, no. 7, pp. 959–971, Jul. 2011. [Online]. Available: <http://www.sciencedirect.com/science/article/pii/S0954611111000552>
- [17] E. D. Chan, M. M. Chan, and M. M. Chan, "Pulse oximetry: Understanding its basic principles facilitates appreciation of its limitations," *Respiratory Medicine*, vol. 107, no. 6, pp. 789–799, Jun. 2013. [Online]. Available: <http://www.sciencedirect.com/science/article/pii/S095461111300053X>
- [18] P. D. Mannheimer, "The light-tissue interaction of pulse oximetry," *Anesthesia and Analgesia*, vol. 105, no. 6 Suppl, pp. S10–17, Dec. 2007.
- [19] "Il monitor indossabile QardioCore per l'ECG per iPhone." [Online]. Available: https://www.getqardio.com/it/qardiocore-wearable-ecg-ekg-monitor-iphone_it/
- [20] "CALM. Wearable ECG sensor with sports and sleep analysis," Feb. 2017. [Online]. Available: <https://www.calm-health.com/>
- [21] "Sito ufficiale Fitbit per i rilevatori di attività e altro." [Online]. Available: <https://www.fitbit.com/it/home>

- [22] J. Lee, K. Matsumura, K. Yamakoshi, P. Rolfe, S. Tanaka, and T. Yamakoshi, "Comparison between red, green and blue light reflection photoplethysmography for heart rate monitoring during motion," in *2013 35th Annual International Conference of the IEEE Engineering in Medicine and Biology Society (EMBC)*, Jul. 2013, pp. 1724–1727.
- [23] F. Lacirignola and E. Pasero, "Hardware design of a wearable ECG-sensor: Strategies implementation for improving CMRR and reducing noise," in *2017 European Conference on Circuit Theory and Design (ECCTD)*, Sep. 2017, pp. 1–4.
- [24] S. Navaretti, E. Pasero, and V. Randazzo, "Vital-ecg: a portable wearable hospital," *2018 IEEE Sensors Applications Symposium*, pp. 361–366, Mar. 2018.
- [25] "CC2640r2f SimpleLink™ Bluetooth® low energy Wireless MCU." [Online]. Available: <http://www.ti.com/product/cc2640r2f>
- [26] S. Bible, "Crystal Oscillator Basics and Crystal Selection for rfPIC™ and PICmicro® Devices." [Online]. Available: <http://ww1.microchip.com/downloads/en/appnotes/00826a.pdf>
- [27] "SOT23 Dual-Input USB/AC Adapter 1-Cell Li+ Battery Chargers." [Online]. Available: <https://www.maximintegrated.com/en/products/power/battery-management/MAX1555.html>
- [28] "Buck/Boost Regulating Charge Pump in μMAX." [Online]. Available: <https://www.maximintegrated.com/en/products/power/charge-pumps/MAX1759.html>
- [29] "REF20xx Low-Drift, Low-Power, Dual-Output, VREF and VREF/2 Voltage." [Online]. Available: <http://www.ti.com/product/REF2033>
- [30] "3 μA 1-Cell/2-Cell Fuel Gauge with ModelGauge." [Online]. Available: <https://www.maximintegrated.com/en/products/power/battery-management/MAX17048.html>
- [31] "Modelgauge battery fuel gauge technology." [Online]. Available: <https://www.maximintegrated.com/en/design/partners-and-technology/design-technology/modelgauge-battery-fuel-gauge-technology.html>
- [32] F. Kervel, "CC26xx HW Training - RF Front End options and Antennas." [Online]. Available: http://processors.wiki.ti.com/images/4/45/CC26xx_HW_training_RF_Frontends_and_Antennas.pdf
- [33] A. Andersen, "Application Note AN043 - Small Size 2.4 GHz PCB antenna." [Online]. Available: <http://www.ti.com/lit/an/swra117d/swra117d.pdf>

- [34] “INA333 - Low-Power, Zero-Drift, Precision Instrumentation Amplifier.” [Online]. Available: <http://www.ti.com/product/INA333>
- [35] “OPA4330 - 1.8 V, 35 μ A, microPower, Precision, Zero Drift CMOS Op Amp.” [Online]. Available: <http://www.ti.com/product/OPA4330>
- [36] J. Karki, “Active Low-Pass Filter Design.” [Online]. Available: <http://www.ti.com/lit/an/sloa049b/sloa049b.pdf>
- [37] “HDC2010 - Low Power Digital Humidity and Temperature Sensor.” [Online]. Available: <http://www.ti.com/product/HDC2010>
- [38] “High-Sensitivity Pulse Oximeter and Heart-Rate Sensor for Wearable Health.” [Online]. Available: <https://datasheets.maximintegrated.com/en/ds/MAX30102.pdf>
- [39] “MAXREFDES117: HEART-RATE AND PULSE-OXIMETRY MONITOR.” [Online]. Available: <https://www.maximintegrated.com/en/design/reference-design-center/system-board/6300.html>
- [40] “Bluetooth Core Specifications.” [Online]. Available: <https://www.bluetooth.com/specifications/bluetooth-core-specification>
- [41] “SYS/BIOS (TI-RTOS Kernel) - User’s Guide.” [Online]. Available: <http://www.ti.com/lit/ug/spruex3t/spruex3t.pdf>
- [42] “Core threading modules for the SYS/BIOS kernel.” [Online]. Available: http://software-dl.ti.com/dsps/dsps_public_sw/sdo_sb/targetcontent/sysbios/6_35_01_29/exports/bios_6_35_01_29/docs/cdoc/index.html
- [43] “BLE-Stack User’s Guide for Bluetooth 4.2.” [Online]. Available: http://dev.ti.com/tirex/content/simplelink_cc2640r2_sdk_1_40_00_45/docs/blestack/ble_user_guide/html/ble-stack-3.x-guide/index.html
- [44] “Recommended Configurations and Operating Profiles for MAX30101/MAX30102 EV Kits.” [Online]. Available: <https://pdfserv.maximintegrated.com/en/an/AN6409.pdf>
- [45] E. W. Weisstein, “Wiener-Khinchin Theorem.” [Online]. Available: <http://mathworld.wolfram.com/Wiener-KhinchinTheorem.html>
- [46] W. H. Press, S. A. Teukolsky, W. T. Vetterling, and B. P. Flannery, *Numerical Recipes in C (2Nd Ed.): The Art of Scientific Computing*. New York, NY, USA: Cambridge University Press, 1992.

- [47] R. Matusiak, "Implementing Fast Fourier Transform Algorithms of Real-Valued Sequences With the TMS320 DSP Platform," Aug 2001.
- [48] J. Pan and W. Tompkins, "A Real-Time QRS Detection Algorithm," *IEEE Transactions on Biomedical Engineering*, vol. 32, no. 3, pp. 230–236, Mar 1985.
- [49] Y. Tan and L. Du, "Study on Wavelet Transform in the Processing for ECG Signals," in *2009 WRI World Congress on Software Engineering*, vol. 4, May 2009, pp. 515–518.
- [50] M. Susi, V. Renaudin, and G. Lachapelle, "Motion Mode Recognition and Step Detection Algorithms for Mobile Phone Users," *Sensors (Basel, Switzerland)*, vol. 13, no. 2, pp. 1539–1562, Jan. 2013. [Online]. Available: <https://www.ncbi.nlm.nih.gov/pmc/articles/PMC3649428/>
- [51] R. Wang, W. Jia, Z.-H. Mao, R. J. Sclabassi, and M. Sun, "Cuff-Free Blood Pressure Estimation Using Pulse Transit Time and Heart Rate," *International conference on signal processing proceedings. International Conference on Signal Processing*, vol. 2014, pp. 115–118, Oct. 2014. [Online]. Available: <https://www.ncbi.nlm.nih.gov/pmc/articles/PMC4512231/>